VILNIUS UNIVERSITY

Birutė Pudžiuvytė

PHOTOSENSITIZED DAMAGE TO *ESCHERICHIA COLI* MEDIATED BY NEW TETRACATIONIC PORPHYRIN

Doctoral dissertation
Physical sciences, Biochemistry (04 P)

Vilnius, 2011

This dissertation was prepared at the Department of Biochemistry and Biophysics, Faculty of Natural Sciences, Vilnius University, the Department of Quantum Electronics in cooperation with Biophotonics group, Faculty of Physics, Vilnius University and Department of Biology, Padova University.

Scientific supervisor:

Assoc. prof. dr. Elena Bakienė (Vilnius University, physical sciences, biochemistry – 04 P).

Scientific advisor:

Assoc. prof. dr. Saulius Bagdonas (Vilnius University, physical sciences, physics – 02 P).

VILNIAUS UNIVERSITETAS

Birutė Pudžiuvytė

NAUJO TETRAKATIJONINIO PORFIRINO SUKELTOS *ESCHERICHIA COLI* FOTOPAŽAIDOS

Daktaro disertacija
Fiziniai mokslai, biochemija (04 P)

Vilnius, 2011

Disertacija rengta 2006-2011 metais Vilniaus universiteto Gamtos mokslų fakultete, Biochemijos ir biofizikos katedroje bei Fizikos fakultete, Kvantinės elektronikos katedroje ir Paduvos universiteto Biologijos mokslų katedroje.

Mokslinis vadovas:

Doc. dr. Elena Bakienė (Vilniaus universitetas, fiziniai mokslai, biochemija – 04 P).

Mokslinis konsultantas:
Doc. dr. Saulius Bagdonas (Vilniaus universitetas, fiziniai mokslai, fizika – 02 P).

Table of contents

ABBREVIATION LIST

ALA – γ-aminolevulinic acid

ATP – adenosine 5'-triphosphate

BSA – bovine serum albumin

CL – cardiolipin

CMC – critical micellar concentration.

DMMB – dimethyl methylene blue

DNA – deoxyribonucleic acid

DNP – 2,4-dinitrophenol

EDTA – ethylenediaminetetraacetic acid

F – fluorescence

HIV – human immunodeficite virus

HpD – hemathoporphyrin derivative

HSV – herpes simplex virus

IC – internal conversion

ITC – intersystem crossing

LED – light emitting diode

LPS – lipopolysaccharides

MAL – methyl aminolevulinate

MB – methylene blue

NA – nucleic acids

OM – outer membrane

PDT – photodynamic therapy

PACT – photodynamic antimicrobial chemotherapy

PE – phospahatidylethanolamine

PG – phosphatidylglycerol

PH – phosphorescence

PMBN – polymyxin B nonapeptide

PMB – polymyxin B

PPIX – protoporphyrin IX

RNA – ribonucleic acid

ROS – reactive oxygen species

SDS – sodium dodecyl sulphate

SEM – scanning electron microscopy

TBO – toluidine blue O

TEM – transmission electron microscopy

THPP – tetrahydroxyphenylporphine

TLCK – L-1-chlor-3-(4-tosylamido)-7-amino-2-heptanone-hydrochloride

T_4MAP – tetra(4N,N,N-trimethyl-anilinium)porphine tetraiodide

TMPyP – 5,10,15,20-tetra[4-N-methylpyridyl] porphine

T_4MPyP – tetra(4N-methylpyridyl) porphine tetraiodide

TN-Et-PyP – tetrakis(N-ethylpyridinium-4-yl)porphyrin tetratosylate

TPP^+ – tetraphenylphosphonium ions

$TPPS_4$ – 5,10,15,20-tetra(sulphonatophenyl)porphine

VR – vibrational relaxation

INTRODUCTION

Undoubtedly the discovery of antibiotics represented one of the most important advances in twentieth century medicine (Chopra, 2002). It gave rise to the belief that infectious diseases could be controlled and, eventually, mastered. Although antibiotics have saved countless lives, the initial widespread optimism has proven to be premature, since massive antibiotic application to clinic practice resulted in substantial stress on the target bacterium, which rapidly selected for resistant subpopulations equipped with different inheritable defence mechanisms (Nikaido, 2009). The first signs of bacterial resistance to commonly used antibiotics were recognized very soon after their introduction, while the first multi-drug resistant bacteria strain had been isolated only a decade later. Nowadays almost every known bacterial pathogen has developed resistance to one or more antibiotics in clinical use (Todar, 2011; Goldstein *et al*, 2011) and the situation is still getting worse due to increasing inappropriate use of existing antibiotics in human and veterinary medicine (Taylor *et al*, 2002; Fernandes, 2006; French, 2010). Therefore, such novel treatments of bacterial infections that give no possibilities to develope the resistance and are better targeted to specific infecting pathogen are in great demand (Willing *et al*, 2011).

Many strategies based on very different concepts are currently being investigated. Since the total elimination of antibiotics from the clinic seems unrealistic these days (Isturiz, 2010), the changed strategies in prescribing of already known antibiotics as well as usage of particular antibiotics along with the compounds inhibiting resistance mechanisms in the cells (e.g. inhibitors of key genes encoding proteins responsible for antibiotic resistance, efflux pumps inhibitors) are expected to reduce the amount of multidrug resistant pathogens (Taylor *et al*, 2002; Moellering, 2011). Apart from further improvements of antibiotic application, the investigation of potentially novel antimicrobials are gaining increased popularity. The

mechanisms by which bacteria attach to and invade mammalian cells, as well as the toxin production mechanisms, represent ideal targets for antimicrobial therapy. Targeting the virulence factors of pathogens is expected to prevent bacteria from colonizing the host and facilitating bacteria eradication by the immune system (Rasko & Sperandio, 2010). Small cationic peptides, mimetics of host defence proteins, manifesting themselves as membrane active drugs, or application of pathogen specific lytic bacteriophages represent still other promising branches of search for novel antimicrobials (Moellering, 2011; Fernebro, 2011). In addition, the application of light activated antibacterial agents is usually considered as technique not promoting the development of resistance, which is of the critical importance nowadays. (Taylor *et al,* 2002; Maish, 2010).

Photodynamic antimicrobial chemotherapy (PACT) is based on application of three initially harmless components: photosensitizer, the appropriate light and oxygen, still the combination of them is highly cytotoxic and leads to the fatal consequences for the cells. The main advantages of this bacteria eradication technique include:

1) target multiplicity and non specificity, that aggravates the development of resistance to the most (but not all) of the photosensitizers used (Soukos & Goodson, 2011),
2) the independence of the degree of antimicrobial photoactivity from the antibiotic−resistance spectra of microbial cells and the efficiency against antibiotic resistant biofilms, that suggest the real opportunity to combat infections which are impossible to treat by administering conventional antibiotics (Cassidy *et al*, 2010; Collin *et al*, 2010),
3) the controlled irradiation of the infected area reduces the risk of undesired side effects, including the low probability of injury to indigenous bacteria remote from the site of the phototreatment, which are often affected during systemic antibiotic therapy (Jori & Roncucci, 2006).

Although all the positive features do not suggest that photosensitization is the answer to all the problems of drug resistant diseases, it is obvious, that the technique will become an inclusive part of the antimicrobial therapy in the future (Wainwright, 2009). The application of this technique in the field of combating periodontal diseases in humans is already gaining increased popularity, however blood sterilization in a large scale still meats some problems and most of other possible applications are being verified in animal models or studied carefully in even earlier experimental stages.

Exploring the photosensitizer interactions with different components of bacterial cell can both facilitate the selection or synthesis of the photosensitizer with desired characteristics and clarify the detailed mechanism of the cell inactivation and death. Numerous researches demonstrate that various sites of the bacterial cell can be affected during the photosensitization process, though it is most likely that the cell wall and the cytoplasmic membrane are altered before the genetic material and represent the main cause of cell death (Salmon-Divon *et al*, 2004; Jori & Coppellotti, 2007). Although several details of the photosensitization mechanisms involved in the photosensitized inactivation of bacteria have been elucidated, there are relatively few data on the morphological alterations induced on the bacterial cell structure during photosensitization.

The aim of this study was to investigate spectroscopic features of a new tetra-cationic photosensitizer tetrakis(*N*-ethylpyridinium-4-yl)porphyrin tetratosylate (TN-Et-PyP), its interaction with the different cellular components and to analyse the photodynamic action of the porphyrin on the integrity and selected functions of *E. coli* KMY1 cell membranes.

The following **tasks** have been formulated:

- To explore TN-Et-PyP spectroscopic features and their changes upon interaction of the porphyrin with selected cellular components (i.e. lipopolysaccharides, lipids, proteins and nucleic acids).
- To determine *E. coli* morphological changes during TN-Et-PyP mediated photosensitization.
- To assay the photodynamic effect of TN-Et-PyP on the permeability of the inner and outer membranes.
- To evaluate the changes of the membrane voltage and respiration efficiency during the photodynamic treatment with the photosensitizer.

Scientific novelty

In this work we explored some details of new tetracationic photosensitizer tetrakis(*N*-ethylpyridinium-4-yl)porphyrin tetratosylate (TN-Et-PyP) mediated photoinactivation of Gram-negative bacterial cells. In order to meet the aim of the work we employed some spectroscopic techniques for studying the interaction of the photosensitizer with selected cellular components, enzymatic assays to clarify the physical state of the bacterial envelope, microbiological and electrochemical methods to assay the viability and changes in the physiological state of the bacterial cells.

It was demonstrated that the molecular symmetry of TN-Et-PyP strongly depends on the ionic nature of the solvent. Furthermore the photosensitizer molecules form complexes with negatively charged nucleic acids and lipopolysaccharides in buffer solution, the interaction being of electrostatic nature. Using low concentrations of photosensitizer, damage is inflicted to the outer membrane and results in a higher permeability of the membrane to fairly small molecules such as deoxycholate; however, larger molecules such as periplasmic alkaline phosphatase are not released or are released after their extensive inactivation, as we could not register any enzyme activity outside the cells. Increasing the TN-Et-PyP concentration correlates with the inactivation of the respiratory chain, drop in plasma membrane voltage, the release of compounds with absorption band at 260 nm, and a decrease in intracellular enzyme β-galactosidase activity, though this activity has not been noticed to increase outside the cells, suggesting that enzyme inactivation probably occurs in inner cell districts. The careful analysis of TEM micrographs also revealed the increased porosity of the photosensitized bacteria envelope and damage inflicted to inner compartments of the cells.

We present here evidences for the presumable mechanism of TN-Et-PyP mediated photosensitized inactivation of Gram-negative *E. coli* cells, which includes several steps, namely: 1) binding of TN-Et-PyP to *E. coli*

outer membrane components (LPS); 2) photosensitized modification of the membrane; 3) diffusion of porphyrin to inner membrane and cytoplasm; 4) photoinduced loss of enzymatic activities and inner membrane functions; 5) amplification of the bacterial envelope permeability and 6) *E. coli* cell death.

The findings presented in this work give more detailed pattern in understanding the photosensitized bacterial inactivation mechanism.

1. BACKGROUND

1.1. Photosensitization as a process from the physical point of view

Photosensitization is a process when the light energy is absorbed by one type of molecule (photosensitizer) and the resulting energy rich state of the photosensitizer then undergoes reactions, that ultimately results in the chemical alteration of any other molecule in the system (the substrate molecule). In other words, the photosensitization is a reaction to light that is mediated by a light-absorbing molecule, which is not the ultimate target. The photosensitizer molecule returns to initial state when photosensitization reaction is complete, however in some cases it is converted to chemically different molecular form, which have completely different spectroscopic characteristics. The latter process named photobleaching usually competes with photosensitization and the final outcome depends on the balance between those two processes (http.www.photobiology.info).

The description of photosensitization mechanism generally starts from acquaintance with the most important diagram in photobiology – Jablonski diagram, which depicts electronic transitions following the absorption of light and energy dissipation or transfer events leading back to the initial state. Generally, the energy of the molecule is made up of electronic energy and energy due to vibrational and rotational nuclear motion: i.e. electronic energy, vibrational energy and rotational energy respectively (Rotomskis *et al*, 2007; Wardle, 2009). Normally, the electrons of the atoms composing photosensitizer molecule are placed in their usual low energy molecular or atomic orbitals, consequently the energy of the molecule is not high enough to enable the photosensitized reactions – such energetic level is denoted as ground state (or S_0). The situation changes when the photon of light is absorbed. According to the first law of photochemistry, only absorbed photons can produce photochemical changes and absorption can occur only when the energy of the photon matches the energy of transition to the excited state. The energy in ultraviolet (UV), visible (VIS) spectral regions answers the

energy requirement for different molecules, since the extent of absorption of light varies a great deal from one substance to another (Wardle, 2009). Light absorbing molecules contain antennae groups known as chromophoric groups, which are responsible for the absorption of light. In the case of organic chromophores the absorption of light causes excitation of electrons in lower energy bonding molecular orbitals (particularly π) or non bonding atomic orbitals (denoted n). They are promoted to higher energy antibonding molecular π* orbitals, the transitions being described as π→ π* or n→π*. Less energetic σ orbitals usually are not involved. (Prasad, 2003; Rotomskis *et al*, 2007; Wardle, 2009). Furthermore, due to the extreme rapidity of light absorption which lays in the range of femtoseconds (1 fs = 10^{-15} s), the massive nucleus of the molecule stays fixed during the transition, whereas much more lighter electron is promoted to a higher electronic energy level; as a consequence the distribution of electrons surrounding the nucleus changes and finally molecule is driven from the ground state S_0 to electronically excited state denoted S_1, S_2…, which differ from ground state in chemical and physical properties. These excited states are short – lived (lifetime ranges in nanoseconds) and rapidly lose their excess energy through a variety of deactivation processes, returning to a ground – state configuration (Fig. 1.1.). If the excited molecule returns to its original ground state, then the dissipative process is a physical process, but if a new molecular species is formed, then the dissipative process is accompanied by a chemical change (Wardle, 2009).

In summary the acquired energy can be lost in three possible ways:

1. The excess of energy is given off as heat in the processes known as internal conversion (IC), vibrational relaxation (VR) and intersystem crossing (ITC) ,
2. The energy is lost by emission of photon (respectively fluorescence (F) or phosphorescence (PH),

3. The energy is transferred to the molecule residing nearby (usually to molecular oxygen) or lost due to participation in photochemical processes.

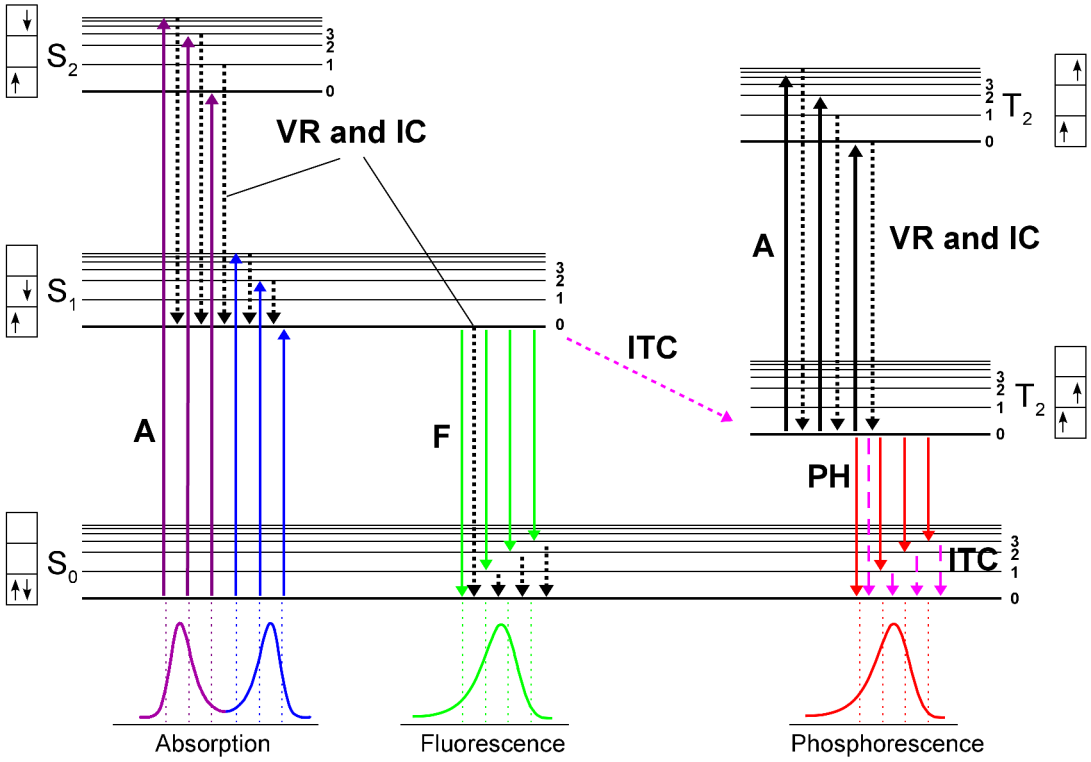

Fig. 1.1. Jablonski diagram represents the electronic states of a molecule and the transitions between them. The electronic states are arranged vertically by increased energy levels and denoted with letters S (for singlet) or T (for triplet) and appropriate numbers. The boxes detail the electronic spins in the molecular orbital, with the spins shown as up and down arrows, denoting opposing directions. Thin horizontal lines illustrate vibrational levels of each electronic state of the molecule. Solid arrows indicate radiative transitions – absorption or emission of a photon. Dotted arrows represent non-radiative transitions. The conception of radiative transitions includes absorbtion A (purple and blue lines), fluorescence F (green lines) and phosphorescence PH (red lines). Non radiative transitions encompass internal conversion IC, vibrational relaxation VR (dotted arrows) and intersystem crossing ITC (dashed magenta arrows). Adapted from „Basic Photobiology" (http://www.photobiology.info/Visser-Rolinski.html) and „Biofotonika" (Rotomskis et al, 2007).

An internal conversion as well as vibrational relaxation is a radiationless transition of a molecule between electronic states having similar electronic spin (between singlet or between triplet states). The energy is released in the form of heat and the process ends when the lowest vibrational level of appropriate electronic state is reached, no matter what level is initially populated by light absorption. It is a very rapid process that takes place in the

range of picoseconds (1 ps = 10^{-12} s). The dissipation of energy as heat drives the molecule either to the ground state $S_{0,0}$ when the whole excitation energy is lost, or to $S_{1,0}$ and $T_{1,0}$ levels when only a part of it is released by internal conversion. In the latter cases the left energy can be released in two possible pathways. The first one leads to the dissipation of energy as heat in a radiationless process denoted intersystem crossing, described as a transition of a molecule between electronic states having different electronic spin, i. e. from singlet $S_{1,0}$ to triplet state $T_{1,n}$ or from triplet $T_{1,0}$ to singlet state $S_{0,0}$. Alternatively, the left energy can be released as light from $S_{1,0}$ in a process named fluorescence. The energy of the emitted photon corresponds to the energy difference between the emitting and final state of fluorescing molecule, moreover both states should have similar electronic spin i.e. both singlet states. Fluorescence always originates from the same $S_{1,0}$ level irrespective of which electronic level is excited. At this point it is important to remember that absorbed energy is greater than emitted energy (either from excited singlet or triplet states), therefore peaking of fluorescence (as well as phosphorescence, described below) spectra is shifted to lower energy and longer wavelength than the absorption spectrum. This phenomenon is named Stokes shift. Fluorescence takes place in nanosecond scale (1ns = 10^{-9}s), being more rapid light emission than phosphorescence, which lasts for miliseconds time (1ms = 10^{-3}). Phosphorescence is a light emission process similar to fluorescence with only one exception – the light emitting and final states have different electronic spin. Typically it starts from a triplet state $T_{1,0}$ and ends in ground state $S_{0,n}$.. However, as transitions between triplet and singlet energy states are relatively forbidden, it results in much longer lifetime of the excited triplet state to compare with excited singlet states. The longer lifetime allows more time for energy or electron transfer from excited photosensitizer molecule to adjusting molecules in the natural systems, thus photochemical reactions occur (Visser & Rolinski, http://www.photobiology.info/Visser-Rolinski.html). The molecules, characterised by inefficient internal conversion, are believed to be good

photosensitizers, hence typically the excitation energy is dissipated by intersystem crossing to the triplet state which participates in photochemical reactions. (Oleinick, http://www.photobiology.info/Oleinick.html). According to the type of molecules which become the substrates and reaction nature two types of photosensitizer mediated reactions are distinguished (Foote, 1968; Streckytė et al, 2008).

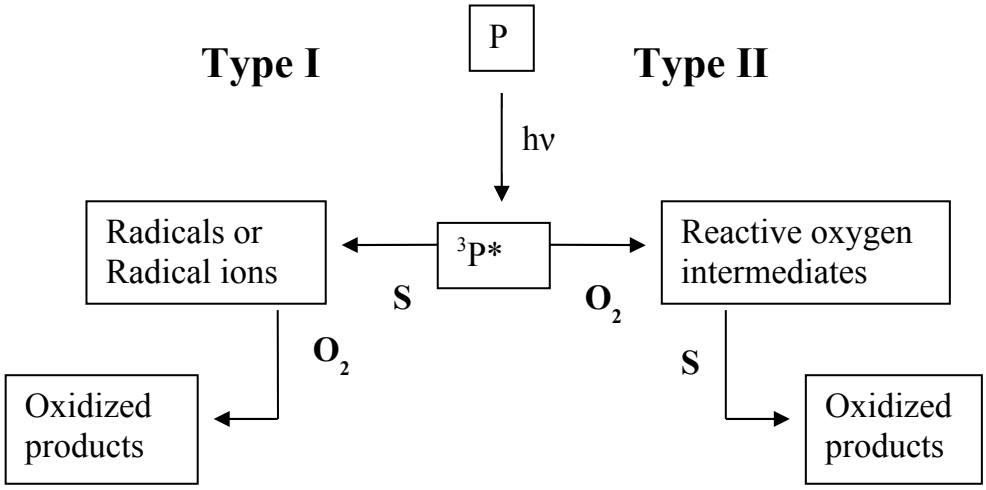

Fig. 1.2. Type I and Type II reaction pathways. P denotes photosensitizer in the ground state, ^{3}P* – photosensitizer in the triplet state, S – substrate. Taken from „Photodynamic therapy and fluorescence diagnosis in dermatology" ch. 2 (Aveline, 2001).

The figure presents very simplified model of both photosensitization reaction pathways. Situation is much more complicated and even raised arguments among scientists concerning attribution of reactions involving triplet state sensitizer and triplet state oxygen interaction (described below) resulting in superoxide radical anion formation. Regardless to the fact, that initially Foote attributed this reaction to Type II process, it is often considered to be the Type I reaction nowadays. (Wainwright, 2009). Further description of both photosensitized reactions types will demonstrate all the complexity and possible interconectivity of them.

Type I reaction mechanisms involve direct interaction between ^{3}P* molecule and a substrate molecule, localised in close vicinity, with a hydrogen abstraction or electron transfer between these molecules. It results in the production of radicals and ion radicals, that have an uneven number of

electrons, therefore they are highly reactive. These intermediate species can undergo further reactions with other substrates, solvent molecules or oxygen. The latter process results in production of cytotoxic reactive oxygen species (ROS) and subsequent generation of oxidized products. More details are presented in Fig. 1.3.

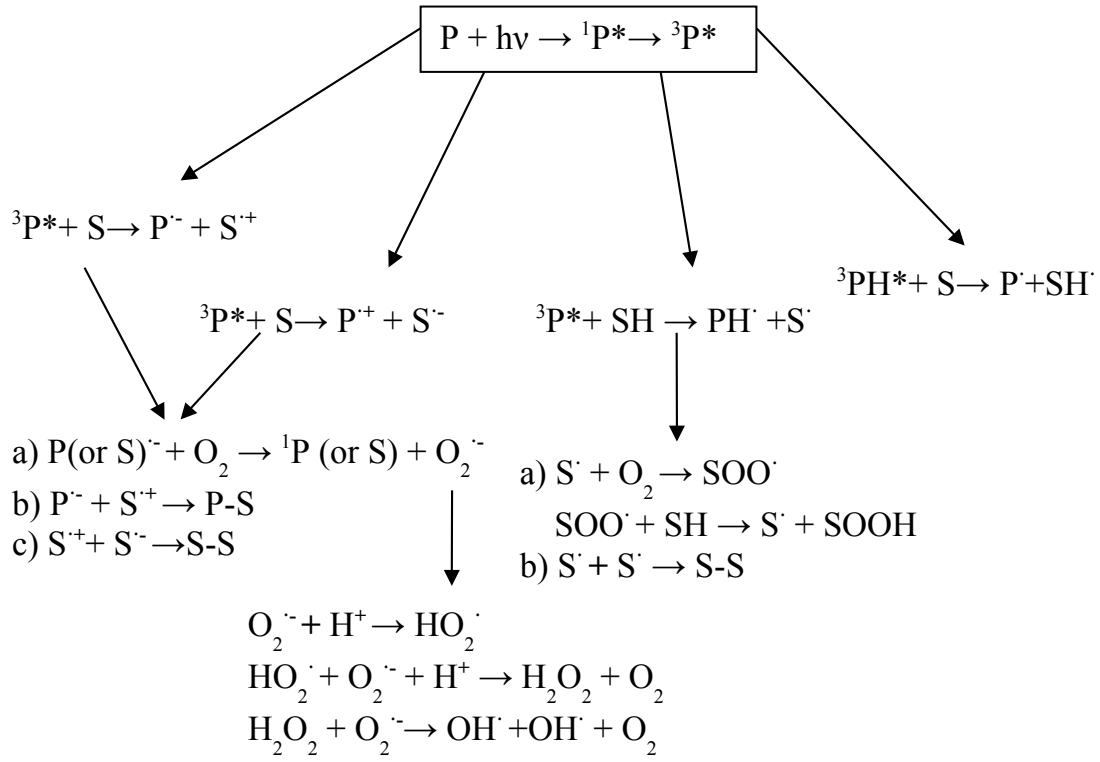

Fig. 1.3. The simplified scheme of Type I reactions. P denotes photosensitizer in the ground state, ^{3}P* – photosensitizer in the triplet state, S- substrate. Adapted from „Fotosensibilizacija biosistemose: taikymas ir perspektyvos“ (Streckytė *et al*, 2008).

Generally it is assumed that excited photosensitizer (^{3}P) reacts directly with the substrate (SH or S), in a one-electron or hydrogen transfer reaction, to produce a radical or radical ion in both the sensitizer ($PH^{\cdot}$ or $P^{\cdot+}$, $P^{\cdot-}$) and the substrate ($S^{\cdot}$ or $S^{\cdot+}$, $S^{\cdot-}$). An electron transfer can proceed in two possible directions: either substrate donates an electron to sensitizer, resulting in substrate radical cation ($S^{\cdot+}$), and sensitizer radical anion ($P^{\cdot-}$) or *vice versa* – substrate receives an electron from photosensitizer, the products of this reaction being substrate radical anion ($S^{\cdot-}$) and sensitizer radical cation ($P^{\cdot+}$). The same type of reactions lay in the background of a hydrogen donation, the products being photosensitizer or substrate radicals ($P^{\cdot}$, $S^{\cdot}$).

The radicals produced in primary reactions can further react in several pathways depending on the amount of oxygen in their microenvironment. The radicals of substrate and photosensitizer can react in between to form covalently bound photosensitizer and substrate aducts or aducts of two substrate molecules (P-S, S-S), if there is a lack of oxygen in surrounding media. However, such conditions are not very common in natural systems, hence, in the presence of oxygen, oxidised forms of the sensitizer or of the substrate readily react with O_2 to give peroxyl radicals, thus initiating chain autooxidation reactions. Semireduced forms of the photosensitizer or the substrate ($P^{\cdot-}$ or $S^{\cdot-}$) interact efficiently with oxygen molecule to produce the superoxide radical anion ($O_2^{\cdot-}$), and regenerating the original sensitizer (P). Formed superoxide radical anion can react directly with different substrates or serve as a precursor of other reactive oxygen species (such as hydrogen peroxide (H_2O_2) or the most dangerous hydroxyl radical ($OH^{\cdot}$)). Under physiological conditions H_2O_2 is produced by the dissmutation of $O_2^{\cdot-}$. The hydroxyl radical can then be generated via Fenton reaction between H_2O_2 and $O_2^{\cdot-}$ (Streckytė *et al*, 2008). In summary, the Type I photosensitization processes can produce different kinds of reactive intermediates. Although, oxygen is not required for the first steps of the mechanism, the concentration of it in the surrounding milieu strongly influences the subsequent chemical reactions. Furthermore, it is important to remember that presence of oxygen facilitates production of ROS, such as H_2O_2, $O_2^{\cdot-}$and especially $OH^{\cdot}$ which are known to be aggressive oxidators of various types of biomolecules, subsequently inducing substantial damage to the cells (Streckyte *et al*, 2008; Aveline, 2001).

Type II mechanisms proceed via energy transfer processes during a collision of triplet state photosensitizer ($^3P^*$) with oxygen ($^3O_2$) and involve electron spin exchange between the two molecules, regenerating the ground state photosensitizer (P) and producing an excited singlet state of oxygen ($^1O_2$)

(Fig. 1.4.). The photosensitizer is not consumed during this type of photosensitized reaction.

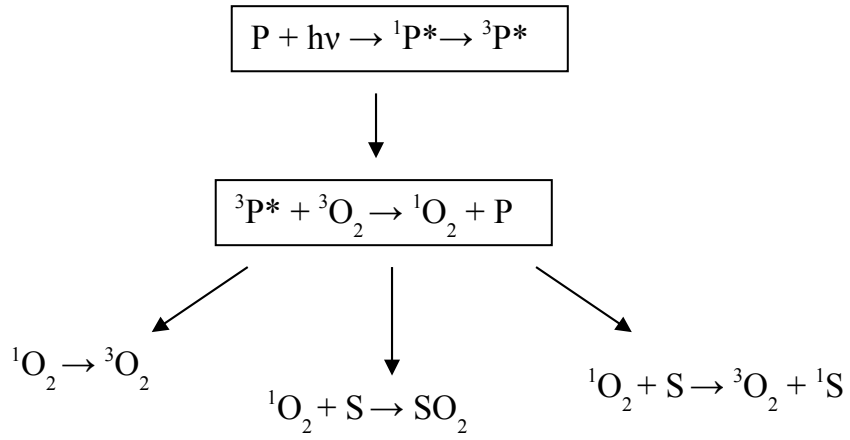

Fig. 1.4. The shorted scheme of Type II reactions. P denotes photosensitizer in the ground state, $^3P^*$ – photosensitizer in the triplet state, S – substrate. Adapted from "Fotosensibilizacija biosistemose: taikymas ir perspektyvos" (Streckytė *et al*, 2008) and (De Rosa & Crutchley, 2002).

The ground state of oxygen has a triplet multiplicity, discriminating the compound from all other organic molecules. The transfer of energy between triplet state of photosensitizer and triplet state of oxygen is not forbidden since it does not require a change in spin direction, consequently it proceeds effectively. Several forms of excited singlet oxygen denoted as $^1\Sigma^+_g$, $^1\Delta_g$ and dimer forms marked as $^1\Sigma^+_g\,^1\Sigma^+_g$, $^1\Delta_g\,^1\Sigma^+_g$ and $^1\Delta_g\,^1\Delta_g$ are known to exist in various solvents and gasses (Rotomskis *et al*, 2002; Buettner, http://www.photobiology.info/Buettner.html). Unfortunately, dimeric forms have particularly short life time and cause a lot of problems in registration, therefore their chemical activity and properties are not properly investigated. It has been demonstrated that only $^1\Delta_g$ form participates in photosensitized reactions and is converted to primary product of type II photosensitization mechanism – singlet oxygen, which is characterised by greater electrophilicity, therefore oxidizes biomolecules very rapidly (Foote, 1968). However, singlet form of oxygen has a short lifetime of approximately 0.01-0.04 μs estimated in the cells, therefore it can diffuse approximately 0.01μm from production site

before being deactivated (Moan, 1990; Moan & Berg, 1991). Apparently, only structures localised adjacent to the photosensitizer are consequently damaged (De Rosa & Crutchley, 2002; Castan*o et a*l, 2004). Several fates of singlet oxygen in cell suspensions have been reported. Firstly, generated singlet oxygen can rapidly decay to the ground state or transfer energy to adjacent molecules driving them into excited state (^{1}S). Alternatively, it can react with adjacent molecules and form cyclic peroxides which appear to be very unstable and decompose rapidly in successive thermal and enzymatic reactions (see Fig. 3.14) (Aveline, 2001).

Obviously, the Type II mechanism is favoured over the Type I (radical) mechanism by lower substrate concentration and higher oxygen concentration, whereas under hypoxic conditions Type I process will predominate (Aveline, 2001). Both: the radicals and ROS can further interact with biological substrates producing changes in their structure and impairing the function as a consequence.

1.2. The methods to achieve the desired characteristics of the photosensitizers, improvements in the targeting of bacteria cells

The photosensitizers are usually defined as molecules with strong absorption of appropriate wavelength capable to transfer the excess energy to other molecules (particularly biomolecules). It results in shifting of the acceptor molecules into unstable excited energy state or transforming them into highly reactive radicals via electron transfer, therefore photochemical reactions are initiated. Consequently the photosensitized cells are damaged or even eradicated (Streckyte *et al*, 2008). The most popular photosensitizers have aromatic structure which is appreciable for long-lived triplet excited states. However, the absorbed light differs in wavelength (and consequently photon energy) depending on the molecular structure of aromatic system involved: furocoumarin photosensitizers (psoralens) absorb relatively high energy ultraviolet (UV) light (c. 300–350 nm), whereas macrocyclic, heteroaromatic molecules such as the phthalocyanines absorb lower energy, near-infrared light

(c. 660-700 nm) and porphyrins absorb light of visible region (c. 395-650), though with decreasing intensity towards the red region of the spectrum (Wainwright, 1998). However, not every light absorbing aromatic compound is considered to be a good photosensitizer. Summarising all successes and failures during long years of photoresearch studies, carried out in a great number of laboratories, and different characteristics of innumerable compounds investigated, it have been concluded, that an ideal photosensitizer should have following physicochemical and pharmacological characteristics:

■ Photosensitizer synthesis should be relatively simple, initial materials available, so that large-scale production is feasible (Phoenix & Harris, 2006).

■ Photosensitizer should be chemically pure compound with a constant composition, because the administration of a mixture makes the situation much more complicated, due to the required identification of useful and deleterious constituents and investigation of their fate in the natural systems (Wainwright, 2009).

■ Ideal photosensitizer should be water soluble or soluble in non hazardous aqueous solvent mixture (Sternberg *et al*, 1998). It is well established that hydrophilic species are rapidly cleared from the organism, whereas lipophilics are metabolized longer, since the production of more hydrophilic derivatives are required in the first step of the drug removal. Since a more lipophilic compound will remain for a longer period within the system, the chances for deleterious events to happen will be increased also (Wainwright, 2009). However, hydrophobic or amphiphilic photosensitizers are sometimes preferred.

■ Photosensitizer molecule should be relatively inert, as it will be subjected to the systems responsible for detoxifying xenobiotics upon administration. Consequently half life of the dye should be also considered, as the compound remaining in the organism for longer periods increases chances of deleterious events, whereas too short lifetime will not secure desirable effect (Wainwright, 2009).

■ It is desirable for a good photosensitizer to have a strong absorbance with a high extinction coefficient at an appropriate wavelength. Generally it is assumed, that a good photosensitizer should absorb the light of longer wavelength (600 – 900nm) in so called "optical window", since only minor absorption of the most human tissues occur within this region, consequently the deeper penetration of the incident light is allowed. Furthermore, it is desirable that the photosensitizer should not strongly absorb light in wavelength region of 400 – 600 nm in order to minimize the risk of generalized photosensitivity due to sunlight (Rotomskis *et al*, 2002; Jorri & Coppellotti, 2007; Streckytė *et al*, 2008; Soukos & Goodson, 2011). However, the irradiation with the light of shorter wavelength is also practiced in topically applied photosensitized antimicrobial chemotherapy (Nitzan & Ashkenazi, 2001).

■ Photostability of the compound provides the ability to avoid photosensitizer bleaching before it reaches the target (Wainwright, 2009).

■ High yields and long lifetimes of the triplet state of photosensitizing compound enables effective production of radicals and ROS that leads to high photochemical reactivity (Rotomskis *et al*, 2002).

■ In addition, photosensitizer molecules should not show significant self-aggregation in the solvents as it lowers singlet oxygen yield (Φ_{Δ}) and triplet state yield (Φ_t) (Phoenix & Harris, 2006; Rotomskis *et al*, 2002)

■ Minimal dark toxicity is very important for escaping allergic reactions and other side effects on healthy tissue adjoining infection site (Wainwright, 2009)

■ Photosensitizing compound should selectively accumulate in the target cells and be eliminated from the patient body sufficiently quickly to avoid generalized photosensitization, especially skin photosensitization as it is constantly exposed to sun light (Jori, 2003).

In spite of the amount of photosensitizers synthesized and tested, there is no single compound having all characteristics needed, however it is important to remember that sometimes the absence of some features can be

compensated with the other characteristics. For example exact targeting and good accumulation in bacteria cells can compensate lower singlet oxygen yield (Streckytė *et al*, 2008). The successful outcome of photosensitizer mediated antimicrobial phototherapy depends on the choice of a photosensitizer with optimal properties for specific application (Jori, 2003).

The chemical modification of photosensitizer offers wide opportunities for choosing the best agent for a particular case. It was shown that the modification of photosensitizer molecule can change light absorption characteristics (λ_{max}, ε_{max}), singlet oxygen yield (Φ_{Δ}), lipophilicity properties (log P) and other physicochemical characteristics, which determine dye accumulation and localization in the cell, consequently influence photosensitization efficiency. Generally it is desirable for a good photosensitizer to have strong absorption in "optical window" – red area of the visible light spectrum. The shift of absorption maximum to the further red region of the spectrum (so called bathochromic effect) is achieved either by the expansion of macrocycle through condensation of a benzene or naphthalene moiety with each pyrrole ring or hydrogenation of a carbon-carbon double bond in one or two pyrrole rings. The fine-tuning of the position and intensity of the absorption maxima can be obtained by further modifications of the photosensitizer molecule such as the insertion of a metal ion in the centre of macrocycle (Redi & Jori, 1998; Jori, 2003). Another problem resolved via chemical modification is aggregation of the photosensitizer molecules, which is highly undesirable because in this case excitation energy is dissipated through nonradiative pathways, thus drastically shortening the lifetime of the dye triplet state and decreasing photosensitization efficiency. Aggregation is more characteristic to porphyrin derivatives dissolved in aqueous media, because the hydrophobic parts of tetrapyrrolic macrocycles are prone to interact in between trying to minimize the contact area with the polar milieu, consequently the dimmers or oligomers of porphyrins are formed (Jori, 2003). Modifying the chemical structure of porphyrins and their analogues by adding

long or charge bearing periferial substitutes and/or axial ligands helps to minimize detrimental tendency to undergo aggregation (Pushpan *et al*, 2002; Streckytė *et al*, 2008; Wainwright, 2009). Additionally, the incorporation of the charge into a photosensitizer molecule increases compound solubility in water based solutions, whereas the addition of a halogen such as iodine results in a much more lipophilic molecule along with considerably increased singlet oxygen generation efficiency. The hydrophilicity/lipophilicity plays an important role in photosensitizer uptake and localization in the cell, consequently it partly determines the extension of damages inflicted upon irradiation. Accordingly, changing this feature by chemical modification of photosensitizer molecule may change the compound accumulation site to completely different microbial compartment, inducing damages to the photosensitized cell in much wider range comparing to initial compound, thus increasing photosensitization efficiency (Wainwright, 1998).

Although, the usage of photosensitizer linked to nanoparticles (made of various materials such as glass, gold, polystyrene, carbon nanotubes etc) is gaining increased popularity in cancer treatment, comparatively much less reports about attempts to use this technique for combating antimicrobial infections have been published recently (Pagonis *et al*, 2010; Perni *et al*, 2011; Soukos & Goodson, 2011; Allaker, 2010). The most popular structure appears to be fullerenes, which can be turned into considerably effective photosensitizers when appropriate groups are bound (Huang *et al*, 2010). The fullerenes initially have some photophysical features required for a good photosensitizer due to specific ball shaped structure composed of 60 carbon atoms (Kroto *et al*, 1985; Hadon *et al*, 1986). The condensed aromatic rings lead to an extended π conjugation of the molecular orbitals resulting in significant absorption of visible light; furthermore the fullerenes have a long lifetime of triplet excited state (Arbogast *et al*, 1991, Perni *et al*, 2011). The addition of quaternary pyrrolidinium groups to fullerene molecule helps to overcome such problems as low solubility in polar solvents turning cationic

fullerenes into effective antimicrobial photosensitizers (Tegos *et al*, 2005; Spesia *et al*, 2008;).

It may appear that the chemical modification provides immense abilities to construct a photosensitizer with particular properties. However, the situation is not so simple at a closer look. Even though a lot of various photosensitizers have been extracted from the natural sources or synthesized artificially, only several of them are approved for clinical use. A lot of problems such as availability of initial materials in large quantities, some difficulties in modification steps or absence of technologies for synthesis in industrial scale still have to be solved (Sternberg *et al*, 1998).

A photosensitizing agent with potentially optimal properties for the treatment of microbial infections should be endowed with specific features in addition to the expected photophysical characteristics described above (Jori *et al*, 2006). A large affinity to microbial cells and extensive killing of the disease-inducing bacteria, with minimal damage to the host tissue and ability to distinguish between pathogen and commensal bacteria, not damaging the latter, should not be overlooked. Moreover, pathogenic bacteria are not expected to develop the resistance to the compound even after multiple applications (Jori *et al*, 2006; Tavares *et al*, 2010). The constantly developing technologies provide appropriate equipment which enables to deliver the light to the site of infection and restrict irradiation to a very small area in order to minimize host tissue damage, however it can not be eliminated totally (Calin & Parasca, 2009). The use of targeted photosensitizers so that the cytotoxic effect is directed to the pathogen entirely could improve the situation. The antibody-based, bacteriophage linked and liposome mediated drug delivery techniques have been proposed for bacteria targeting. Despite the fact that some of these techniques were hypothesized several decades ago, practical aspects of targeted photosensitization are still in the experimental laboratory level, because high cost of research and certain problems limit manufacture and development.

The advantages of targeted photosensitization include high selectivity and increased drug concentration around the target cells which enables increase in the number of kills, due to exposure to a greater amount of singlet oxygen upon irradiation, thus contributing to the photosensitizing compound saving (Yacoby & Benhar, 2007). A very few researches have been done on antibody – targeted photosensitization, yet even the very first results appeared to be encouraging. The toluidine blue TBO and tin (IV) chlorine e6 were the first photosensitizers conjugated to antibodies against surface structures of *Porphyromonas gingivalis* (Bhatti et al, 2000)*, Staphylococcus aureus* (Embleton *et al*, 2002), *Pseudomonas aeruginosa* (Strong et al, 1994) The conjugates showed considerable improvement of photosensitization efficiency and selectivity. Although conjugate architecture has varied over the years, design criteria have remained the same, namely: (1) photochemical and immunochemical stability, resistance to photodecomposition and stability against enzymatic attack (2) capacity of inflicting precise selective injury to targeted cells, and (3) plasma stability along with good target uptake in vivo. Critical point in targeted photosensitization efficiency is the choice of antibody which should meet not only criteria mentioned above but also is required not to interfere with photophysical properties of the conjugated photosensitizer molecule, including quenching of singlet oxygen, shortening of triplet state lifetime or extreme changes in absorption properties (Strong et al, 1994). The target of antibody is equally important and failure to choose a proper bacterial surface structure can decrease photosensitization efficiency, when growth phase dependent bacterial surface structures are targeted.

The therapeutic potential of bacteriophages is based on their ability to infect a specific bacterial host. According to the ideal scenario the filamentous phages are genetically modified to display a special moiety on their surface. The photosensitizer is linked to phages by chemical conjugation through a labile linker which is needed to controlled release. Thus, in the conjugated state, the photosensitizer can be considered as a prodrug, which is

activated upon its dissociation from the phage at the target site after the phage carrier tethers to the target cell. This controlled release helps to ensure reduction of general toxicity (Yacoby & Benhar, 2007). In order to enhance selectivity antibodies can be linked to the phages minor coat protein, thus combining the best features of both antibody and bacteriophage based techniques (Yacoby *et al*, 2006). The first researches on *Staphylococcus aureus* photosensitization with tin (IV) chlorine e6 conjugated to Phage 75 demonstrated real ability of bacteriophage to deliver the photosensitizer to target bacteria. It occurred that recognition of the target is enough for photosensitization efficiency and phage abilities to lyse the target bacteria are not important. However, the attitudes to the usage of bacteriophages as drug carriers vary from optimistic to sceptic due to a lot of difficulties such as the choice of the phage (since the lysogenic viruses can contribute to spreading of antibacterial resistance or virulence genes among bacterial populations), special conditions required for phage adsorption to bacteria (which are not so easy achievable *in vivo*), a high mutability rate both phage and bacteria, leading to loss of special surface receptors or inability to recognize them (Carlton, 1999; Levin & Bull, 2004). In addition, phage growth, purification and storage protocols are needed to assure therapeutic safety and to reduce the possibility of contamination of pharmaceutical preparations with toxins and bacterial debris, because potential adverse reactions, such as anaphylactic shock must be considered when repeated treatment is required (Merril *et al*, 2003).

The liposomes as the analogues of natural membranes are generally assembled by spontaneous self-organization from pure lipids or lipid mixtures and the liposomal shell can enclose or bind many different classes of compounds, therefore liposomes can be used as various antibacterial drug carriers including photosensitizers. Liposomes have many superior features, particularly biocompatibility, biodegradability, low toxicity, capability for big load of drug and structural variability which is very important for filling

interior of the vesicle with different photosensitizers. The problem of releasing liposome-encapsulated or –associated compounds to the target cells is resolved by incorporating special substances which participate in specific reactions at the target site or promotes structural changes of lipid bilayer as a response to an external stimulus such as irradiation (Benkoski *et al*, 2006). This technique appears to be most promising and fast developing though it is more widely used for antibiotic and cancer therapy than for antimicrobial photosensitized therapy (Immordino *et al*, 2006; Samad *et al*, 2007), yet investigations on liposome application for drug carrying are constantly accelerating also in antimicrobial photosensitization field (Bombelli *et al*, 2008; Nisnevitch *et al*, 2010). It was demonstrated that composition of liposome determines efficiency of photosensitized bacteria eradication, for example vesicles composed of neutral phospholipid bilayer form a barrier preventing the initial interaction between positively charged functional groups in the photosensitizer molecule with the negative bacterial envelope moieties, therefore naturally only the liposomes composed of cationic phospholipids appear to be efficient drug carriers (Ferro *et al*, 2007). However apart from a lot of beneficial features certain problems such as instability, short circulation half-lives, low entrapment efficiency and leaking of the internalized substances through the boundaries, irreproducibility of preparation conditions, immune system mediated neutralization and premature removal of administered immunoliposomes have to be solved before applying it to photosensitized antimicrobial chemotherapy (Jesorka & Orvar, 2008).

In spite of immense possibilities in chemical modification of photosensitizers, promising achievements in targeting them to exact pathogenic bacterial cell and rapid development of equipment for appropriate light emitting and channelizing to infected sites, it is obvious that a lot of difficulties still have to be overcome. Therefore it is not surprising that phenothiazinium dyes (toluidine blue O and methylen blue) and protoporphyrin IX are the only photosensitizers that have been widely used in clinic to treat infectious

(particularly dental) diseases or to sterilize the blood products. A lot of optimized photosensitizers' molecules are available having hundreds or even thousands of time the potency than their predecessors, however they have never been subjected to the costly toxicological and safety studies necessary for approval for clinical use (Dai *et al*, 2009).

1.3. The photophysical photochemical and biological features typical to the most popular groups of photosensitizers used in antibacterial chemotherapy

At present, members of three classes of photosensitizers have been proposed as antimicrobial chemotherapeutics, namely phenothiazine, porphyrin, and phthalocyanine derivatives, while porphyrin related chlorines are just gaining popularity in antibacterial photodynamic therapy (Jori & Coppellotti, 2007). The basic chemical structures of the photosensitizing agents are shown in Fig. 1.5.

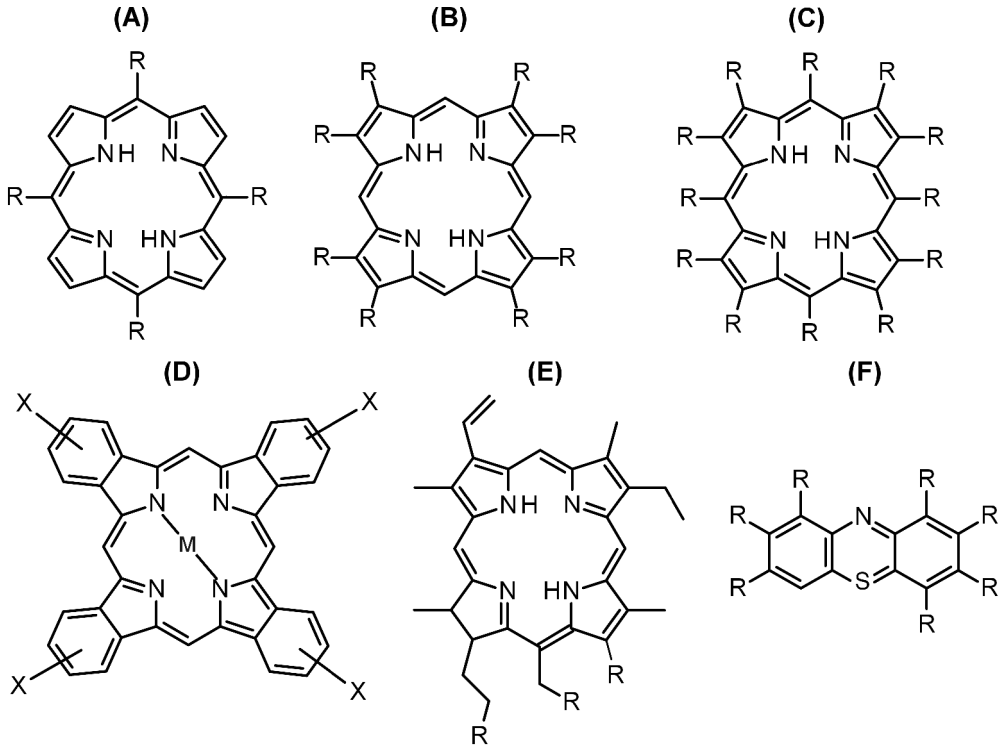

Fig. 1.5. The basic chemical structure of porphyrines (A-C), phthalocyanines (D), chlorins (E) phenothiaziniums (F) (Wainwright, 2009).

The mentioned groups of photosensitizers need to be reviewed in more details, particularly stressing special points of photophysical and photochemical features, photosensitization mechanism or special applications typical to each group of photosensitizers.

1.3.1. Phenothiaziniums

The compounds are closely related in structure which is rather simple – namely aromatic tricycle to which other functional groups are attached. The chemical structure of compound core determines long-wavelength absorption in the region 590 – 660 nm of visible light. However, the absorption maximum is shifted to the longer wavelength if such modifications as amino side chain alkylation, chromophore heteroatom substitution take place. Increasing the alkyl content can provide the phenothiazinium molecule with greater lipophilicity as well as addition of anionic or cationic functional groups increase hydrophilicity – the features considerably influencing the cellular uptake of the photosensitizer (Wainwright, 2009).

Although there are plenty of phenothiazinium based compounds synthesized, only two of them, namely methylene blue (MB) and toluidine blue O (TBO), are acknowledged to be the leader compounds in drug research against bacterial infection and approved for clinical use (Dai et al, 2009; Wainwright, 2009). Similarly to other photosensitizers the phenothiaziniums are more effective against Gram-positive strains such as *Enterococcus faecalis*, *Streptococcus pneumoniae* and *Staphylococcus aureus, Baccilus cereus,* and less effective against Gram-negative strains such as *Escherichia coli*, *Haemophilus influenzae* and *Pseudomonas aeruginosa* (Usatheva *et al*, 2001). The phenothiaziniums, particularly dimethylmethylene blue (DMMB), methylene blue and toluidine blue O have been reported to eradicate highly resistant spores of various *Baccilus* species (Demidova & Hamblin, 2005). Several reports have demonstrated the photoeradication of *Helicobacter pylori*

using TBO (Milson *et al*, 1996) and MB (Choi *et al*, 2010). The photosensitizers had antimicrobial effect against *Mycobacterium fortuitum keratitis* (Shih & Huang, 2011) and oral pathogens *Actinomyces actinomycetemcomitans, Fusobacterium nucleatum, Porphyromonas gingivalis, Prevotella intermedia, Streptococcus sanguis* (Raghavendra *et al*, 2009), *Candida albicans* (Wilson & Mia, 1994) and *Streptococcus ssp*. (Wilson, 1993) both in planctonic form and as the part of a biofilm (Wilson *et al*, 1995). Consequently, the tricyclic dyes have been successfully used for dental cavities sterilization, proposed for treatment of periodontitis (Wainwright, 2003; Nastri *et al*, 2010; Biel, 2010), plaque-induced peri-implantitis, endodontic infections (Soukos & Goodson, 2011) and wound infections (Zolfaghari *et al*, 2009; Dai *et al*, 2009) caused by antibiotic resistant bacteria strains. Recently some attempts have been made to apply MB for combating the main cause of cystic fybrose – multidrug resistant lung pathogens (Cassidy *et al*, 2011). However, the situation had become more complicated after a few studies demonstrated the existence of active protein mediated efflux of phenothiaziniums from the cell. In other words, the dyes have been acknowledged to be the substrates for microbial multi-drug efflux pumps, thus staggering the generally accepted concept of bacterial inability to develop resistance to photosensitizer mediated eradication (Tegos & Hamblin, 2006a; Tegos *et al*, 2008). Taking into account, that efflux pumps are coded in bacteria genome, thus particular genetic elements can be inherited or spread inside pathogen populations and even beyond it, the intense use of phenothiaziniums may cause some bacterial resistance problems in the future. Therefore phenothiazinium application safety has to be investigated in more detail.

It is common knowledge that both TBO and MB have a similar chemical structure and most of photophysical properties. The only substantially distinguishing characteristic is the partitioning coefficient, which appears to be almost 3 fold higher for TBO than for MB, resulting in the greater

accumulation of TB molecules in the hydrophobic region of cellular membrane, therefore gaining a greater photobactericidal activity (Usatheva *et al*, 2001). Conversely, high water solubility of MB contributes to poor uptake of the compound. The uptake pathway depends on the type of bacteria involved in phenothiazinium-mediated photosensitization and can proceed either via diffusion through the envelope (more common for Gram-positive bacteria) or so called "self-promoted" penetration passage (typical to Gram-negative bacteria). The absence of any protein transporter involved in the uptake has been reported (George *et al*, 2009).

The size and planar shape of phenothiazinium-type chromophore, regardless of the substitution pattern, make them ideal nucleic acid intercalators, however, due to different partitioning coefficient, they localize in separate cellular compartments and their ability to damage DNA differs. It has been shown that after TBO accumulates in the outer membrane it is able to penetrate into plasma membrane and damage photolabile proteins (Bhatti *et al*, 1998) and LPS (Usatcheva *et al*, 2007), consequently TBO is membrane active (Wakayama *et al*, 1980), however slight breakage of DNA have also been reported, though it was considerably lower than demonstrated with MB-mediated photosensitization. Although MB effectively photodegrades isolated DNA (Bellin & Grossman, 1965), conditions for the dye interaction with DNA inside the cell are more complicated, since it require the penetration through cytoplasmic regions of bacteria. Therefore bacterial eradication efficiency with MB-mediated photosensitization is sufficiently lower comparing to TBO-mediated.

The situation of photosensitization efficiency reverses when viruses are concerned, MB is much more efficient in eradication of cell free viruses (particularly adenoviruses, HSV and influenza viruses) than TBO, which is not surprising taking into account their partitioning coefficient differences (Usatheva *et al*, 2001; Wainwright, 2004). The sites of damage involve viral envelope, viral core proteins such as reverse transcriptase and

viral nucleic acid, where various types of damage are inflicted upon irradiation, including base modification rather than direct strand breakage, and the formation of nucleic acid–protein crosslinks (Bachmann *et al*, 1995; Abe & Wagner, 1995; Wainwright, 2004). The wide range of lesions displayed by the MB-mediated viral photosensitization was so convincing, that encouraged several European transfusion services to apply MB for photodecontamination of blood plasma with particularly effective outcome (Lambrecht *et al*, 1994, Wainwright, 2004). However, for sufficient sterilization of blood preparations both extra- and intracellular viruses should be susceptible to the photodynamic agent. Unfortunately, MB would not be of use in the disinfection of red blood cell concentrates for it is much less effective against internalized viruses and causes significant membrane damage and hydrolysis of the red blood cell itself (Wainright, 2004). Moreover, as far as collateral effects are concerned, the dye also mediates photodamage to some plasma proteins, resulting in a drop of clotting factor activity (Wainwright, 1998). In order to eliminate MB drawbacks the compound undergone some chemical modifications such as methylation and demethylation, resulting in development of demethylated MB derivatives and dimethyl methylen blue with improved antiviral photosensitizing properties. Demethylated MB derivatives were found to be suitable for virus inactivation both in plasma and platelets preparations with lower collateral damage compared to MB (Wainwright, 1998). Other type of MB derivative dimethyl methylene blue (DMMB) represents a significant advance, being highly efficient against both extra- and intracellular viruses (Skripchenko & Wagner, 2000; Wainwright, 2004), however it is highly toxic to blood recipient. In the field of total blood product disinfection, an ideal candidate photosensitizer would need to be effective in the inactivation of bacteria, viruses, yeasts and protozoa, while being essentially non-toxic and non-mutagenic in a human recipient. It is hardly surprising, that none of the currently available agents (including MB) is completely satisfactory in all of these criteria (Wainwright, 2009). Although MB still remains the main

compound used for blood sterilization, phenotiaziniums are relinquishing their leading positions to macrocyclic photosensitizers such as porphyrins and phthalocyanines.

1.3.2. Macrocyclic photosensitizers

Most widely used and investigated photoantimicrobials belong to the group of macrocyclic photosensitizers. The parent form has a structure known as porphine, which is composed of four modified pyrrole subunits interconnected via methine bridges. The molecules represent aromatic highly conjugated system, which typically has intense absorption bands in the visible region of the spectra. The chemical structure of porphyrin derivatives may vary a lot because the hydrogen atoms localized in pyrrole rings and in methine bridges can be substituted by a wide range of various functional groups. The reduction of one or two double bonds in the macrocycle periphery gives rise to closely related compounds such as chlorins, bacteriochlorins and isobacteriochlorins along with a bathochromic shift in their absorption spectra comparing to parent porphyrin absorption (Pushpan *et al*, 2002; Rotomskis *et al*, 2002, Streckytė *et al*, 2008). Isomeric porphyrins, such as porphycen, are modified porphyrins obtained by scrambling the four pyrrolic subunits and the four bridging carbon atoms. Phthalocyanines are the porphyrin derivatives where four isoindolic rings are bridged by a nitrogen atom and this arrangement enlarge absorption intensity at longer wavelengths compared to parental compound absorption intensity at the same spectral region. The naphthalocyanines are obtained by fusing another benzene ring to the periphery of isoindolic ring of phthalocyanines. These compounds are absorbing light at still further wavelength compared even to phthalocyanines. The other porphyrin based photosensitizers such as texaphyrins, core modified expanded porphyrins etc. have been synthesized, however they are considered to be anticancer drugs and have not been applied for antimicrobial chemotherapy yet (Pushpan *et al*, 2002; Sternberg *et al*, 1998).

1.3.2.1. Porphyrins

Whereas azine derivatives evolved from vital staining, both in oncology and in microbial pathology, the use of porphyrins has originated from anticancer PDT (Wainwright, 2009). The first photosensitizer approved for clinical use namely hematoporphyrin derivative (HpD) in fact was the mixture of porphyrin oligomers and dimers interconnected by etheric and esteric bonds (Daugherty *et al*, 1984). Hematoporphyrin and its derivatives were entitled the first generation photosensitizers. However, the compounds had a lot of drawbacks which aggravated their utilization either in cancer or antimicrobial chemotherapy. Taking into account nonhomogenic structure of the first generation photosensitizers and the fact that physicochemical properties of monomers, dimmers or oligomers differ greatly, it is obvious that the photosensitization efficiency will vary in different biological milieu, where aggregated part of the photosensitizer can monomerize or change the aggregation type depending on the dye concentration, acidity, polarity and temperature of the milieu. All these factors make the prediction of the process proceeding and its efficiency very difficult if not impossible. Furthermore, non homogeneity of the compounds is a big obstacle for studying their structure, aggregated states and photosensitizing features (Rotomskis *et al*, 2002). In addition, hematoporphyrin derivatives have a low excitation to triplet state yield and a singlet oxygen generation yield, accordingly high concentrations of the photosensitizer are required to achieve desirable effect. However, applying increased concentrations of the dye is dangerous for the patient, since the excess of the photosensitizer may accumulate in adjacent tissues and cause permanent toxic effect (Streckytė *et al*, 2008). Obviously the poor physicochemical characteristics of hemathoporphyrin derivatives increased the demand for new improved photosensitizing compounds namely second generation photosensitizers with reduced or eliminated drawbacks typical to the first generation photosensitizers and stimulated their synthesis and studies. The new generation photosensitizers belong to homogenic tetrapyrrolic

compounds of well defined structure characterized by better absorption in red part of the spectrum, higher singlet oxygen generation yield, increased photostability and low dark toxicity. The scaffold of second generation macrocyclic photosensitizers is hydrophobic and hydrophilicity can be increased by addition of sulphonated, hydroxyl, alkoxy and other functional groups (Sternberg *et al*, 1998; Rotomskis *et al*, 2002; Wainwright, 2009). A further enhancement in the photoinactivation activity was obtained by the insertion of the spacer, such as propoxy bridge, between the macrocycle and charge bearing (particularly cationic) groups, though providing higher flexibility of the molecule and facilitating the orientation of functional groups for a tighter binding to charged (generally anionic) groups placed on bacterial surface (Jori *et al*, 2006).

Porphyrins are the most extensively studied group of photosensitizers and numerous reports on efficiency of different derivatives have been published in the last few decades. Although it is difficult to compare the results of reports, because in the absence of standard protocol the experiments were performed under different conditions, however, some consistent pattern can be pointed out. It was demonstrated that the photosensitization efficiency against different bacteria type correlated with the charge of the dye molecule. According to the results obtained by various groups of researches the neutral or anionic charge bearing derivatives of porphyrins exhibit photoeffect only on Gram-positive bacteria (such as *Staphylococcus aureus, Streptococcus faecalis, Bacillus cereus, Clostridium perfringens, Bacteroides fragilis, Enterococcus seriolicida* and others), but are incapable to eradicate Gram-negative species (such as *Escherichia coli*, *Pseudomonas aeruginosa, Vibrio anquillarum*) and yeasts *Candida albicans*, unless some cell envelope permeabilising agents are employed. Conversely, the cationic derivatives even in the absence of additives were generally more photoactive against Gram-negative species both planctonic and residing in biofilms than the anionic or neutral porphyrins (Merchat *et al*, 1996; Jori &

Coppellotti, 2007; Dai *et al*, 2009; Engelhardt *et al*, 2010; Collins *et al*, 2010). The most extensively studied neutral porphyrin type photosensitizers are tetrahydroxyphenilporphine (THPP), anionic compounds include 5,10,15,20-tetra(4-sulphonatophenyl)porphine ($TPPS_4$), and there is a great variety of cationic compounds, namely *meso*-substituted porphyrins such as 5,10,15,20-tetra(4-N-methylpyridyl)porphine (TMPyP), tetra(4N-methylpyridyl)porphine tetraiodide (T_4MPyp), tetra(4N,N,N-trimethyl-anilinium)porphine tetraiodide (T_4MAP) (Nitzan *et al*, 1995; Merchat *et al*, 1996; Jori *et al*, 2007; Dai *et al*, 2009; Wainwright, 1998, 2009). Data on relationship among the number of cationic charges and photosensitization efficiency against Gram-positive and Gram-negative bacteria appeared to be rather controversial in the case of cationic porphyrins. Some studies have shown that the number of charges does not affect the activity of photosensitizer (Merchat *et al*, 1996), other studies reported contradictory results, that increasing number of charges located on the photosensitizer peripheries has the positive effect on the photosensitization activity of the compound (Caminos *et al*, 2006). Moreover, charge distribution and nature of *meso*-substituted groups are of importance for photosensitization efficiency. It has been assumed that charged groups localized in adjacent positions make the compound more efficient than the same groups transferred to the opposite positions. Additionally, a high number of positive charges increases hydrophilic character of the molecule but decreases efficiency, and *vice versa* positive charges combined with highly lipophylic groups may enhance dye affinity to bacteria, however direct correlation can not be established in every particular case (Alves *et al*, 2009). The role of growth phase in photosensitization efficiency is the second controversial topic. Some authors acknowledged the certain degree of resistance to photosensitizers of stationary phase cultures, whereas others witnessed its independence from physiological state (Banfi *et al*, 2006). In addition, it was proposed that microbial cells growing in colonies appear to be more resistant than cultures grown in suspension in liquid media (Quiroga *et al*, 2010).

In spite of extensive knowledge of porphyrins and their properties only protoporphyrin IX (PPIX) precursors ALA or MAL are clinically approved for treating of infectious diseases, such as microbial skin infections caused by nosocomial colonization of the skin by multi-resistant bacteria and particularly acne vulgaris (Gold, 2007; Dai *et al*, 2009; Hörfelt *et al*, 2009; Maish *et al*, 2004, 2010). Some attempts to treat osteomyelitis and gastric *H. pylori* infections were also fairly successful, furthermore *H. pylori* appeared to produce a high amount of porphyrins without the addition of precursor, exhibiting high initial susceptibility to irradiation. The researches, designed to explore the utilization of other porphyrin derivatives in photosensitized antibacterial chemotherapy, revealed their potential to treat burn wound infections (Orenstein *et al*, 1998; Dai et al, 2010), and localized infections such as brain abscess (Hamblin & Hasan, 2004) as well as blood plasma sterilization (Lambrechts *et al*, 2005), however toxicological and safety studies are very expensive and a wide variety of porphyrin type photosensitizers are still under investigation.

Although numerous porphyrinic compounds are not used in clinic, the interaction between targeted cell and photosensitizer is being subjected to extensive studies. It has been demonstrated that only those photosensitizer molecules that are interacting with the inner membrane of the microbial cell, are effective in promoting phototoxic effects, because of short lifetime of highly reactive transients generated upon irradiation and protective features of outer membrane layer typical for Gram-negative bacterial cells (Jori & Coppellotti, 2007). The peptidoglycan layer in Gram-positive bacteria does not represent a strict permeability barrier for macrocyclic photosensitizers and it can readily be crossed by diffusion, consequently reaching inner membrane (Jori & Coppellotti, 2007). Obviously the situation is more complicated when Gram-negative bacteria are concerned. Although the application of anionic and neutral photosensitizers is feasible due to employment of cell envelope permeabilising agents, the cationic photosensitizers are capable to make their

way into the cell by "self-promoted uptake" pathway (Maish *et al*, 2004). Porphyrin precursor ALA is actively taken up into the cells by the dipeptide permease tansport system (Vercamp *et al*, 1993). Upon usual ALA metabolism in the cell, the compound is converted to the porphyrins and the excess of these compounds have been shown to be exported from the cell by TolC-dependent efflux system (Tatsumi & Waschi, 2008), thus protecting bacteria from severe photosensitization damage upon irradiation. The inability of efflux systems to cope with the huge excess of porphyrins accumulated inside the cell, when high concentrations of artificially added ALA are present in close vicinity of bacteria, usually results in damaging cell inner compartments particularly inactivation of intracellular proteins, ribosomes and mutagenic effect on cell genetic material, leading to the cell death (Nitzan *et al*, 2004; Fotinos *et al*, 2008). Unlike hydrophilic ALA, amphiphilic nature and extensive molecular mass of ready-synthesized porphyrins and their derivatives aggravates photosensitizer penetration into the cell, generally restricting the photodynamic activity to external regions of the cell. Although the porphyrins have been reported to accumulate in the envelope of the cell, the photosensitized damage does not confine to the membrane damage, but also involves damages to intracellular components, thought to the lesser extent (Jorri & Coppellotti, 2007).

Unlike utilization of porphyrinic compounds in photodynamic antibacterial chemotherapy, the use of photosensitizers as antivirals has been slow in gaining acceptance, although the photodynamic effect against viral targets have been demonstrated. Porphyrins such as haematoporphyrin derivative and dihaemathoporphyrin ether as well as porphyrin precursor ALA have been found to exhibit antiviral activity against papillomavirus infection (Bauman & Smith, 1996). Benzoporphyrin derivative has been tested against HIV in blood and is reported to be more selective than methylene blue against intracellular virus (North *et al*, 1993). Alkylated porphyrins have been demonstrated to be efficient against HBV, HCV and showed some antiviral

effect against such exotic viruses as Dengue, Marburg and Junin viruses (Guo *et al*, 2011). As a consequence of little popularity of the porphyrins in antiviral chemotherapy, merely innumerous reports published in this field, especially little attention is given to the site of damage inflicted upon irradiation. It is usually assumed that the porphyrins resemble close related chlorins and cause photodamage to viral envelope (North *et al*, 1993).

1.3.2.2. Phthalocyanines

Formally, phthalocyanines are tetrabenzotetraazaporphyrins. Unlike the general group of porphyrins their pyrrole rings are linked by nitrogen atoms instead of methine bridges. The extension of a molecule by fused benzene rings in the periphery of macrocycle results in increasing of aromatic character and consequently more intense near-infrared absorption of these compounds compared to that of parent porphyrin nucleus. Similarly to other photosensitizer groups a wide range of compounds are available due to modification of phthalocyanine chemical structure: such as introduction of substituents in the peripheral positions of tetraazaisoindole macrocycle, coordination of metal ions with the central nitrogen atoms and the addition of axial ligands (Segalla *et al*, 2002; Wainwright, 2009). The nature of incorporated metal ion significantly influences photophysical properties of phthalocyanines. Complexes with Zn^{2+}, Al^{3+}, Ga^{3+} are characterized by higher triplet state quantum yield and prolonged lifetime, therefore they are approved as the best photosensitizers among phthalocyanine type compounds (Rotomskis, 2002). By contrast, incorporation of Fe^{2+}, Cr^{2+}, Ni^{2+}, Cu^{2+} decreases phthalocyanine triplet state lifetimes and such compounds appear to be unsuitable as photosensitizers (Wainwright, 2009). The incorporation of various polar groups helps in attaining greater solubility of the compounds in the polar milieu (Wainwright, 2009). However, the aggregation of phenothiazinium molecules in the aqueous milieu is a very common phenomenon in this family of compounds due to their large π-conjugated

systems. The forming of aggregates dramatically shortens the lifetime of triplet state, herewith decreasing singlet oxygen generation quantum yield, therefore the photosensitizing activity of dimers and aggregates is significantly lower (Atsay *et al*, 2009) than that of monomers, which produce higher yields of singlet oxygen compared to standard photosensitizers such as methylene blue (Griffiths *et al*, 1997). The aggregation is less likely in three-dimensional structures rather than the planar shapes, therefore situation may be improved using multiple bulky ring substituents or similarly charged groups. As the presence of such a high charge may undesirably increase hydrophilicity, it is advisable to add some lipophilic groups, providing molecules with regions of different hydrophilicity/lipophilicity and warranting effective solubility along with efficient uptake into the cell (Wainwright, 2009). However, it is important to note that microenvironment also makes a substantial contribution to aggregation along with efficiency and mechanism of phthalocyanines-mediated photosensitization process, it is especially evident in complex biological systems with different physicochemical features and biochemical composition (Segalla *et al*, 2002).

Structure-activity relationship studies suggest that amphiphilic derivatives exhibit the greatest activity for Gram-positive bacteria and yeast, while more hydrophilic octa-substituted phthalocyanines, bind to Gram-negative bacteria (Jori *et al*, 2006). Phthalocyanines were demonstrated to be effective against microorganisms in planctonic state including Gram positive bacteria such as *Staphylococcus aureus*, *Streptococcus sanguis* (Wilson *et al*, 1996) *Streptococcus mutants, Streptococcus sobrinus, Lactobacillus casei* (Burns *et al*, 1994), Gram-negative bacteria such as *Escherichia coli, Pseudomonas aeruginosa* (Mantareva *et al*, 2010)*, Aeromonas hydrophila* (Kussovski *et al*, 2009) and yeast such as *Candida albicans* (Segalla *et al*, 2002; Mantareva *et al*, 2007; Mantareva *et al*, 2010) as well as against biofilms of mixed dental plaque derived strains (Wood *et al*, 1999). The research on susceptibility of bacterial stains derived from dental plaque biofilms revealed

that both aerobic and anaerobic bacteria are susceptible to phthalocyanines-mediated photosensitization, which could have significant clinical importance, particularly for treatment of infections caused by obligatory anaerobic periodontopathogenic bacteria. Series of cationic phthalocyanine derivatives have been patented for use against bacterial infections occurring in burn wounds (Dai *et al*, 2010).

Phthalocyanines, being related to porphyrins in chemical structure, share the same cell envelope penetration pathway. Any transport system which facilitates the envelope barrier passing has not been reported for the meantime. As the target sites in bacterial cell are concerned, the phenothiaziniums have been shown to interact with cell envelope and increase its permeability due to inflicted damage especially it is typical for cationic dye derivatives (Segalla *et al*, 2002; Spesia *et al*, 2009). Alternatively it is known that cationic phthalocyanines form complexes with nucleic acids and induce breaks upon irradiation as well as base oxidation (Spesia *et al*, 2009).

Additionally, some pthalocyanines have shown significant potential in the area of blood products disinfection (Ben-Hur & Horowitz, 1996). Although aluminium and silicon phthalocyanines were demonstrated to be efficient against HIV, the cationic silicon phthalocyanine was not only active against cell-free HIV, but also against the actively replicating virus and latently infected red blood cells, although with some collateral damage (Allen et al, 1995; Wainwright, 2009). It is generally assumed that there is no general correlation between antiviral potency and the central atom of the phthalocyanine. Conversely, the degree of phthalocyanine sulphonation and butylation has been reported to affect both the antiviral activity and the extent of haemolysis (Wainwright, 2009). The increased susceptibility of enveloped viruses suggested that the viral envelope may be a target for phthalocyanine-mediated photosensitization (Wainwright 2009). It was more substantially demonstrated when the changes in structural proteins of HSV envelope have been discovered (Smetana et al, 1998). Despite all the positive results obtained,

the utilization of phthalocyanines neither for blood sterilization nor for multidrug resistant or biofilm forming bacteria eradication has not gained clinical approval yet.

1.3.2.3. Chlorins

The chlorins is another porphyrin-like photosensitizer group, rapidly gaining popularity in photosensitized antimicrobial chemotherapy over the past decade. The main characteristics already described for porphyrins and phthalocyanines are typical also for chlorins, but then it is important to revise some special points of chlorin-mediated photosensitization to complete the picture of bacterial photosensitization. The chlorins (e.g. chlorin e6) are superior to standard HpD-type photosensitizers in several ways such as higher triplet state generation yields, or stronger red light absorption, which render them better photosensitization efficiency (Wainwright, 2009).

Distinctly from cancer photodynamic therapy, where a great variety of chlorines have been examined, very few chlorines, particularly ce6, its derivatives and conjugates with antibodies or policationic compounds have been extensively studied in antibacterial photodynamic inactivation field. It was demonstrated that chlorin ce6 and its conjugates with polilysine (pL-ce6) exhibited different efficiency against various strains of Gram-positive *Streptococcus*, *Staphylococcus aureus* and Gram-negative *Porphyromonas gingivalis*, *Actinobacillus actinomycetemcomitans*, *Bacteroides forsythus*, *Escherichia coli,* accordingly free ce6 inactivated only Gram-positive bacteria, whereas the polycationic chain was necessary to mediate killing of Gram-negative bacteria and likewise eradication of Gram-positive bacteria (Rovaldi *et al*, 2000; Tang *et al*, 2007). Furthermore, the polylysine chain length had crucial effect on capability to inactivate Gram-negative bacteria, hereby the conjugates with higher cationic charge (composed of 37 lysine residues) significantly improved photosensitization efficiency (Hamblin *et al*, 2002). It was also demonstrated that the amount of polycationic chlorine conjugate

taken up by bacteria cells exceeded the amount of conjugate bound to eucaryotic cells, suggesting good perspectives in eliminating undesirable side effects in clinical application (Soukos *et al*, 1998). However, in spite of very encouraging results obtained *in vitro*, there are numerous problems to be solved before chlorins can be applied to the clinics. The attempts to use both free chlorine ce6 and conjugated photosensitizer form for treating soft tissue infections in animal models resulted in regrowth of the infecting bacteria after the treatment (Gad *et al*, 2004). Another problem which was encountered during the studies is susceptibility of the conjugate to proteolytic activity of the enzymes present in the infected areas of tissue. The polylysine substitution to polyethylenimine in conjugates with ce6 resulted in a new efficient photosensitizer, resistant to proteolytic activity, however this feature hindered removal of the conjugate from the tissue after completion of the illumination (Tegos *et al*, 2006b). In the course of further structure developments, conjugates of tin(IV) chlorine e6 with specific or non specific monoclonal antibodies have been designed and tested against *Pseudomonas aeruginosa* infections in mice. The chlorine conjugates with specific antibodies showed convincing antibacterial activity, while normal bacteria growth was observed in animals that were treated with conjugates including non specific antibodies (Bertiaume *et al*, 1994). Furthermore, the immunoconjugates specific to *Staphylococcus aureus* have been reported to exhibit high efficiency in killing the bacteria in all phases of growth, while conjugates with non specific antibodies were growth phase dependent (O'Riordan *et al*, 2005). In the light of available experimental data, chlorine conjugates have been successfully tested on Gram-negative bacteria formed biofilms in root canals of extracted teeth and periodontal infections (Meisel & Kocher, 2005; Dai *et al*, 2009), wound infections (Hamblin *et al*, 2003), soft tissue infections (Bertiaume *et al*, 1994; Dai *et al*, 2009), suggesting the considerable potential for treating these sometimes life threatening infections in the future.

Due to similar chemical structure and photophysical features, the targets of chlorins in bacterial cell do not differ from those of porphyrins and phthalocyanines. Alike in the case of porphyrins and phthalocyanines the damage to some membrane and inner cell components, possibly chromosomic DNA has been reported (Hamblin *et al*, 2002).

In spite of increasing amount of research on antibacterial features of chlorines and their conjugates, very few data concerning antiviral chlorine-mediated photosensitization are available (Gramdadam *et al*, 1995; O'Riordan *et al*, 2005). This group of photosensitizers has been reported to cause photodamage to viral envelope, resembling the antiviral activity of porphyrins and phthalocyanines (Wainwright, 2004).

In summary, there are enormous amount of available photosensitizers characterized by good photophysical properties, having high affinity to selected targets in bacterial cell, consequently exhibiting sufficient antibacterial efficiency, however very few of them are applied to clinics due to high cost of clinical trials and various problems encountered.

1.4. Photosensitizer – mediated photodamage inflicted to bacterial cells

Photosensitization is generally assumed to be a promising approach for combating bacterial infections. The main advantage of this technique is target multiplicity, which is enabled by the photosensitizer relocation to the deeper compartments of a cell upon irradiation, thus inflicting gradually increasing damage to biomolecules such as proteins, lipids, nucleic acids etc. Furthermore, the order of preference for modification of particular biomolecule depends upon a number of factors, such as location of the photosensitizer, ROS production efficiency, relative ability of the biomolecule to be oxidised, and availability of metal ions. Amino acid residues, particularly those of cysteine, methionine, tyrosine, histidine, and tryptophan are the primary targets of an oxidative attack on proteins (Santus & Reyftmann, 1986). The reaction mechanisms are rather complex and lead to a number of final

products. Cysteine and methionine are oxidized mainly to sulfoxides, histidine yields a thermally unstable endoperoxide, tryptophan reacts by a complicated mechanism to give *N*-formylkynurenine, tyrosine can undergo phenolic oxidative coupling (Berlett & Stadtman 1997; Stadtman & Levin, 2003). Unsaturated lipids typically undergo ene-type reactions to give lipid hydroperoxides, however it is not so common for bacteria comparing to eucaryotic cells (Hussain *et al*, 2006). DNA can be oxidatively damaged at both the nucleic bases and at the sugars resulting in DNA base oxidative damage, strand breaks and DNA-protein cross-linking (Castano *et al*, 2004). The mutagenic potential varies depending on the type of a cell, possibly reflecting differences in repair capability or damage surveillance mechanisms. The living cells have acquired a number of defence mechanisms to combat attack from ROS and free radicals. The simplest type of defence are antioxidants such as vitamin C and vitamin E, which intercept free radicals, becoming radicals themselves, albeit much less reactive, therefore decreasing damage to cellular biomolecules. More complex oxidative stress defence strategies involve enzymes such as superoxide dismutase, catalase and glutathione peroxidase, which have evolved to limit the levels of ROS (Farr & Kogoma, 1991). Despite the fact that all cells have some capability of preventing and repairing the oxidative damage to various cellular components, excess of the oxidative stress leads to severe damages, mutations and consequently cell death (Castano *et al.*, 2005). Although, the detailed mechanism of the photosensitized bacterial cell killing is still under investigation, the hypothesis on the most plausible course of events has been already presented. (Jori & Coppelloti, 2007). The alterations of bacterial envelope and genetic material were the most extensively studied items, for they were supposed to be the general points in bacterial cell eradication. Although, the recent findings rendered them a different importance to evoke the cell death, the available facts about the damage of these two essential bacterial structures need to be discussed in detail.

1.4.1. Cell envelope damage

Gram-positive and Gram-negative bacteria are characterized by large differences in their subcellular organization, which has obvious influence in modulating the interaction of such cells with externally added chemotherapeutic agents including photosensitizers (Jori *et al*, 2006). The cells of both bacteria groups are covered by a plasma membrane and a cell wall which differs in permeability determined by the distinct composition of the wall. As shown in Fig. 1.6. Gram-positive bacteria are surrounded by 15-80 nm thick cell wall containing up to 100 peptidoglycan layers which form a mesh traversed by negatively charged teichoic acids, some of them anchored in a plasma membrane by a lipid anchor, thus denoted lipoteichoic acids (Salyers & Whitt, 2001).

It is generally accepted that such arrangement of the cell wall displays high degree of porosity and can carry out "molecular sieving" for relatively large molecules (up to 50-60 kDa) which have been found to readily diffuse to the inner membrane (Friedrich *et al*, 2000; Hamblin *et al*, 2002). Although it is obvious that the envelope of Gram-positive bacteria does not act as a strict permeability barrier, though in theory, some minor obstacles of electrostatic repulsion nature can be created for anionic compounds in the absence of Ca^{2+} and Mg^{2+} which usually bind to carboxylate groups (in proteins and peptidoglycan cross-links) and phosphate groups (in lipoteichoic and teichoic acids) neutralizing their anionic charges (George *et al*., 2009).

However, this problem has been neither widely discussed, nor encountered in experimental work. The situation becomes more complicated when Gram-negative bacteria are concerned, since they posses an additional 10-15nm thick outer membrane with heterogenous composition, situated external to the thin layer of peptidoglycan (Jori & Coppellotti, 2007). The inner leaflet of outer membrane consists of phospholipids, whereas the outer leaflet is composed of densely packed lipopolysaccharides, whose negatively charged polysaccharide portion is exposed to the cell surface (Salyers & Whitt, 2001).

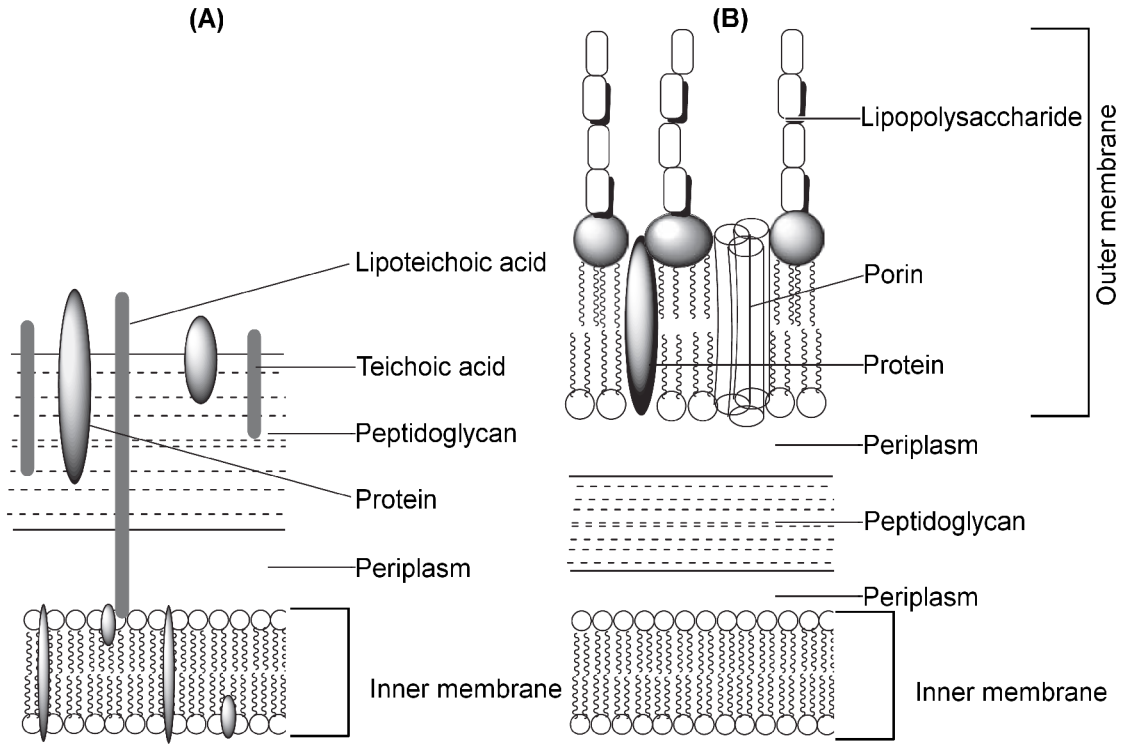

Fig. 1.6. The structure of Gram-positive (A) and Gram-negative (B) bacteria envelope. The picture taken from Wainwright, 2009.

Divalent cations (Mg^{2+}, Ca^{2+}) intercalated between LPS molecules are crucial for the stability of OM structure, as they prevent repulsion between the negatively charged phosphate groups of adjacent LPS molecules (Nikaido, 2003). In addition to neutralization of negative charges by divalent cations, interactions between fatty-acid chains and between the sugar components allow LPS to be compacted, giving the OM a highly organized arrangement that is crucial for its barrier function. (Nikaido, 2003; Ruiz *et al*, 2006). Consequently, the intact outer membrane of wild-type Gram-negative bacteria is impermeable to macromolecules and does not allow diffusion of hydrophobic substances due to lipopolysaccharide (LPS)-covered surface and the lack of glycerophospholipids, the effective channels for hydrophobic diffusion. Small hydrophilic compounds diffuse through the OM via the water-filled porin channels, but the narrowness of these channels remarkably restricts their diffusion (Vaara, 1992), only compounds with a molecular weight lower than 600-700Da can penetrate into the cell through porins (Nikaido, 2003). It is

generally accepted that the permeability of the cell wall, particularly outer membrane, is crucial for the efficiency of photosensitization process. It was assumed that the organization of lipid layers either stops any photosensitization intermediate products such as singlet oxygen or hydroxyl radicals from being transported through these layers and reaching sensitive target sites within the Gram-negative cell or acts as buffering targets or quenchers of the singlet oxygen. (Nitzan *et al*, 1992; Ehrenberg *et al*, 1985). It is obvious that photosensitization generated reactive species diffuse short distances before they are deactivated, consequently the dye localization adjacent to the target is critical to photoinactivation of the bacterial cell (Malik *et al*, 1992; Soukos & Goodson, 2011), thus it is not enough to disturb the outer membrane structure alone to kill bacteria cell, the cytoplasmic membrane structure must be damaged as well. (Nitzan *et al*, 1992). Obviously, such features of the outer membrane as restricted transport of hydrophilic compounds, negative charge of the cell surface and capability of the outer membrane to stop any photosensitization intermediate products from reaching sensitive target sites within the cells, explain the resistance of Gram-negative bacteria to photosensitized inactivation, particularly applying neutral and negatively charged photosensitizers with higher molecular weight.

The specific approaches developed in order to enhance the permeability of the outer membrane and subsequently increase the photosensitization efficiency against Gram-negative bacteria include the addition of membrane-permeabilizing agents: EDTA (Bertoloni *et al*, 1990) or PMBN (Nitzan *et al*, 1992; Nitzan *et al*, 1995), the association of the photosensitizer molecules with polycationic compounds (Hamblin *et al*, 2002), as well as the use of cationic photosensitizers (Alves *et al*, 2009) or precursors of photosensitizers such as ALA (Nitzan *et al*, 2004; Szocs *et al*, 1999). Some of those strategies are related (though not identical) in the principle by which photosensitization efficiency is increased. The addition of metal chelator ethylenediaminetetraacetic acid (EDTA) was found to cause the displacement

and, respectively, the removal of Mg^{2+} and Ca^{2+} ions which neutralize the superficial negative charges: as the consequence electrostatic repulsion is promoted with destabilization of the outer membrane native organization, inducing the release of a large fraction of the lipopolysaccharides into the medium (Vaara, 1992, Jori *et al*, 2006). It was reasonable to suggest that the loss of LPS will lead to appearance of phospholipids in the outer leaflet of the OM, since EDTA induced massive and instantaneous loss of LPS must be compensated. The formed phospholipid patches would then act as channels through which hydrophobic compounds can diffuse. EDTA is usually applied together with Tris solutions which also facilitates LPS release by replacing Mg^{2+} and Ca^{2+} (Vaara, 1992). In contrast, polymyxin derivative which lacks the fatty acid tail – polymyxin B nonapeptide (PMBN) does not cause the release of LPS. It was proposed that upon binding to LPS, PMBN increases the permeability via expanding the outer leaflet of the OM, thus altering the physical structure of the OM bilayer. Clearly in such expanded layer the hydrocarbon chains may become less "crystalline" and allow the partition of hydrophobic molecules from the external medium. (Vaara, 1992; Malik *et al*, 1992). Even though these findings improve the susceptibility of Gram-negative bacteria to photodynamic therapy, it would be highly preferable for clinical applications to avoid the use of a chemical in addition to the photosensitizer. The further development started with the discovery that the addition of polycationic peptides to neutral photosensitizer molecules provides sufficient improvements due to electrostatic interaction between positive charge of connected polycationic part and negatively charged LPS. Originally the term 'self promoted uptake' was used to describe the uptake of cationic peptides across outer membrane of Gram-negative bacteria. The first step encompasses interaction of polycations with divalent cation-binding sites on the cell surface and since these peptides have much higher affinities for LPS compared with the native divalent cations Ca^{2+} and Mg^{2+}, they competitively displace the ions. Furthermore the displacement of divalent cations may weaken the

intermolecular interaction of LPS constituents, disorganize the structure and disrupt the normal barrier properties of the outer membrane, since the affected membrane is thought to develop transient "cracks" that permit the passage of a variety of molecules, including hydrophobic compounds and promote the uptake of the perturbing peptide together with bound photosensitizer (Hamblin *et al*, 2002). Similar "self-promoted uptake" mechanism has been proposed for positively charged photosensitizer molecules. The presence of positive charges enables the dye molecule to interact with negatively charged LPS moieties on the cell surface and neutralize them, thus presumably facilitating the relocalisation of the hydrophobic chromophoric portion of macrocyclic photosensitizer molecule into the lipid bilayer of the outer membrane (Jori & Coppellotti, 2007; Engelmann *et al*, 2007; George *et al*, 2009;). It has been reported that the depth of insertion along with photosensitization efficiency depends on the membrane physical parameters such as bilayer phase transitions and pH (Nitzan *et al*, 1987; Ricchelli & Jori, 1990; Ricchelli, 1995 Bronshtein *et al*, 2005). As the photosensitizer molecule is inserted deeper in the membrane, singlet oxygen is also produced in deeper sites of the bilayer and therefore has a higher probability of inflicting damage to a membrane residing target, consequently the photosensitizer is more efficient. The addition of δ-aminolevulinic acid (ALA) suggests very different approach of bacteria eradication to those mentioned above. It is well known that ALA – a precursor of endogeniously synthesized porphyrins – is actively taken up by cellular dipeptide permease, thus facilitating the penetration through the inner membrane. This approach, in contrast to exogenously added photosensitizers, offers wider abilities to destruct inner cellular components since reactive intermediates are generated inside the cell adjacent to DNA and important intracellular enzymes as well as destruction of the inner membrane (Ricchelli, 1995). The findings presented above clearly demonstrate the significance of photosensitizer localization in the cell, obviously the amount of damage

inflicted upon irradiation is higher if the dye is localized in close vicinity of the targeted site.

Although, the detailed mechanism involved in bacterial cell photokilling is still under investigation, some details of the cellular damage have been revealed by innumerous TEM and SEM studies, X-ray elemental microanalysis and electrophoretic analysis of proteins. However, the absence of standard protocol for photosensitization along with the application of photosensitizers of a different structure and homogeneity aggravates the summarizing of obtained results, which are rather sketchy. Photosensitized Gram-positive bacteria exhibited the elongated shape of a cell, irregular cell wall and a multivesicular-mesosome structure formed near the septum, which was attributed to disturbances in the synthesis of the membrane and cell wall by photosensitized reaction (Nitzan *et al*, 1992; Bertoloni *et al*, 1984), additionally, some cells showed asymmetrical septation (Nitzan & Ashkenazi, 1999). The damage of membrane residing ionic pumps, resulting in an efflux of potassium and magnesium, have already been reported (Nitzan & Ashkenazi, 1999 ; Malik *et al*, 1993). Furthermore, it has been suggested that such serious membrane damage is presumably leading to altered electrolytic balance and finally to osmotic shock and death of the cell (Bertoloni *et al*, 1984). The photosensitized damage of Gram-negative cells closely resemble that typical to gram-positive cells including the rupture of the cell envelope and the induction of disorders disabling the formation of the septum, as well as the malfunction of sodium – potassium pump resulting in increased levels of sodium inside the cell (Nitzan *et al*, 1992; Salmon-Divon *et al*, 2004; Nitzan & Ashkenazi, 2001). Both inner and outer membrane proteins appear to exhibit a different susceptibility to photosensitized inactivation, transmembrane sites being more protected from photodamage than protruding lipid bilayers or proteins only connected but not residing entirely in the envelope (Valduga *et al*, 1999). The protective features of lipids constituting prokaryotic membranes have been attempted to explain by the lack of polyunsaturated fatty acids in

their composition, resulting in less susceptibility to lipid peroxidation comparing to eukaryotic cells Martin & Logsdon, 1987; Tuite & Kelly, 1993). In addition, photosensitizer-mediated photodamage is not confined to the cell envelope, but expands further to cytoplasmic regions where aggregation of ribosomal complexes (Nitzan & Ashkenazi, 1999) and other cytoplasmic macromolecules (Spesia *et al*, 2009) as well as the disturbances of nucleic acids have been reported (Nitzan et al, 1992; Nitzan & Ashkenazi, 2001).

1.4.2. DNR damage

It has been demonstrated that cellular DNA damages produced by intermediates of type II reactions occur with significantly higher yield than those produced by type I reactions. The application of quenchers revealed that singlet oxygen is the ultimate DNA damaging species in photosensitization reactions, however slight traces of superoxide, hydrogen peroxide, hydroxyl radical participation in the process also have been observed. Therefore, the DNA damage resulting from both types of photosensitized reactions need to be discussed in parallel (Tuite & Kelly, 1993; Chatterjee *et al*, 1997). It was assumed that the heterocyclic bases and sugar scaffold are two main targets for nucleic acid oxidation by ROS and radicals generated in photosensitization process. Free radicals (particularly $^{\bullet}OH$) react with heterocyclic bases either by adding to the most electron dense sites, resulting in pyrimidine-OH adduct radicals, or through the abstraction of hydrogen atom from methyl groups, resulting in allyl radicals. Heterocyclic base OH-adduct radicals and allyl radicals are further oxidized or reduced (depending on their redox properties and the environment) yielding a variety of products (Evans *et al*, 2004). $^1O_2$-mediated heterocyclic base oxidation is specifically caused at guanine, since it has the lowest redox potential of the four DNA bases and therefore is most readily oxidized. The final products are generated through formation of unstable endoperoxide which undergoes complicated sequence of reactions to give 8-oxo-7,8-dihydroguanine (also known as 8-oxodG) and 2,6-diamino-4-

hydroxy-5-formamidopyrimidine (FapyGua) (Sies & Menck, 1992, DeFedericis *et al*, 2006). 8-oxodG can further mispair with adenine leading to G → A transversion which is easily converted to mutation while replicating DNA (Cavalkante *et al*, 2002). In the case of sugar scaffold damaging, $^{\bullet}OH$ abstract an hydrogen atom from the carbon atoms in the sugar moiety of DNA, resulting in radicals, which undergo further reactions to yield a variety of sugar modifications and DNA strand breakage. Some sugar products are released from DNA as free modified sugars, whereas others remain within DNA or constitute end groups of broken DNA strands (Evans *et al*, 2004). $^1O_2$ -mediated DNA modifications also lead to formation of alkali-labile sites along with DNA strand breaks, which contribute to overall DNA degradation. While the direct cleavage reactions occur equally on both strands of the isolated duplex DNA, the yield of alkali-labile sites varies with the guanine content of the strand. It suggests that guanine bases available for attack rather than the amount of singlet oxygen produced upon irradiation is the limiting factor (Croke *et al*, 1993). DNA hydration level appeared to be important for protonation/deprotonation of heterocyclic bases and sugar moieties, which are required for formation of single strand breaks and base release (Seah & Burgoyne, 2001). More complex damages such as covalent DNA–protein cross-links are formed by mechanisms involving the addition of a DNA base radical to an aromatic amino acid of proteins or the combination of DNA base radical with an amino acid radical, however, they are more typical to eukaryotic cells where chromatin is present in close vicinity to DNA (Evans *et al*, 2004). The removal and repairing of DNA lesions, particularly purine and pyrimidine-derived base lesions by cellular repair systems are crucial for survival of the cell, since the failure to repair these lesions lead to mutagenesis and consequently cell death.

It is assumed that only cationic charge bearing photosensitizers can interact with DNA and subsequently damage it. Cationic molecules have been reported to bind the DNA in three distinct ways, namely intercalating into

DNA base pairs, binding to external groove and external binding with self-stacking. The binding types can be readily distinguished according to several spectroscopic characteristics, biochemical features and constants (Sari *et al*, 1990; Munson & Fiel, 1992; Kang *et al*, 2005; Wang et al, 2008):

■ First characteristics, denoted specially for porphyrin type compounds, comprise the absorption intensity and position of Soret peak in the spectrum. The red shift (approx 10nm) and decrease of the Soret peak is typical to intercalation, whereas no (or minor) changes of the absorption spectrum are seen if the photosensitizer binds externally to the groove. External binding to polynucleotides or DNA with self-stacking are characterized by red shift and decrease of the porphyrin Soret peak especially in solutions with high ionic strength. This type of interaction was proposed for porphyrins having a marked tendency to aggregate. Such photosensitizers appeared to bind externally and form long-range stacked structures

■ Clear decrease of the intensity of fluorescence emission and excitation spectra is observed if the dye is intercalating, though no (or minor) changes of the photosensitizer fluorescence spectra are seen in the case of external groove binding.

■ A 2- to 4-fold increase of fluorescence quantum yield for an excitation around 260 nm corresponding to an energy transfer between DNA and the photosensitizer is a feature of intercalation and obviously no energy transfer between DNA and photosensitizer can be seen if the dye is binding to the groove, since the distance between a dye molecule and DNA is too big for energy transfer.

■ Intercalation of the dye usually lengthens the DNA molecule, whereas other binding types do not.

■ Photosensitizers capable to intercalate into DNA base pairs have sufficiently higher DNA binding constants comparing to the constants typical to externally binding dyes.

The binding type greatly depends on the nature of photosensitizer molecule and steric position of the functional groups. The main feature required for DNA intercalation is the planarity of the molecule, at least half of the molecule, in the case when porphyrinic photosensitizers are concerned (Sari *et al*, 1990). Only those molecules which can exist at least temporarily in a planar conformation can intercalate the DNA (Sari *et al*, 1990), whereas photosensitizers that cannot exist in such a conformation usually bind externally. Phenothiaziniums, being planar tricycles, favour intercalation type interaction with DNA, though porphyrinic compounds due to great variety of their derivatives can display all known types of interaction (Zupán *et al*, 2005**)**. Accordingly, porphyrins have been investigated more extensively comparing to other types of compounds, though some regularities of interaction share similarity with the interaction typical to other types of photosensitizers.

The photosensitizer structural features influencing the intercalating and nonintercalating DNA binding efficiency are adversative. The affinity for DNA is much higher for intercalating dyes and does not depend on number of cationic charges, however the position of positively charged pyridinium substituents (*meta- , para-* or *ortho-*) is crucial in determining both the mode and the strength of binding. Accordingly, *para-* substituted compounds freely intercalate since their substituents are capable of unhindered rotation, *meta-* substitution introduces the element of steric hindrance, though does not prevent intercalation, whereas *ortho-* substitution prevents intercalation because of strong hindrance to rotation of the ring substituents (Sari *et al*, 1990). The nonintercalating dyes have much lower affinity for DNA than intercalating photosensitizers, but it depends mainly on the number of cationic charges, whereas the position of substituents is of much lower importance. Additionally, the photosensitizers (particularly porphyrins) complexed with metals such as Fe(III), Co(III), Zn(II) and Mn(II) with axial ligands have been found to be incapable of intercalations, however those with metal ion such as Cu(II) or Ni(II) without axial ligands readily intercalate into DNA (Pasternack *et al*,

1983a, 183b). Moreover, the intercalation appeared to be sequence dependent both for phenothiazinium and porphyrin type photosensitizers, preferring GC containing sequences at low [photosensitizer]:[DNA] ratio and low ionic strength, whereas when [photosensitizer]:[DNA] ratio and ionic strength increases the mode of binding becomes more complex and involves both intercalation at GC sites and outside binding which occurs predominantly at AT sites in the case of porphyrins (Ford *et al*, 1987). Similarly, phenothiazinium type photosensitizers are shifted from a site in close contact with guanine further, possibly close to AT sites at higher ionic strength and presence of Mg^{2+} (OhUigin *et al*, 1987).

Cationic photosensitizers which are capable to interaction with DNA via electrostatic groove binding or external binding with self stacking are more efficient in strand scission of DNA compared to intercalating photosensitizers (Chatterjee *et al*, 1997). The most frequently used model for studying bacterial DNR strand scissions is plasmid DNA such as pBR322, which is more handy because of rather small size and multiple copies that are relatively easy isolated from the bacterial cells. It has been demonstrated that double-strand scissions are enhanced once the DNA has already undergone a single-strand scission, implying either free access of the reactive species ($^1O_2$) to the site of the first cleavage or plasmid with single strand break binds more photosensitizer molecules due to more flexible conformation. (Praseuth *et al*, 1986) It has been proposed that the nature of interaction between photosensitizer and DNA does not play the major role in the induction of second cleavage. Studies of DNA residing inside the cell at the moment of photosensitization revealed only plasmid DNA relaxation after prolonged irradiation, whereas chromosomic DNA was not affected. It was suggested that plasmid relaxation is associated with the damage of some other cellular components upon irradiation. Considering, that DNA superhelicity in bacterial cell is maintained by the equilibrium between ATP requiring supercoiling activity of DNR gyrase and the relaxing activities of DNA topoisomerases, two

possible explanations had been presented. The first was attributed to photosensitizer-mediated oxidation and inactivation of the cellular components involved in the maintenance of DNR superhelicity, the other proposed the depletion of ATP as a consequence of plasma membrane damage, resulting in broken equilibrium between both DNR conformation maintaining enzymatic activities (Horiuchi *et al*, 1984). However other mechanisms can not be completely ruled out since DNA relaxation was observed in the strain deficient in topoisomerase (Caminos *et al*, 2008). Only few reports describing DNA damage (such as presence of filamentous chromosomes and aggregates attributed to DNA-protein rich complexes) inside the cell observed in TEM micrographs have been published (Nitzan & Ashkenazi, 1999).

Although there are some controversial data on the main cause of bacterial cell death during photosensitization mediated by the most externally added photosensitizers (Salmon-Divon *et al*, 2004), most reports that discuss the photodynamic inactivation of bacteria generally agree that the cell envelope damage is a lethal event, whereas DNA modifications and subsequent damage occur at a later stage of the process. (Jori & Coppellotti, 2007).

2. MATERIALS AND METHODS

2.1. Photosensitizer

The photosensitizer tetrakis(N-ethylpyridinium-4-yl)porphyrin tetratosylate (TN-Et-PyP) was a generous gift from prof. R. Bonnett. It was prepared by treating tetra(pyridin-4-yl)porphyrin with ethyl *p*-tosylate in dimethylformamide using the general procedure of Pasternack and coworkers (Pasternack *et al*, 1972). The chemical structure of the porphyrin is shown in Fig. 2.1.

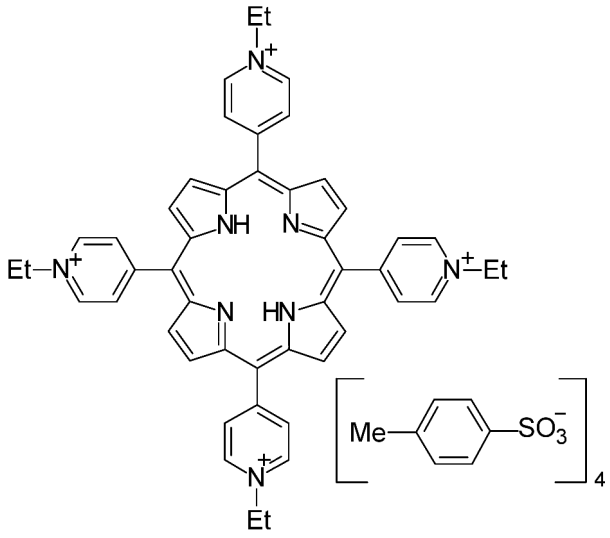

Fig. 2.1. Chemical structure of tetrakis(N-ethylpyridinium-4-yl)porphyrin tetratosylate (TN-Et-PyP).

Stock solutions of TN-Et-PyP were prepared in PBS (pH=7.3) at a concentration of 100 μM and stored at -20°C in the dark.

2.2. Plasmid DNA transformation, amplification

E. coli KMY1 strain was transformed with 5 μg pTz19 (length 2862 bp) using the modified procedure described by Cohen *et al* and Sambrook & Russell with application of ice-cold $CaCl_2$ and subsequent rising of the incubation temperature from ice cold to 42°C for 2 min (Cohen *et al*, 1972; Sambrook & Russell, 2001). After transformation procedure the cells were preincubated in 200 μl liquid LB before plating on LB agar with 100 μg/ml ampicillin and grown at 37°C overnight. The appropriate transformants have been selected after screening ampicillin resistant colonies.

2.3. Plasmid DNA purification.

600 ml overnight culture of selected *E. coli* KMY1 transformants were harvested by centrifugation (7500 g, 15 min) and resuspended in 30 ml TEG buffer (0.025 M Tris-HCl (pH=8), 0.01 M EDTA and 0.05 M glucose). The alkaline lysis with SDS procedure described by Sambrook & Russell (Sambrook & Russell, 2001) was applied with modifications. The lysozyme was added to the concentration of 5 mg/ml and the preparation was incubated for 10 min in 20°C before addition of 60 ml of another lysing solution consisting of 0.2 M NaOH and 1% SDS (alkaline lysis solution II in Sambrook & Russell). Afterwards the preparation was incubated on ice for 10 min and 45 ml of ice cold 5 M potassium acetate (pH=4.8) was added before incubating another 10 min on ice. After centrifugation (15000 g, 20 min) 0.6 volume of isopropyl alcohol was added to the supernatant and incubated for 1 hour at 20°C. After next centrifugation (15000 g, 20 min), the pellet was dried, resuspended in TE buffer and 1 volume of 9 M LiCl was added. The suspension was incubated for 3 hours at -80°C and centrifuged (15000 g, 10 min). The plasmid DNA was precipitated from supernatant with 2 volumes of ethanol, dried and resuspended in 300 μl of TE buffer. The purified plasmid DNA was evaluated electrophoretically and concentration was determined referring to the fact that OD_{260} = 1 corresponds to 50 μg/ml double stranded DNA in the tested solution. The samples were frozen for storage until the spectroscopic measurements were performed.

2.4. The preparation of phospholipid vesicles

Multilamellar lipid vesicles were prepared from commercially available phospholipids phospahatidylethanolamine (PE), phosphatidylglycerol (PG) and cardiolipin (CL) (Sigma). They were diluted separately in chloroform – methanol solution (9:1 v/v) and mixed in the molar ratio resembling the composition of *E. coli* plasma membrane, e.g. PE:PG:CL = 65:18:12 (Tanford, 1980). The vesicules were prepared as described by Cvirkaitė-Krupovič

(Cvirkaitė-Krupovič *et al*, 2010). In order to avoid aggregation or decomposition of vesicles, they were prepared immediately before spectroscopic measurements.

2.5. Preparation of LPS samples

Commercially available LPS (Sigma) purified by ion-exchange chromatography from *E. coli* O111-B4 was dissolved in PBS (pH=7.3) at the concentration of 10 mg/ml immediately before spectroscopic measurements.

2.6. Spectroscopic measurements

Instrumentation

Absorption spectroscopic measurements were made on fiber optics based spectrofluorimeter AvaSpec-2048 in a spectral range of 173-1100 nm. Fluorescence emission and excitation spectra were recorded by Perkin-Elmer spectrofluorimeter 55B. Both excitation and emission band-pass were set at 10 nm, scan speed was 200 nm/min.

Interaction studies

The interactions of cationic porphyrin with BSA, LPS, NA, lipids and SDS were studied by recording absorption spectra, while titrating 1.5 μM TN-Et-PyP solution in PBS (pH=7.3) with increasing concentrations of the mentioned compounds until no further changes in the Soret band position were observed. The experiments were carried out in a quartz cuvette (1.0 cm optic path length) with stirring. Buffer blanks were used to compensate for the dilution effect. The percentage of hypochromicity was counted from the equation:

$$[(OD_f - OD_b)/OD_f] \times 100$$ (Mettath *et al*, 1999)

OD_f and OD_b represent the optical density of the free porphyrin and the mixture of free porphyrin along with porphyrin bound to particular supplement, respectively.

More complicated experiments were performed with bacterial cells (both alive and heat inactivated) suspension in PBS (pH=7.3), which was mixed with the same amount of TN-Et-PyP (total concentration 1.5 μM) and irradiated with 415 nm LED at the increasing light dose up to 72 J/cm^2, maintaining the same stirring mode. In the next set of experiments, everything was repeated with some modifications: after irradiation the cells were harvested by centrifugation (15000 g, 15 min) and resuspended in sterile PBS. The absorption spectra of the obtained cell suspension and supernatant containing the larger portion of unbound porphyrin were recorded separately under the same conditions as they were registered for modelling systems. The scattering background was subtracted from the absorption spectra by Origin 7.5 software.

Fluorescence emission and excitation spectra have been obtained by titrating TN-Et-PyP solution in PBS (pH=7.3) diluted to optical density OD_{423} = 0.1 with selected concentrations of BSA, LPS, NA, lipids and SDS added in small increments to avoid significant dilution of the sample. 104F-QS, Hellma semi Micro fluorescence cuvette was used in order to create the conditions for the most possible even excitation of the sample and to minimize the optical filtering effect. The fluorescence emission was recorded in the range of 550-800 nm exciting the sample with light of several appropriate wavelengths (see the section “Appendix”). Fluorescence excitation spectra were registered at selected maximum values of emission wavelength (see “Appendix”). Fluorescence emission and excitation spectra for cell samples and supernatant (prepared as described above) were measured after diluting them to optical density OD_{423} = 0.1. Afterwards Origin 7.5 software was used both to subtract the scattering background from the spectra obtained and to analyse them.

2.7. Bacteria growth, photosensitization procedure and viability assay

Escherichia coli KMY1 strain (MK12 λRS45[Φ(emrK'-lacZ)] (Kato *et al*, 2000; Egushi *et al*, 2003) a generous gift from Prof. R. Utsumi (Kinki University, Japan) was used in this study.

Typically, *E. coli* KMY1 strain was plated on BHI agar and grown overnight. The cells were suspended in sterile liquid BHI media and harvested by centrifugation after 40 min (or one generation) incubation at 37°C. The pellet was washed twice with a sterile PBS (pH=7.3) solution and diluted in PBS to the concentration of $\sim 1x10^8$ colony forming units (cfu/ml) in a 96 well plate. The porphyrin was added to a final concentration of 0.1 μM, 0.25 μM, 0.35 μM, 0.5 μM, 0.75 μM, 1 μM , 1.5 μM, 1.775 μM, 2.5 μM, and 3.5 μM. The plate was incubated in the dark for 30 min at room temperature with shaking. After that, samples were irradiated with 415 nm LED or 400 nm LED at the dose of 20 J/cm^2. In order to measure the cell viability, samples were diluted in sterile PBS (pH=7.3) and plated in duplicate on solid BHI agar after irradiation. Colonies were counted after overnight incubation at 37°C. Each experiment was repeated three times.

2.8. TN-Et-PyP uptake studies

E. coli KMY1 cell suspension was prepared as described in the previous paragraph. The porphyrin was added in triplicate samples up to the concentrations of 0.25 μM, 0.5 μM, 1 μM, 1.5 μM, 2.5 μM, 3.5 μM. The samples were incubated in the dark for 30 min at room temperature with stirring. After incubation the samples were harvested by centrifugation (3000 g, 10 min) and washed from 1 to 3 times in PBS (pH=7.3). The pellet was resuspended in 1 ml of 2% aqueous SDS and left in the dark for 24 hours. The fluorescence emitted by each sample was measured after appropriate dilution in 2% SDS in the 550-720 nm wavelength range, excitation being 430 nm. The BCA assay ("Thermo Scientific" Pierce protein assay) was applied for

measuring the amount of protein in the samples. Uptake of the porphyrin by the cells was expressed in nanomoles of dye per mg of protein.

2.9. Sample preparation for TEM studies

E. coli KMY1 strain was plated on BHI agar and grown as described above. Bacteria were diluted in sterile PBS (pH=7.3) to the concentration of ~ $5x10^8$ cfu/ml after washing and TN-Et-PyP added to a total concentration of 0.25 μM and 1 μM. The samples were incubated in the dark for 30 min at room temperature with stirring. After incubation the samples were irradiated with 415 nm LED (dose 20 J/cm^2). After the treatment the cells were harvested by centrifugation (3000 g, 10 min) and washed with PBS, fixed with 3% glutaraldehyde, which was prepared in 0.1 M cacodylate buffer (pH=7.2) for 30 min. The samples were washed twice in 0.1 M cacodylate buffer (pH=7.2) before fixation with 1% osmium tetroxide. Dehydration step was carried out by washing the sample twice in ethanol solutions, successively 50%, 70%, 95%, 100%. During the next step the samples were embedded in Epoxy Resin 812 and left for 24 hours at 60°C to polymerize. After cutting the samples into slices with an ultramicrotome, they were dyed with 50% uranyl acetate and 1% lead citrate (the procedure was designed with reference to Bozzola & Russell, 1999). Finally the samples were viewed and photographed by means of a transmission electron microscope Hitachi H600.

2.10. The evaluation of membrane integrity

Outer membrane permeability was monitored as cell lysis, the consequence of sodium deoxycholate income into the cells as well as the outcome of periplasmic alkaline phosphatase (described in the section "Enzymatic assays"). In order to determine the inner membrane integrity the cytoplasmic β-galactosidase activity was monitored as well as the release of material absorbing at 260 nm. The protein amount determined by BCA assay inside and outside the cell reflected the integrity of both membranes. The

method of outer membrane disruption evaluation with 0.5% sodium deoxycholate in PBS buffer (pH=7.3) described by J. A. Bengoechea. *et al* and R. Rasul *et al* was applied with some modifications. After photosensitization with 0.1 μM, 0.25 μM, 0.5 μM, 0.75 μM, 1 μM, 1.5 μM, 2.5 μM, and 3.5 μM TN-Et-PyP bacterial cells were washed up to 6 times with PBS (pH=7.3) before resuspension in sodium deoxycholate solution. The suspension was incubated at 37°C for 30 min and cell lysis was measured as a decrease in optical density at 600 nm. Polymixin B sulphate (50 μg/ml) was used for the estimation of the optical density of totally lysed cells.

2.11. Enzymatic assays

After photosensitization with 0.1 μM, 0.25 μM, 0.5 μM 0.75 μM, 1 μM, 1.5 μM, 2.5 μM, and 3.5 μM TN-Et-PyP, bacterial cells were harvested by centrifugation (15000 g, 15 min at 4°C) and the supernatants were analysed for enzymatic activity. The pellets were resuspended in PBS with protease inhibitor L-1-chlor-3-(4-tosylamido)-7-amino-2-heptanone-hydrochloride (TLCK) and sonicated for 30 min to release the proteins. After sonication the cell debris was separated by centrifugation (15000 g, 15 min at 4°C) and enzymatic activities were measured. β-Galactosidase and alkaline phosphatase activities were assayed using *o*-nitrophenyl-β-D-galactopyranoside and p-nitrophenylphosphate, respectively. The assays were modified from previously described techniques (Miller, 1972; Dean, 2002). The amount of proteins was determined by Pierce BCA protein assay according to manufacturer recommendations. The enzymatic activity was expressed as units per mg protein.

2.12. Release of compounds absorbing at 260 nm

The triplicate samples for monitoring the release of material absorbing at 260 nm and determining the protein amount were prepared as described in the section “Enzymatic assays”.

2.13. Measurements of electrochemical parameters

A particularly large amount of biomass is needed for electrochemistry assays, consequently the *E. coli* KMY1 strain was grown in LB medium at 37 °C with aeration to OD_{600} = 1.0; harvested by centrifugation (7500 g, 15 min) and concentrated in PBS buffer (pH=7.3) to obtain the stock solutions for measurements of the electrochemical parameters. The cells were kept on ice until electrochemical measurements were performed. Membrane voltage of bacteria cells was estimated as changes of tetraphenylphosphonium ions (TPP^+) concentration in the media. Briefly, measurements were performed by selective TPP^+ electrodes, elaborated in the Laboratory of Membrane Biochemistry, Vilnius University. The measuring system was calibrated at the beginning of each experiment by adding appropriate amounts of tetraphenylphosphonium chloride to 5 ml of 0.1 M Tris-HCl buffer (pH=8.0) with 10 mM EDTA placed into the measurement vessel thermostated at 37°C. The concentrated cell suspension was added to a final concentration of ~3 × 10^8 cfu/ml and, after reaching a steady state of ion flux in and out of the cells, TN-Et-PyP was added to a final concentration of 0.1 μM, 0.25 μM, 0.5 μM, and 1 μM. Irradiated and dark-incubated samples of each concentration were measured in parallel vessels. Irradiation took place directly in the measuring vessel with 400 nm LED source for a total light dose of 20 J/cm^2. Polymyxin B sulphate was added to the final concentration of 100 μg/ml in order to depolarize the plasma membrane and promote the efflux of TPP^+ ions from the cells at the end of experiment.

The evaluation of the bacteria respiration efficiency was performed in 2.2 ml volume chamber of a high resolution respirometry oxygraph – 2k from Oroboros Instruments, Austria. As it was impossible to irradiate the sample directly in the measurement system, irradiation was performed before estimating the consumption of oxygen. After TN-Et-PyP treatment *E. coli* KMY1 cells were diluted in 0.1 M Tris-HCl buffer (pH=8.0) to a final cell concentration of ~6 × 10^7 cfu/ml in the measurement vessel, in

order to ensure proper initial respiration rate. Uncoupler 2,4-dinitrophenol and glucose which was used as energy source for bacteria were added to final concentration of 2 mM and 0.1 M respectively. The experiments were repeated 2-3 times to make certain that the results obtained were reproducible.

3. RESULTS

3.1. Spectroscopic analysis of TN-Et-PyP interaction with different cellular components

Tetrakis(*N*-ethylpyridinium-4-yl)porphyrin tetratosylate (TN-Et-PyP) belongs to a well investigated group of tetracationic *meso*-substituted porphyrins, consequently is characterized by typical porphyrin-type absorption and fluorescence spectra (Rotomskis *et al*, 2002; Streckytė *et al*, 2008). However, the exact position of the peaks has individual character and varies depending on the structure of the porphyrinic compound. Since we are intending to explore the porphyrin interaction with cellular components by spectroscopic means, it is important to discriminate between spectroscopic features specific to TN-Et-PyP itself and features, occuring due to the porphyrin interaction with cellular components. Therefore, the first step of the work includes investigation of TN-Et-PyP spectroscopic characteristics in different milieu, pH and prolonged time of incubation.

3.1.1. TN-Et-PyP spectroscopy

The information concerning porphyrin molecular structure, aggregation and interaction with different molecules can be derived from the changes in the absorption spectrum, which is characterized by a slight absorption in UV region (γ band), a strong absorption band near 400 – 420 nm (Soret band) and several less intense bands observed in the visible region (450 – 700 nm), named Q bands. Since γ band often coincides with the absorption of different compounds (e.g. nucleic acids, some amino acids etc.), it is rarely used in analysis. Q bands are sensitive to the chemical structure of the photosensitizer (e.g. protonation, metal chelation etc.), while the Soret band changes reflect variations in the porphyrin aggregation state or interaction with the other molecules and complex formation (Rotomskis *et al*, 2002). The fluorescence spectra of the porphyrins are usually composed of two main bands, which intensity and maximum wavelength strongly depend on chemical

structure of the compound along with the nature of solvent. Fig. 3.1. illustrates the influence of solvent nature on the spectroscopic features of TN-Et-PyP.

TN-Et-PyP absorption spectra is composed of γ band with maximum at 260 nm, Soret band peaking at 423 nm, four Q bands with highest absorbance intensity (or optical density) at 519 nm, 555 nm, 585 nm, 646 nm in the aqueous PBS solution (Fig. 3.1. A), which will be used for bacteria suspensions in the further experiments. This type of Q bands' arrangement is called phyllo-type (Q band intensity changes respectively IV>II>III>I). Addition of SDS to aqueous PBS solution results in Soret band shift to 430 nm and Q bands to 591 nm, 557 nm, 594 nm, 648 nm still maintaining phyllo-type arrangement (Fig. 3.1. C and insertion). However, when the photosensitizer is dissolved in ethanol, which is known to disrupt porphyrin aggregates, Soret band peaks at 426 nm, Q bands at 516 nm, 555 nm, 591 nm and 645 nm and the arrangement type changes to aethio-type with Q band intensity decreasing in IV>III>II>I order (Fig. 3.1. E and insertion).

The differences in fluorescence spectra are also obvious (Fig. 3.8. B, D, F): the two typical porphyrin peaks are clearly defined in both ethanol solution and SDS at 665 nm, 715 nm and 662-1 nm, 716 nm respectively. However, it is not the case in aqueous PBS, where fluorescence emission spectrum is bell shaped, indicating that peaks are located very closely to each other. It clearly demonstrates interaction between porphyrin molecules occurring in PBS, which is in concert with the general rule, stating that most porphyrins exist as a mixture of monomers and aggregates in aqueous solutions (Rotomskis *et al,* 2002). In summary, the presented data show that the spectroscopic characteristics of TN-Et-PyP at a certain concentration are solvent dependent, possibly due to variation of ratio between monomers and aggregates. However, this suggestion is more theoretical since such a ratio was not investigated in details.

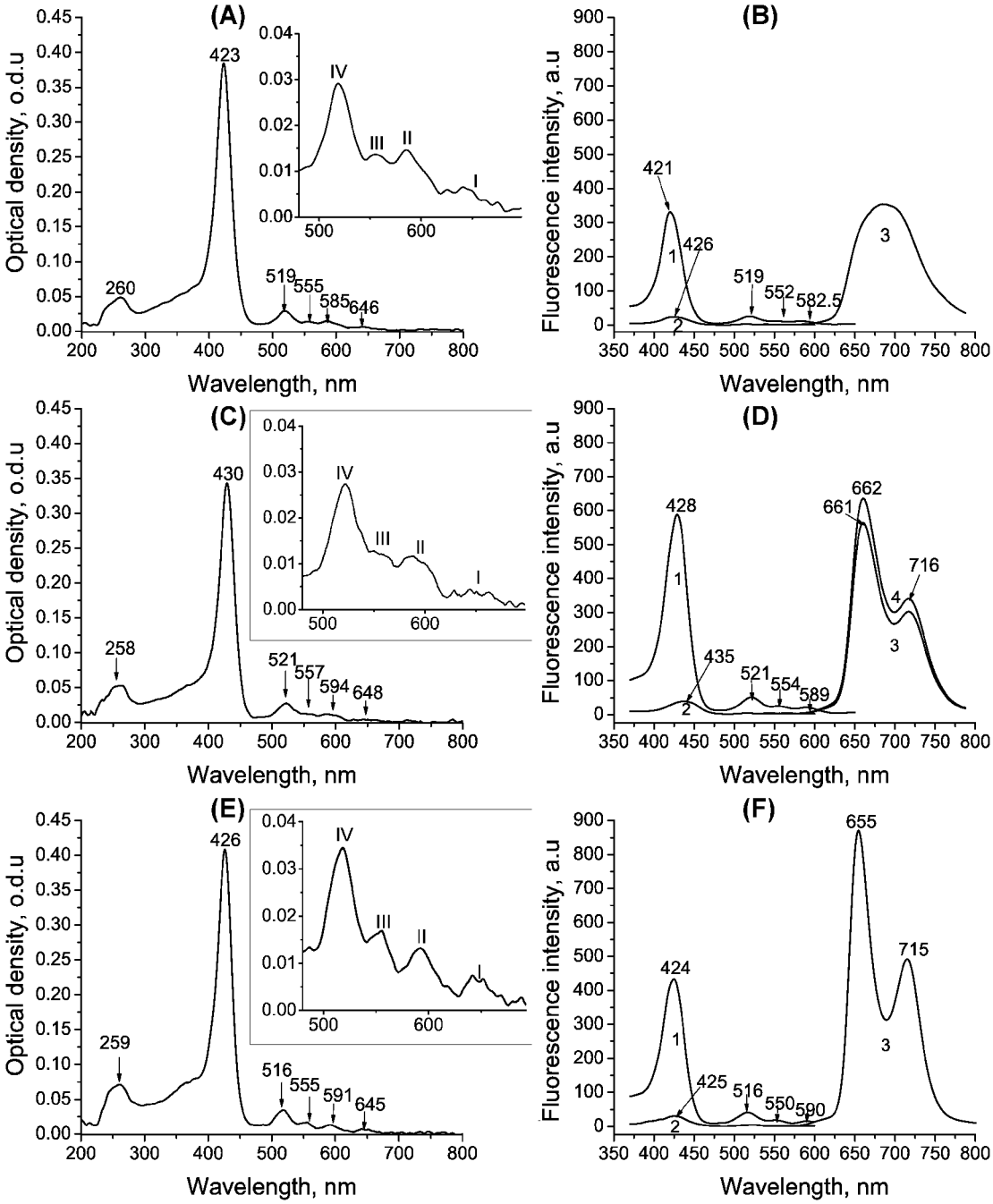

Fig. 3.1. Spectroscopic characteristics of TN-Et-PyP in different milieu: absorbance spectra (A, C, E), fluorescence emission and excitation spectra (B, D, F). A, B- porphyrin dissolved in PBS; C, D- dye dissolved in PBS with addition of 0.02% SDS; E, F- TN-Et-PyP in 96% ethanol. Insertions – enlarged part of absorbance spectra demonstrate arrangement of Q bands. TN-Et-PyP concentration was 1.5 μM for absorption and 0.375 μM for fluorescence measurements respectively. Fluorescence emission spectra were recorded upon excitation at 423 nm (line 3) and 430 nm (line 4 in D), excitation spectra were registered at the emission wavelength of 670 nm (line 1), 623 nm (line 2).

The prolonged incubation of TN-Et-PyP in the room temperature was performed to evaluate the stability of porphyrin spectroscopic properties in

PBS buffer (pH=7.3). The results revealed some purposeful process gradually progressing in one direction (Fig. 3.2.), denoted by the presence of isobestic point in fluorescence emission spectra.

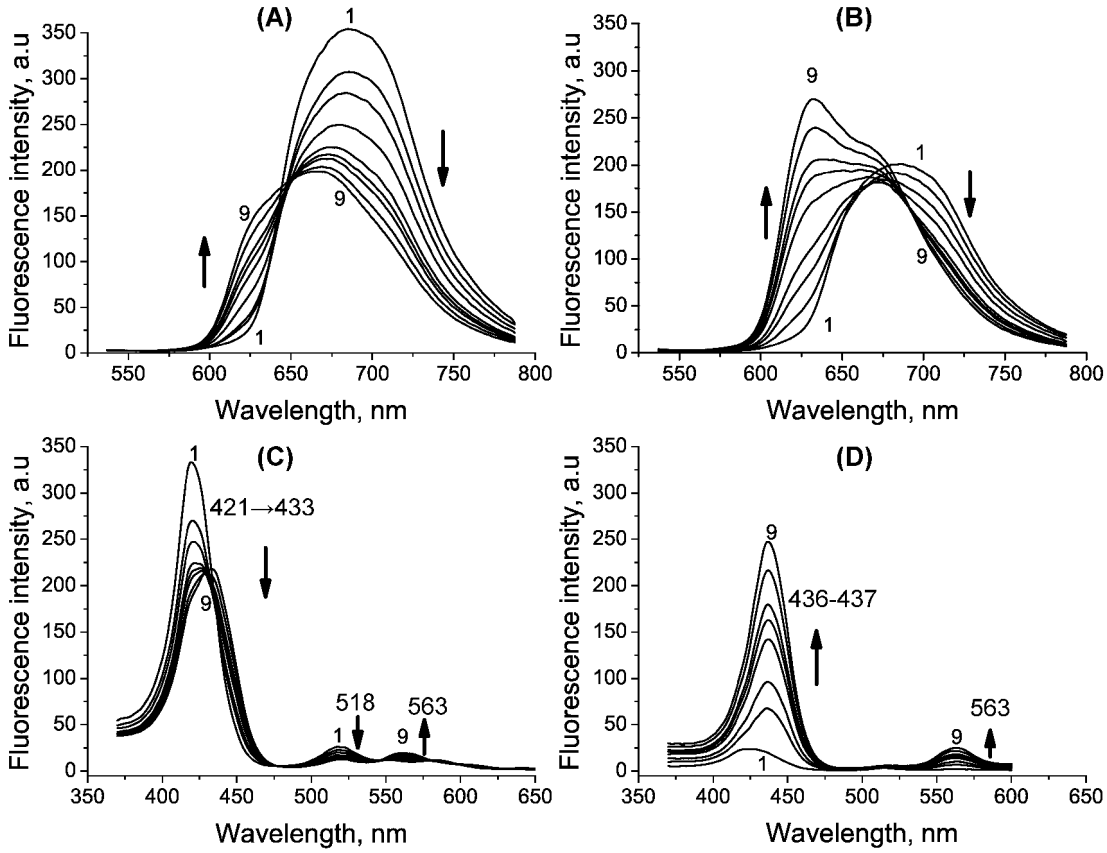

Fig. 3.2. Appearance of two TN-Et-PyP forms when photosensitizer is dissolved in PBS and incubated in the dark. The fluorescence emission (A, B) and excitation (C, D) spectra of TN-Et-PyP solution (OD_{423} = 0.1) have been measured after keeping in the dark for 0 min, 5 min, 30 min, 1 h, 2 h, 2.5 h, 3 h, 4 h, 5 h. (lines 1-9). Fluorescence emission spectra were recorded upon excitation at 423 nm (A), 435 nm (B), excitation spectra were registered at the emission wavelength of 670 nm (C) and 623 nm (D). The arrows show the increase or decrease of the particular peak starting from the line 1 ending at line 9.

In general the isobestic points are obtained in absorbance spectroscopy and indicate that only two species with identical molar absorption coefficients converts from one form to another without forming multiple products (IUPAC Compendium of Chemical Terminology, 1997, http://old.iupac.org/goldbook/I03310.pdf). It is much more complicate to obtain such points in fluorescence spectra, since there are a lot of factors such as the photosensitizer concentration, the conditions of even excitation, the selection of appropriate wavelength for exciting the photosensitizer, the

fluorescence quantum yield etc. influencing the fluorescence emission. Anyway, Fig. 3.2. clearly shows two forms of TN-Et-PyP appearing in buffered solution. One of them, having excitation spectrum peaking at 421 nm and smaller peaks at 518 nm and 563 nm, is gradually decreasing in amount (Fig. 3.2. A, C), the other, having excitation spectrum peaking at 437 nm and smaller peak at 563 nm, is gradually increasing (Fig. 3.2. B, D). Apparently, the first form is turning to the other in time course. Since it is well known, that increased temperature results in disruption of porphyrin aggregates the sample was heated in order to ascertain the two forms of TN-Et-PyP appearing in the buffered solution (Fig. 3.3.).

Although, the increased temperature accelerates the conversion process, the subsequent cooling failed to restore the sample to initial state. However, the gradual red shifting of maximum position and progressive disappearance of 518 nm peak in excitation spectrum clearly indicates the changing symmetry in porphyrin molecule i.e. changing the protonation state of the imino nitrogen or pyrrole nitrogen of the tetrapyrrole nucleus (see also Fig. 3.2. C, D). This hypothesis is strongly supported by decreasing number of Q bands in absorbance spectrum which is also affected by tetrapyrrole ring protonation state (Fig. 3.3. E, F).

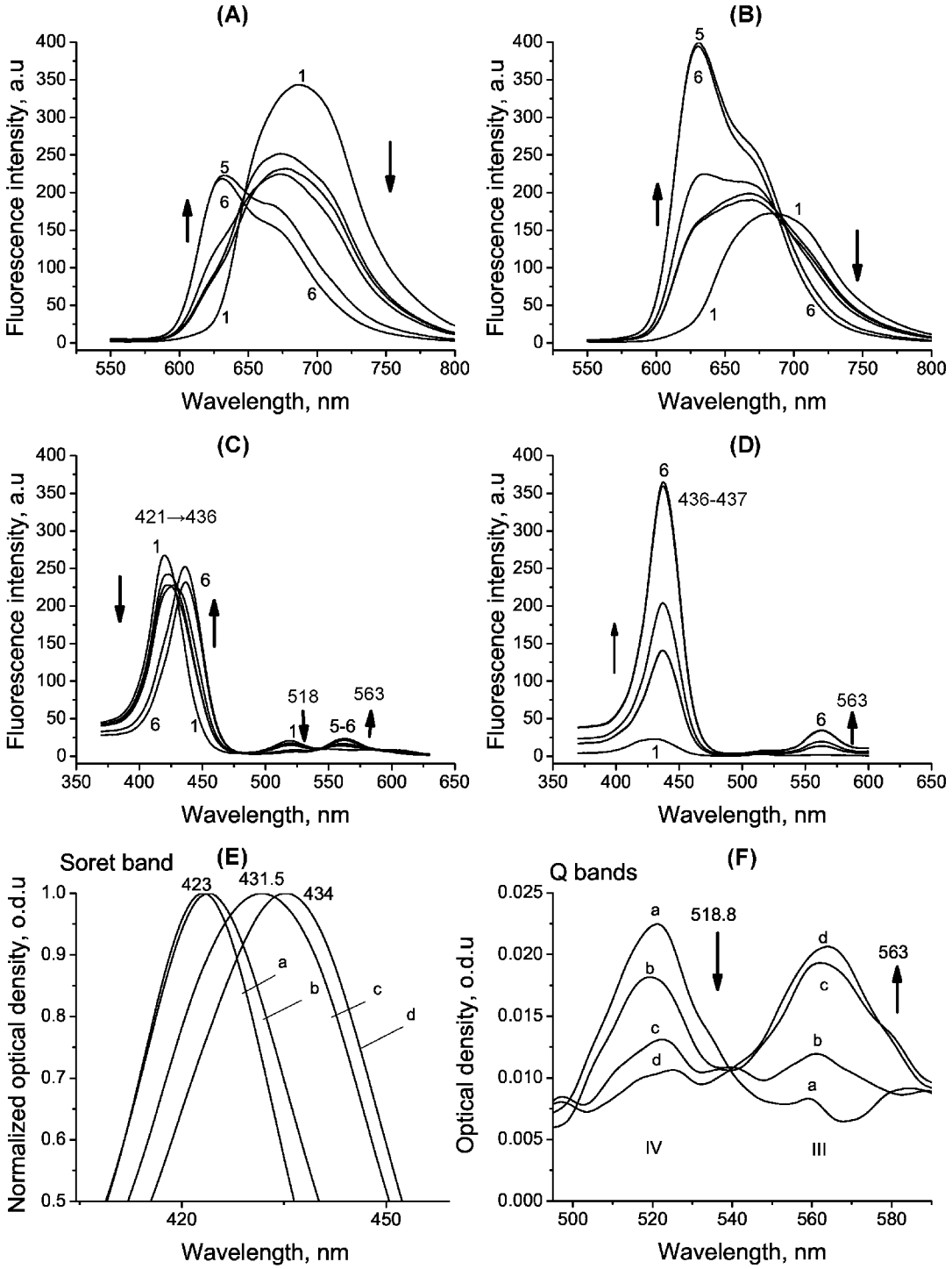

Fig. 3.3. Equilibrium between two forms of TN-Et-PyP dissolved in PBS depending on temperature and time changes. The fluorescence emission (A, B) and excitation (C, D) spectra of TN-Et-PyP solution (OD_{423} = 0.1) have been measured before (line 1) and after heating to 60ºC (line 2) and successive cooling up to +4 ºC (line 3). Additionally spectra of cooled samples kept at +4 ºC were recorded after 3 (line 4) and 5 days after heating (line 6). Fluorescence emission spectra recorded upon excitation at 423 nm (A), 435 nm light (B), the emission registered at 670 nm (C) and 623 nm (D). The arrows show the increase or decrease of the particular peak, starting from the line 1, ending at line 6. The time and temperature dependent variation of Soret band and III – IV Q band intensity in absorption spectra are shown in E, F: a – before heating, b – after heating, c – the sample was cooled and kept at +4 ºC for 3 days after heating, d – the sample was cooled and kept at +4 ºC for 5 days after heating.

Although the appearance of fluorescence emission and excitation spectra (particularly the number of smaller peaks in visible part) slightly reminds the spectra obtained in solutions baring acidic and alkaline pH (see Fig. 3.4.), it is not associated with significant changes of pH in PBS, which slightly varies between 7.0-7.4 during the prolonged experiment time.

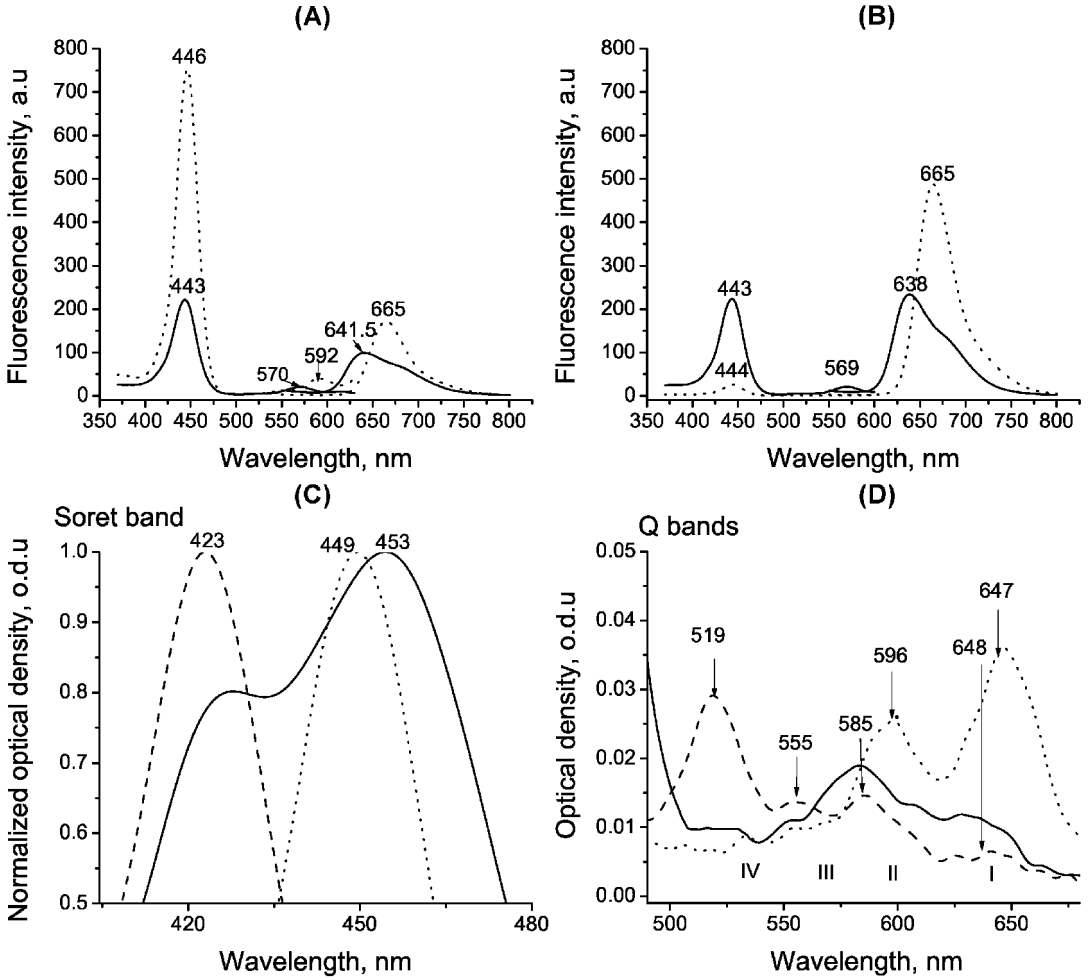

Fig. 3.4. The dependence of TN-Et-PyP absorption, fluorescence emission and excitation spectra on different pH values of PBS solution. pH = 12 – solid line, pH = 1 – dotted line, pH=7.4 – dashed line. TN-Et-PyP solution in PBS was OD = 0.05 for fluorescence, OD_{423} = 0.4 for absorbance measurements. (A) – fluorescence emission spectra recorded upon excitation light of 423 nm, excitation spectra registered at 670 nm, (B) – fluorescence emission spectra recorded upon excitation at 435 nm, excitation spectra registered at 623 nm. (C) – Enlarged view of Soret band in absorption spectra, when spectra were normalized to maximum, (D) – enlarged view of Q bands.

In order to investigate the possible dependence of TN-Et-PyP protonation state on the polarity of the solvent, prolonged porphyrin incubation experiment was performed in ethanol solutions of different concentrations. The data obtained from the spectroscopy of porphyrin dissolved in 96% and 50% ethanol shows, that the conversion still exist in diluted ethanol solution, though is much slower comparing with that appearing in PBS solution (Fig. 3.5. a and 3.5. b).

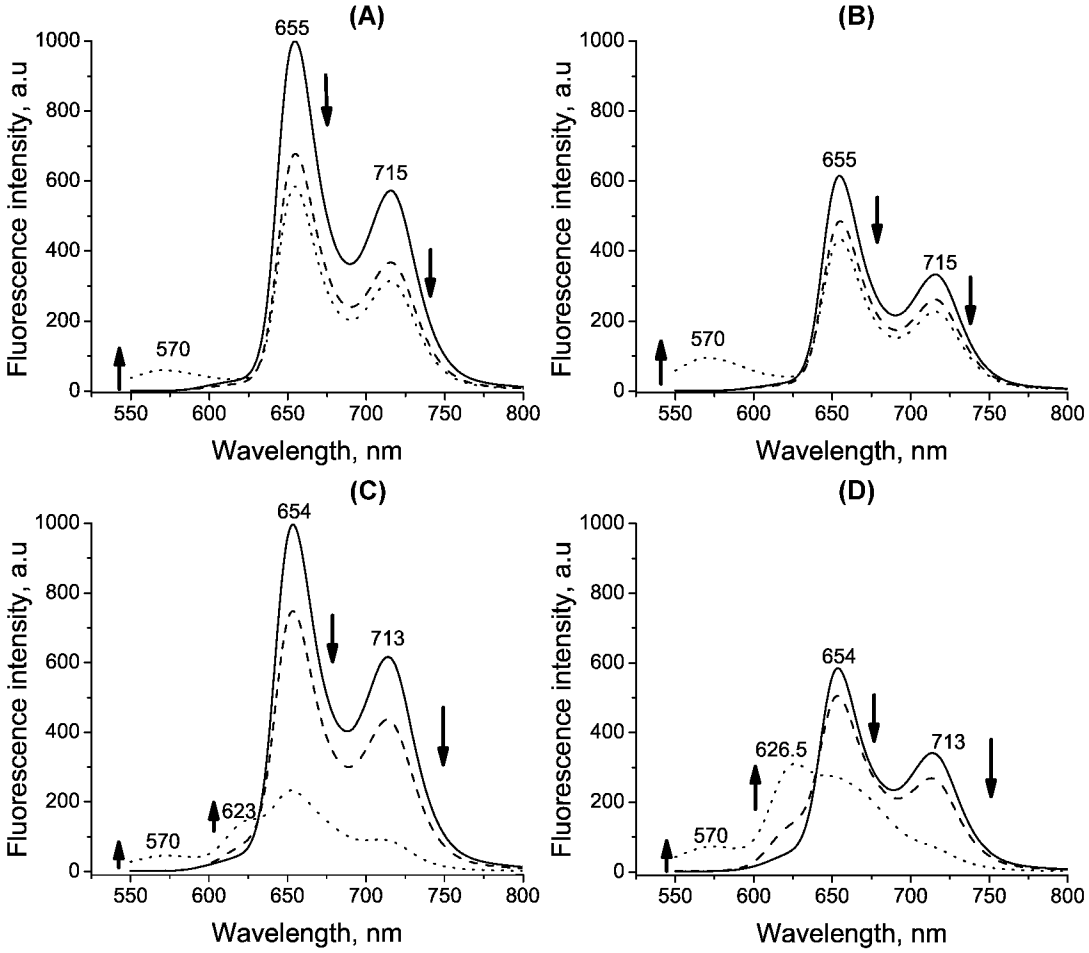

Fig. 3.5. a TN-Et-PyP fluorescence emission in 96% (A, B) and 50% (C, D) ethanol solutions. TN-Et-PyP was diluted to OD = 0.1 with appropriate concentration of ethanol. The fluorescence emission spectra recorded upon excitation at 423 nm (A, C) or 435 nm (B, D). Solid line represents the fluorescence emission of initial TN-Et-PyP solution in ethanol, dashed line – the same solutions kept in the dark for 1 day at +4ºC, dotted line – the same solutions kept in the dark for 3 days at +4ºC.

Considering the results obtained in 96% ethanol the conversion was not detected for the first 24 h after preparation, however after prolonged incubation times a minor part of the porphyrin is converted to different ionic form. A new peak at 497 nm occurred in the excitation spectra of "aged" porphyrin, possibly due to interaction with the solvent.

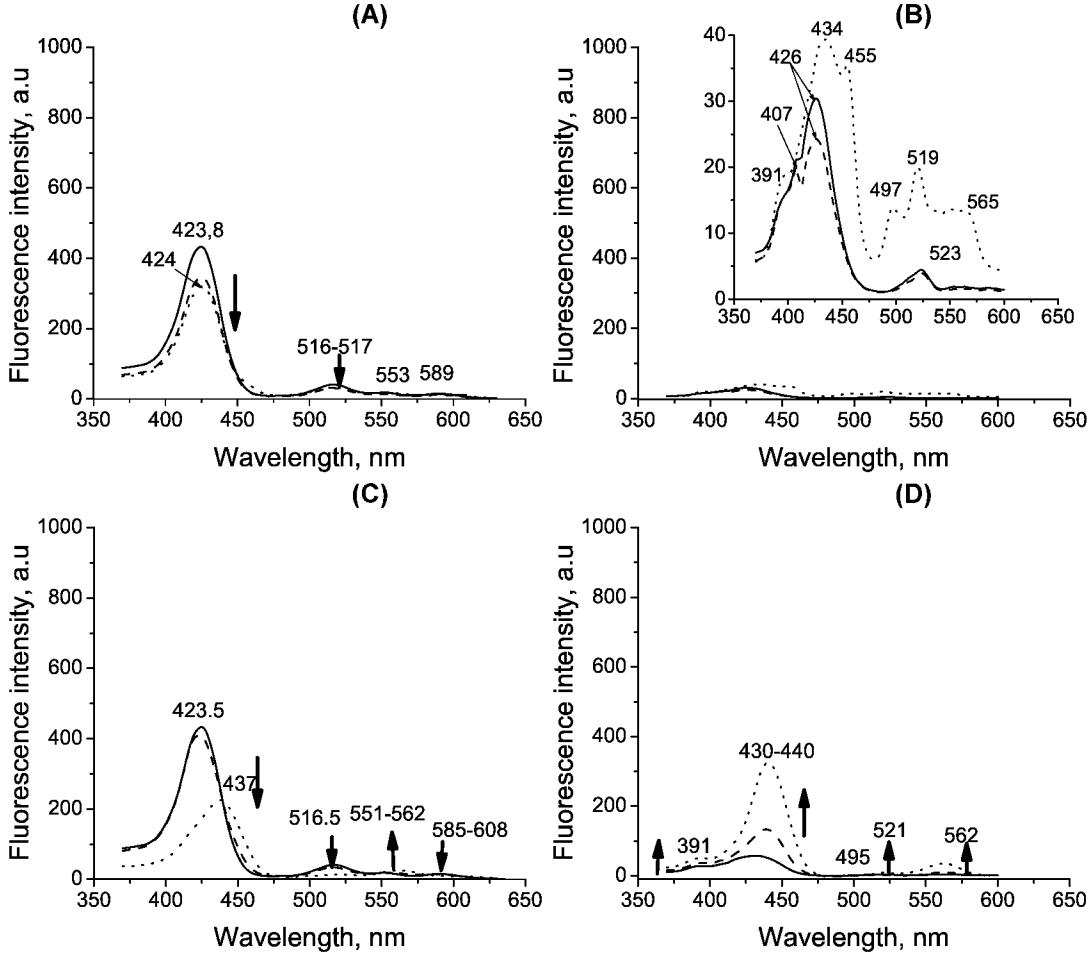

Fig. 3.5. b TN-Et-PyP fluorescence excitation in 96% (A, B) and 50% (C, D) ethanol solutions. TN-Et-PyP was diluted to OD = 0.1 with appropriate concentration of ethanol. The excitation spectra registered at 670 nm (A, C) or 623 nm (B, D). Solid line represents the fluorescence excitation of initial TN-Et-PyP solution in ethanol, dashed line – the same solutions kept in the dark for 1 day at +4ºC, dotted line- the same solutions kept in the dark for 3 days at +4ºC.

The results presented in Fig. 3.3. and Fig. 3.5. suggest, that TN-Et-PyP does not have stable spectroscopic properties in aqueous solutions, this can be attributed to changing symmetry of the molecule. There exist two possible explanations of the finding. In one case tetrapyrrole ring may be deprotonated due to transfer of proton from the pyrrole nitrogen to

methylbenzosulphonic acid, which capability to interact with a tetrapyrrole ring may appear to be sensitive to the ionic nature of the solvent. This hypothesis is supported by the finding that deprotonation of the tetrapyrrole ring is strongly inhibited in 96% ethanol solution, but persists in 50% ethanol solution. The second explanation implies protonation of the tetrapyrrole ring due to formation of dimers, where molecules are orientated in such a way that pyrrole nitrogen of one molecule protonates imino nitrogen of the second molecule. Although, such events are not very likely, they cannot be completely excluded. Accordingly, it is important to consider the spectroscopic changes of the photosensitizer in PBS (pH=7.3), while interpreting the interaction of TN-Et-PyP with cellular components denoted by transformed absorbance and fluorescence emission and excitation spectra.

3.1.2. The interaction of TN-Et-PyP with purified cellular components in model systems.

The TN-Et-PyP interaction with different cellular components are supposed to clarify some details concerning at least initial steps of bacterial photosensitization process. The interaction of the photosensitizer with various cellular components have been studied in model systems, composed of the dye and purified components, since the cell is a system fully packed with different compounds, which might react with the porphyrin, forming various types of products. Consequently the spectroscopic results obtained from such complex systems are difficult to interpret.

Titration of 1.5 μM TN-Et-PyP solution in PBS (pH=7.3) with increasing concentrations of bacterial membrane components such as lipids and lipopolysaccharides (LPS), proteins which may be attributed either to membrane or inner components of the cell and nucleic acids (NA) representing the inner part of the cells, revealed that only porphyrin interaction with LPS and NA caused the pronounced red shift of Soret band by 7.8 nm and 17 nm respectively, indicating complex formation (Fig. 3.6. A). Moreover, the batochromic shift was accompanied by hypochromic (or absorption intensity

decrease) effect. The percentage of hypochromicity (H%) is one of the parametters used for determination of photosensitizer-NA binding mode, accordingly the hypochromicity of 41% along with 17 nm Soret band shift to the longer wavelength may indicate TN-Et-PyP intercalative binding to the nucleic acids.

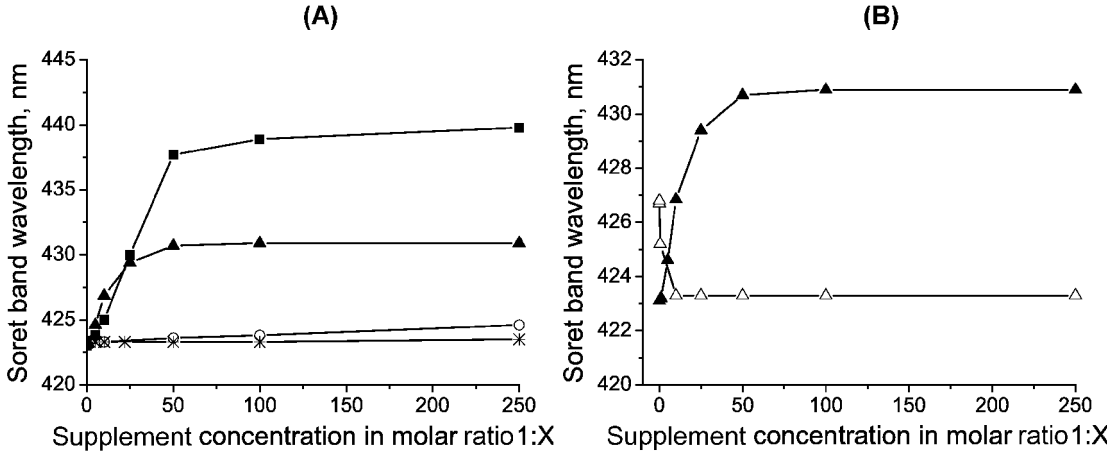

Fig. 3.6. TN-Et-PyP absorption spectra Soret band changes during complex formation with cellular components (A) and during porphyrin-LPS complex dissociation after addition of $MgCl_2$ (B). 1.5 μM TN-Et-PyP solution in PBS (pH=7.3) was titrated by increasing amount of NA(■), LPS (▲), BSA (○) and lipids (*). TN-Et-PyP titration with buffered LPS solution (▲) in increased concentration is placed in graph (B) for comparison with TN-Et-PyP-LPS complex titration with increasing concentration of $MgCl_2$ (Δ). TN-Et-PyP complex with LPS was obtained by mixing buffered solutions of both components in constant molar ratio 1:10. This mixture was titrated with increasing concentration of $MgCl_2$.

Since divalent cations such as Mg^{2+} and Ca^{2+} stabilize outer membrane structure by preventing the repulsion between negatively charged groups localized in the inner core of adjacent LPS molecules in bacterial cells, they may play some role in aggravating porphyrin binding to the bacterial envelope, therefore the fate of porphyrin-LPS complex in the presence of increasing $MgCl_2$ concentrations was investigated. Fig. 3.6. B demonstrates the disassembling of the complex, suggesting, that $MgCl_2$ replaces the dye molecules on LPS as indicated by the gradual restoration of the dye original spectra with increasing concentrations of $MgCl_2$. Therefore, it is reasonable to believe, that TN-Et-PyP-LPS complex is formed by interactions of electrostatic nature and Mg^{2+} ions are competing with TN-Et-PyP molecules for binding to the negatively charged inner core of LPS.

It is well known that fluorescence measurements are more sensitive technique than UV-VIS absorption spectroscopy, therefore the interaction of TN-Et-PyP with different cellular components was studied by examining fluorescence emission and excitation spectra (Fig. 3.7.-3.8., complete and unmodified data on fluorescence emission and excitation are presented in appendix Fig. 3.22. – 3.27.).

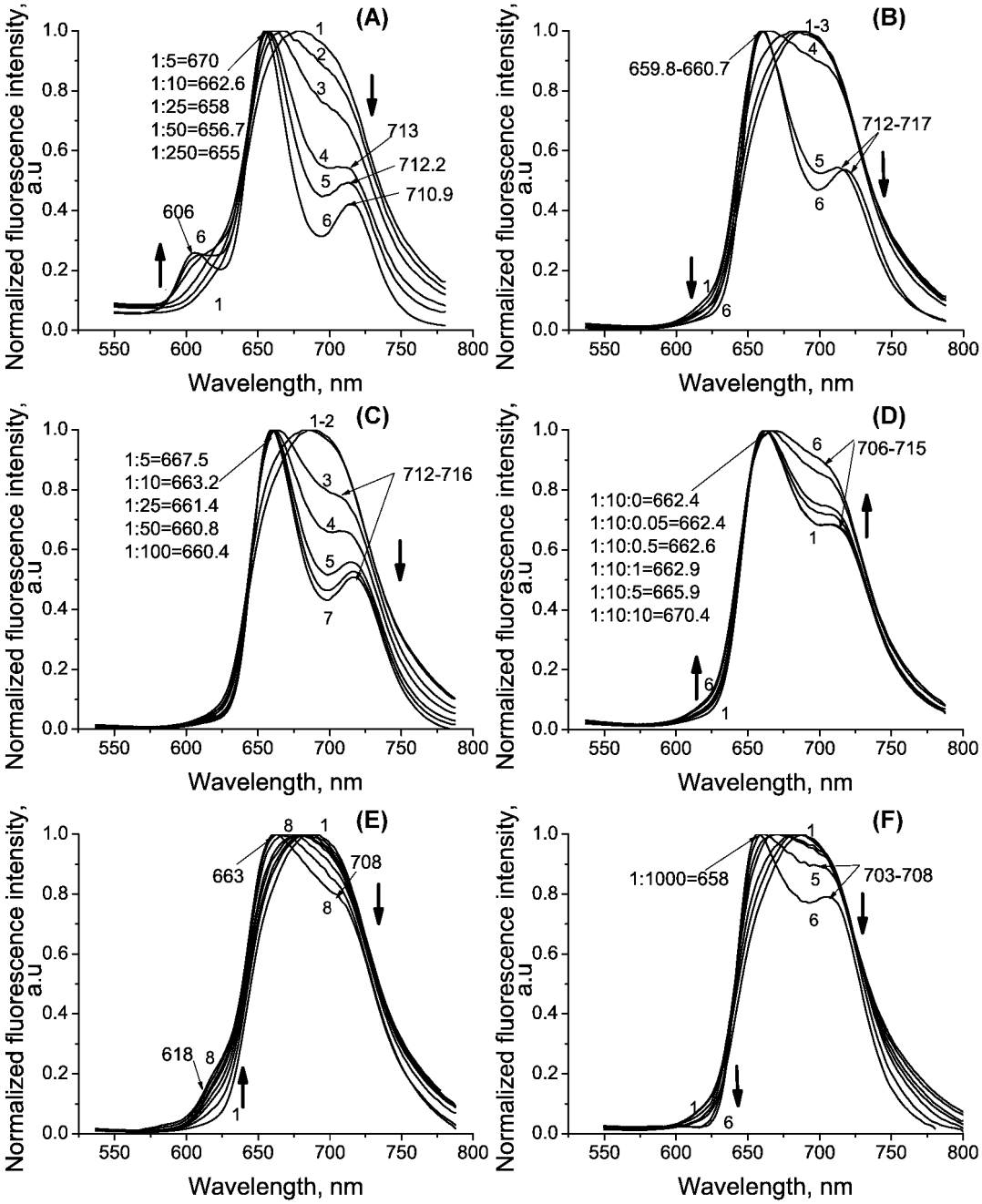

Fig. 3.7. The fluorescence emission spectra (excitation being 423 nm) normalized to maximum. TN-Et-PyP solution in PBS with OD = 0.1 was titrated by increasing concentration of various supplements. The pronounced arrows show the increase or decrease of the particular peak, smaller arrows indicate the peak shift. A – TN-Et-PyP titrated with purified plasmid DNA, concentration expressed in molar ratio Dye:NA = 1:0; 1:5; 1:10; 1:25; 1:50; 1:250 (lines 1-6 respectively). B – TN-Et-PyP titrated with SDS, concentration expressed in molar ratio Dye:SDS = 1:0; 1:10; 1:50; 1:100; 1:250; 1:500 (lines 1-6 respectively). C- TN-Et-PyP titrated with LPS, concentration expressed in molar ratio Dye:LPS = 1:0; 1:0.5; 1:5; 1:10; 1:25; 1:50; 1:100 (lines 1-7 respectively). D – TN-Et-PyP mixed with LPS in molar ratio 1:10 titrated with $MgCl_2$, concentration expressed in molar ratio Dye:LPS:$MgCl_2$ = 1:10:0; 1::10:0.05; 1:10:0.5; 1:10:1; 1:10:5; 1:10:10; (lines 1-6 respectively). E – TN-Et-PyP titrated with lipids, concentration expressed in molar ratio Dye:total lipid= 1:0; 1:5; 1:10; 1:22; 1:50; 1:250; 1:500; 1:1500 (lines 1-8 respectively). F – TN-Et-PyP titrated with BSA, concentration expressed in molar ratio Dye:BSA = 1:0; 1:10; 1:50; 1:250; 1:500; 1:1000 (lines 1-6 respectively).

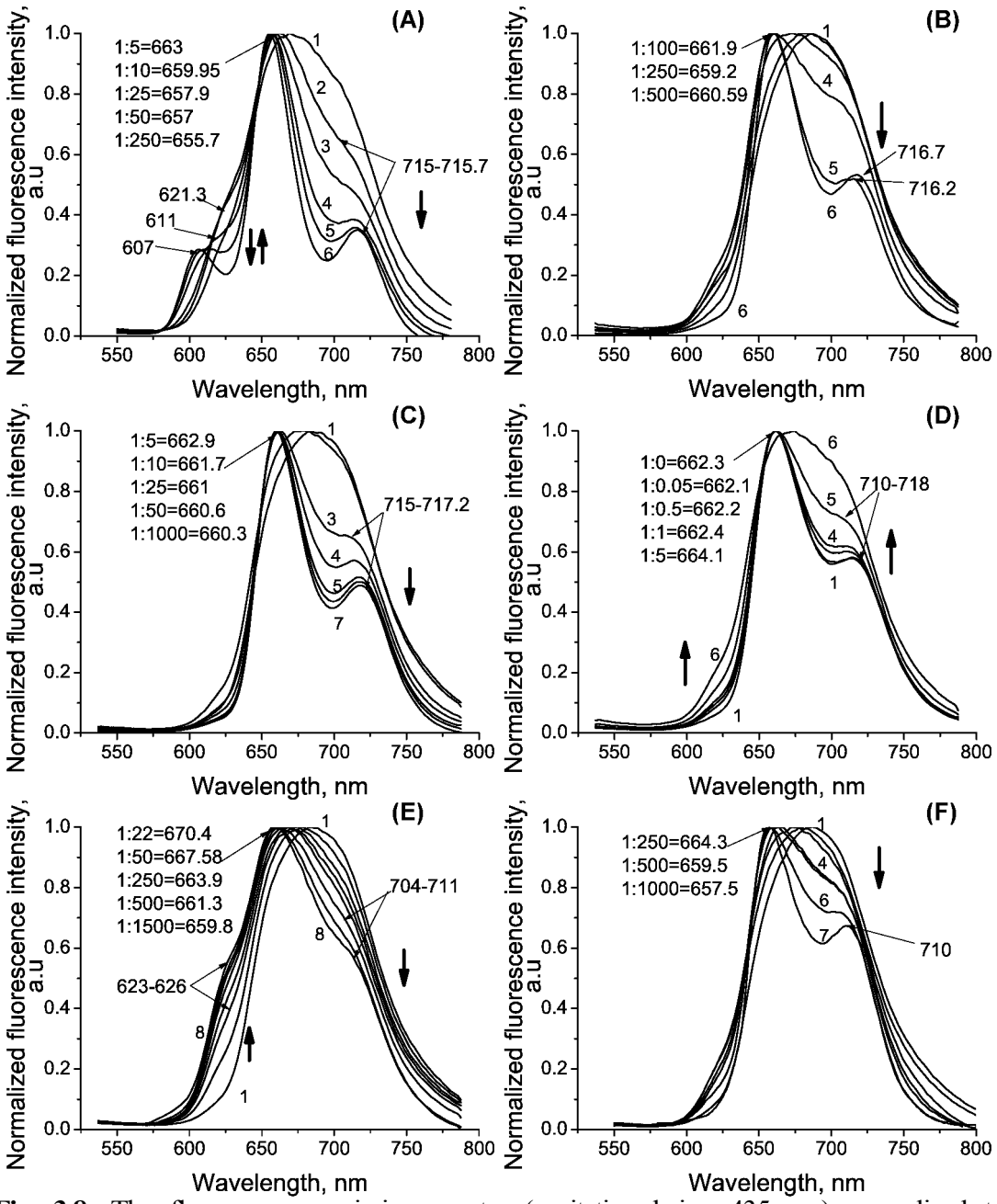

Fig. 3.8. The fluorescence emission spectra (excitation being 435 nm) normalized to maximum. TN-Et-PyP solution in PBS with OD = 0.1 was titrated by increasing concentration of various supplements. The pronounced arrows show the increase or decrease of the particular peak, smaller arrows indicate the peak shift. A – TN-Et-PyP titrated with purified plasmid DNA, concentration expressed in molar ratio Dye:NA = 1:0; 1:5; 1:10; 1:25; 1:50; 1:250 (lines 1-6 respectively). B – TN-Et-PyP titrated with SDS, concentration expressed in molar ratio Dye:SDS = 1:0; 1:10; 1:50; 1:100; 1:250; 1:500 (lines 1-6 respectively). C – TN-Et-PyP titrated with LPS, concentration expressed in molar ratio Dye:LPS = 1:0; 1:0.5; 1:5; 1:10; 1:25; 1:50; 1:100 (lines 1-7 respectively). D – TN-Et-PyP mixed with LPS in molar ratio 1:10 titrated with $MgCl_2$, concentration expressed in molar ratio Dye:LPS:$MgCl_2$ = 1:10:0; 1::10:0.05; 1:10:0.5; 1:10:1; 1:10:5; 1:10:10; (lines 1-6 respectively). E – TN-Et-PyP titrated with lipids, concentration expressed in molar ratio Dye:total lipid= 1:0; 1:5; 1:10; 1:22; 1:50; 1:250; 1:500; 1:1500 (lines 1-8 respectively). F – TN-Et-PyP titrated with BSA, concentration expressed in molar ratio Dye:BSA = 1:0; 1:10; 1:50; 1:250; 1:500; 1:1000 (lines 1-6 respectively).

It showed distinct changes in the shape of the spectra: gradual turning from Gaussian type of the curve to two-peaked fluorescence emission spectra upon addition of cell components in increasing concentration. However, the concentrations of various compounds needed to change the spectra shape differ from very high in the case of BSA and lipid vesicles (0.375 mM or 0.56 mM respectively) to comparatively low in the case of nucleic acids, LPS and especially $MgCl_2$, which can revert the TN-Et-PyP-LPS complex spectrum to the initial position in a concentration as low as 3.75 μM $MgCl_2$.

Considering the capability of the porphyrin molecules to interact in between reflected by discussed changes in absorption, fluorescence emission and excitation spectra (see Fig. 3.2.; 3.3.), it can be presumed, that TN-Et-PyP interactions with BSA and lipid vesicles are fairly negligible. However, the presence of these supplements in PBS solution may aggravate the porphyrin conversion process described above (see chapter "TN-Et-PyP spectroscopy"), since there are neither clearly defined changes in the number of Q bands in absorption spectra, nor strong increase and predominance of 563 nm over 518 nm peak in fluorescence excitation spectra (see appendix Fig 3.26; 3.27). Conversely, the distinct changes in fluorescence emission peaks not typical to porphyrin conversion process (i.e. formation of clearly defined 715 peak and appearance of 607 nm peak in 3.7. – 3.8. A) along with strong red shift of the Soret band in absorption spectra provide a strong reason to believe, that porphyrin interaction with NA, LPS and SDS appear to be much more significant and is possibly associated with complex formation between TN-Et-PyP and supplement molecules.

The analysis of Tn-Et-PyP interactions with anionic surfactant sodium dodecyl sulphate, anionic LPS and lipid vesicles is a promising model for enlightening the initial binding of the photosensitizer to Gram-negative bacteria envelope. Fig. 3.9. demonstrates changes in absorption spectra due to increasing concentration of the supplement.

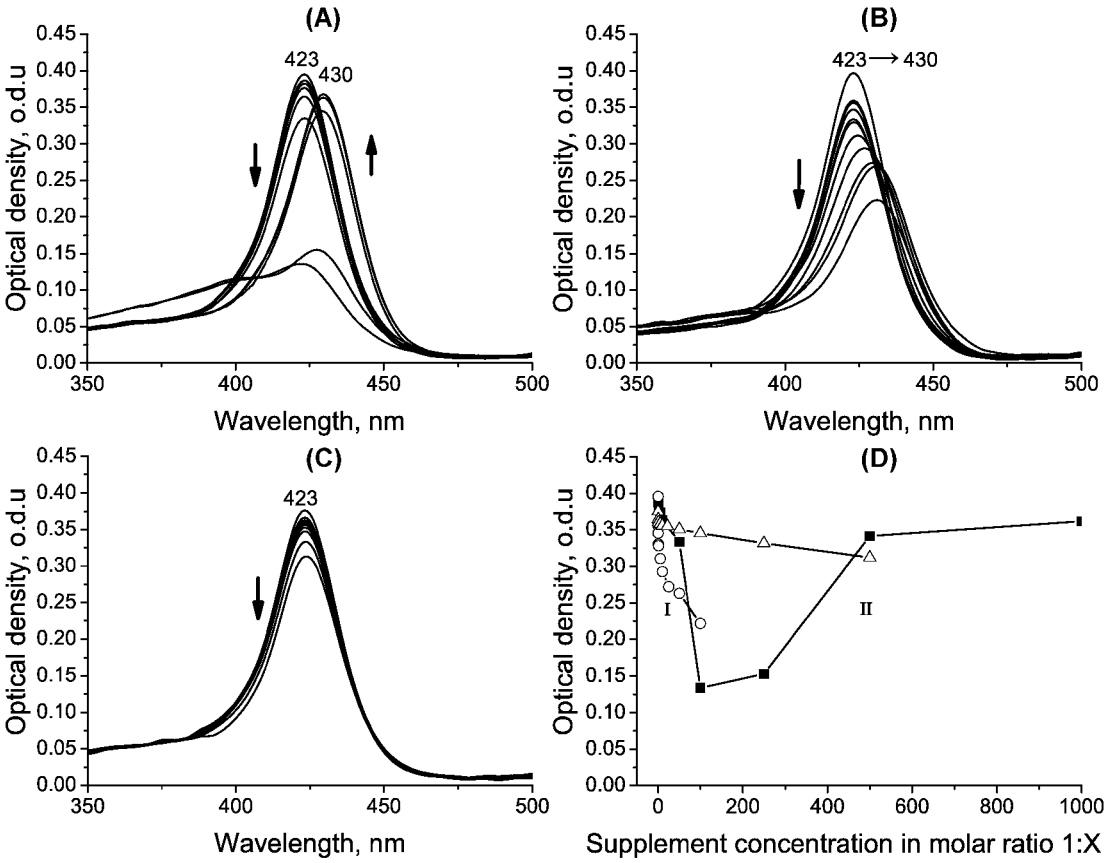

Fig. 3.9. TN-Et-PyP absorption spectra Soret band changes due to dye interaction with SDS (A), LPS (B) and lipid vesicles (C). 1.5 μM TN-Et-PyP solution in PBS (pH=7.3) was titrated with increasing concentration (see Fig. 3.13.) of appropriate supplement and absorption spectra were recorded. The Soret peak intensities are drawn with regard to supplement concentration (D). ■ – represents intensity changes when porphyrin interacts with SDS, Δ – represents intensity changes when porphyrin interacts with lipid vesicles, ○ – represents intensity changes when porphyrin interacts with LPS.

In the absence of supplements, the absorption spectra of TN-Et-PyP in PBS buffer presents Soret maximum at 423 nm. On gradual addition of components a hypochromic effect of different intensity is observed (Fig. 3.9. A-C). However, the variation of absorbance intensity at the maximum as the function of supplements' concentration indicates two processes for model system to study TN-Et-PyP interaction with SDS, though only the first process occurs in the systems designed to study the porphyrin interaction with LPS or lipids (Fig. 3.9. D marked as I and II). Considering SDS capability to form micelles it is reasonable to presume that two opposite processes seen in the Fig. 3.9. D represent interaction events occurring in the

system in premicellar range of SDS concentrations (process I) and at concentrations higher than critical micellar concentration (CMC) (respectively process II). The decrease in absorbance may be explained by neutralization of the dye positive charge by surfactant anions (at the lesser extent by anionic groups in LPS or even in lipid vesicles). That suppresses the repulsion between porphyrin molecules and favors the formation of dye-surfactant aggregates. The increase in absorbance (process II) may be explained by incorporation of TN-Et-PyP into SDS micelles. Unfortunately, it is impossible to predict the positioning of the porphyrin molecule in the SDS micelles since the dye was not studied in organic solvents. Moreover, some intermediate state of the system occurs when SDS concentration is approaching CMC (seen as marked decrease in absorption intensity and gradual Soret band red shift in Fig. 3.9. A). The formation of dye-surfactant pairs and aggregates as well as induced premicellar aggregates have been proposed to be the main processes explaining the behaviour of cationic dyes in the presence of anionic surfactant molecules at the concentrations below the CMC. (Freire *et al*, 2010). Supposedly, porphyrin molecules form two types of complexes with detergent molecules: monomers incorporated in micelles, represented by the 430 nm peak and presumably large aggregates with the absorption maximum shifted to the blue part of the spectrum. The aggregates are surmised to be of different size since there is no strongly expressed peak in the blue region of the spectrum. The aggregates crumble after increasing SDS concentration and turn to monomerised porphyrin molecules which are incorporated into micelles. The process is reflected by rapid decrease and disappearance of the absorption band in the blue region of the spectra and increase of the band peaking at 430 nm. The discrepancies observed in absorbance intensity variation profiles (Fig. 3.9. D) may be explained by the different capability to form vesicles due to number of charges present in SDS and LPS molecules. SDS molecules having one negative charge are neutralized more rapidly comparing to LPS molecules, which bare several negative charges, therefore the formation of LPS micelles is

retarded. Although, the possibility of II process appearance can not be excluded in the latter case, still it will need higher amount of porphyrin molecules to neutralize the negative charge of LPS.

In spite of slightly lipophilic partition coefficient ($logP_{OW}$) of TN-Et-PyP calculated by various modelling programs for water-octanol system (see Table 1.), it seems highly unlikely, that this porphyrin may relocate deeply into lipid vesicles (Fig. 3.9. D), since there are no distinct changes either in absorption nor in fluorescence emission or excitation spectra (see Fig. 3.9.; 3.8.; 3.7.)

Table 1. $LogP_{OW}$ of commonly used photosensitizers, calculated by different computer programs

	ALOGPs	AC logP	miLogP	ALOGP	MLOGP	XLOGP2	XLOGP3
mTHPC	6.10	6.64	9.07	9.77	3.36	6.35	9.60
TN-Et-PyP	7.06	4.02	6.68	8.44	2.87	4.85	7.85
TMPyP	6.47	2.69	5.18	7.05	2.22	3.82	6.65
$TPPS_4$	0.69	-2.05	0.11	7.09	1.97	3.06	5.40

This discrepancy may be explained assuming, that lipophilicity is not the only factor contributing to interaction of cationic porphyrins with lipid vesicles or cell membranes, therefore the predictions based entirely on $logP_{OW}$ values are unsatisfactory. The partitioning coefficient calculated for particular systems such as buffer – lipids may be more relevant for pursuing the photosensitizer sublocalization (Engelman *et al*, 2007). The slight interaction of electrostatic nature occurring on the hydrophilic vesicle surface due to four cationic charges of the porphyrin molecule is the most plausible event. Consequently the dye molecule is not changing microenvironment and there is no “red shift” of the Soret band (Fig. 3.9.).

Considering the results presented above, it is substantial to conclude, that investigated components are modifying the TN-Et-PyP symmetry changes to different extent and possibly by different modes of action. NA, LPS and SDS monomerise porphyrin molecules by forming complexes and it is reflected in spectroscopic features as substantial red shift of

Soret band and fluorescence emission shape turning to the spectra with two clearly defined peaks. Although, the interaction of TN-Et-PyP with other studied components are not so undeniably expressed, the change of microenvironment may modify such physical properties as dielectric constant of the solvent, photosensitizer solubility, the monomers: aggregates ratio etc, which in turn may influence the capability of the photosensitizer to change symmetry.

3.1.3. TN-Et-PyP interaction with *E. coli* KMY1 cells.

Although, it is very difficult to draw interferences from spectroscopy data on photosensitizer interaction with complex systems of the living cells, some interesting findings can be discussed anyway. The interaction of TN-Et-PyP with the cells in suspension upon irradiation reminds that of porphyrin complexing with nucleic acids (compare Fig 3.6. A and 3.10.).

Considering the Soret band changes, which become observable after the cells receive approx 10-20 J/cm^2 light dose and increases along with increasing irradiation, it is reasonable to suppose, that the main cause for gradual Soret band shift in cellular systems is increasing concentration of the inner components (most probably NA) in the media, due to gradual disruption of the bacteria cells (see TEM micrographs in Fig. 3.14.). The appearance of the same Soret band shift to almost 440 nm in the mixture of heat inactivated cells, actually even before any light treatment is applied, also strongly supports the hypothesis (Fig. 3.10.).

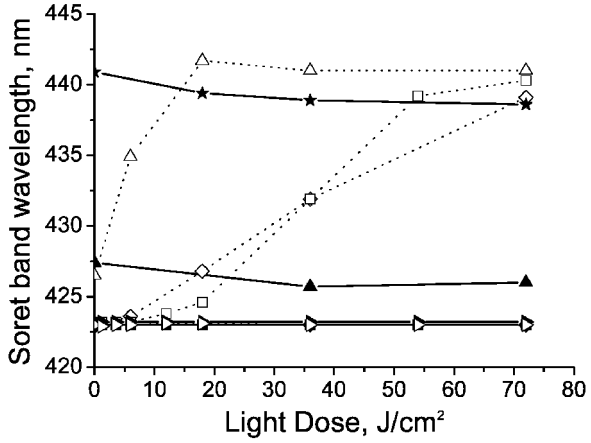

Fig. 3.10. Soret band changes during dark treating or irradiating TN-Et-PyP with *E. coli* KMY1. Cell suspension in PBS (pH=7.3) was mixed with 1.5 μM TN-Et-PyP. Part of the preparation was kept in the dark, another part irradiated with LED λ = 400nm at a dose of 0; 0.6; 1.2; 3.6; 6; 12; 18; 36; 54; 72 J/cm^2. Absorbance was measured against appropriately diluted cell suspension untreated with the porphyrin. The experiment was repeated with cells, harvesting them after irradiation with LED λ = 400 nm at a dose of 0; 6; 18; 36; 72 J/cm^2 or after dark treatment for appropriate time. The absorption of supernatant and cells resuspended in sterile PBS was measured against the supernatant and cell suspension obtained after centrifugation of the preparation immediately after mixing with the porphyrin. For cell inactivation three cycles of heating to 80°C for 20 min and subsequent frozing at -20°C had been applied before treating with porphyrin. (►-TN-Et-PyP in PBS kept in dark, > – TN-Et-PyP in PBS irradiated, ■ – cell suspension dark treated with TN-Et-PyP, □ – cell suspension irradiated with TN-Et-PyP, ▲- cells harvested after dark treatment with TN-Et-PyP, Δ- cells harvested after irradiation with Tn-Et-PyP, ♦ – supernatant from dark treated cells, ◊ – supernatant from irradiated cells, * – heat inactivated and irradiated with TN-Et-PyP cells). The lines denoting the Soret band position of TN-Et-PyP in PBS either irradiated or kept in the dark, cell suspension dark treated with TN-Et-PyP and supernatant from dark treated cells coincide.

In addition, there are no other changes except for bleaching of the porphyrin absorbance spectra during irradiation of the dye with two unvarying concentrations of NA as well as LPS, lipids and BSA in model systems (data not shown), which also agrees with the prediction that the main cause for gradual Soret band shift is increasing NA concentration in the media, due to decomposition of the bacteria cells.

The comparison of fluorescence emission and excitation spectra of the TN-Et-PyP present in the bacterial cells either harvested after particular irradiation time or harvested after dark treatment for the same time, as well as the porphyrin left in supernatant in each case, revealed that irradiating of the

cell suspensions with increasing light dose transform the shape of fluorescence emission spectra from typical for aqueous milieu to two-peaked shaped spectra more common to some different surrounding (Fig. 3.11.).

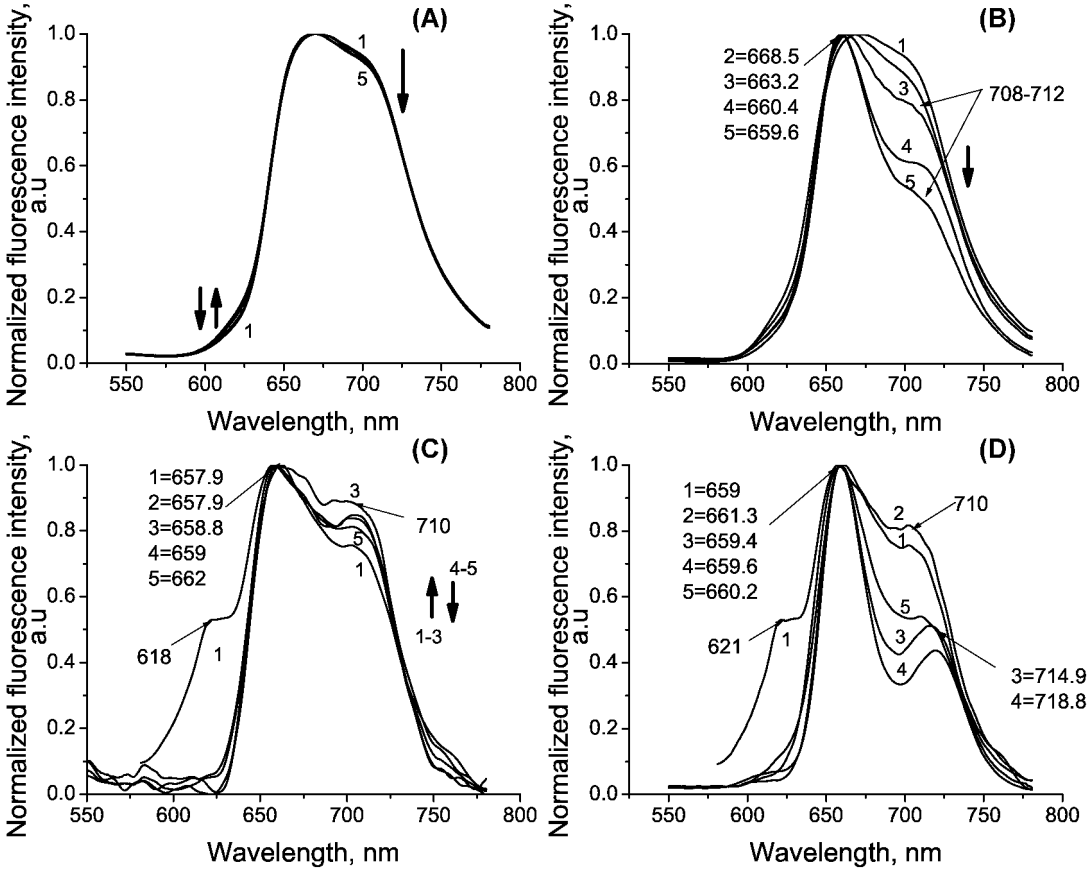

Fig. 3.11. TN-Et-PyP fluorescence emission spectra (excitation being 423 nm) in cell suspension and supernatant normalized to maximum. TN-Et-PyP was mixed with *E. coli* KMY 1 suspension at OD = 0.1. The suspension was irradiated with increasing light dose (6 J/cm^2, 18 J/cm^2, 36 J/cm^2, 72 J/cm^2) or kept in the dark for the time periods equal to irradiation time. Afterwards the cells were harvested by centrifugation and resuspended in sterile PBS (pH=7.3). The porphyrin fluorescence emission spectra were recorded in both: resuspended cell suspensions and supernatant left after centrifugation. A – supernatants from the cells which were dark treated with TN-Et-PyP, B- supernatants from the cells irradiated with TN-Et-PyP, C- cells resuspended in PBS after incubating with TN-Et-PyP in the dark, D – cells resuspended in PBS after irradiating with TN-Et-PyP (0 J/cm^2- line 1, 6 J/cm^2 – line 2, 18 J/cm^2- line 3, 36 J/cm^2- line 4, 72 J/cm^2 – line 5). The pronounced arrows show the increase or decrease of the particular peak, smaller arrows indicate the peak shift.

Furthermore, the changes in the shape of porphyrin fluorescence emission spectra in supernatant, obtained from bacteria irradiated with increasing light dose may be attributed to the cell decomposition and inner material outcome, which interacts with the rest of free porphyrin left after centrifugation. However the fluorescence intensity is gradually decreasing (see

appendix Fig. 3.28.). Similar pattern can be seen in the cells harvested after irradiation and resuspended in porphyrin-free buffer solution, though the intensity changes are more complex. The fluorescence emission intensity increases only for some time, suggesting the increased uptake of the dye into the cell possibly due to increased permeability of the cell outer membrane, afterwards it starts to decrease and the latter effect can be attributed to cell decomposition, wherefore some part of inner components along with bound porphyrin is left in supernatant after centrifugation (appendix Fig. 3.29.). This decrease of fluorescence intensity coincides with increased intensity in supernatant at the appropriate time.

In conclusion the results obtained from spectroscopic analysis clearly demonstrate, that considerable changes in Soret band position in absorbance spectrum, both fluorescence emission and excitation spectra shape and intensity can be associated with the photosensitizer relocalization to another microenvironment and formation of complex with cellular components baring negative charge.

3.2. Photosensitized inactivation of *E. coli* KMY1

In PDT, irradiation of target cells or tissues is generally accomplished by irradiation with red light ($\lambda > 600$ nm). This choice is motivated by the minor absorption of these light wavelengths by the normal constituents of most human tissues, which allows for a deeper penetration of the incident light to inner tissue layers. However, the scenario is in principle different in the case of a phototherapeutic treatment of superficial and localized lesions infected by pathogenic bacterial agents. In actual fact, TN-Et-PyP exhibit a very intense absorption band (Soret) in the blue region which peaks at 423 nm (Fig 3.1.). Since the light of shorter wavelength is characterised by higher energy, the inactivation of the bacterial cells will be less time consuming. These considerations would justify the choice of blue light-emitting sources for the treatment of localized bacterial infections, since a

significant penetration of the light into the host tissue is not required. Preliminary studies from our laboratory, as well as literature reports from other groups (Nitzan & Ashkenazi, 2001), indicate that illumination of *E. coli* with blue light in the presence of porphyrins leads to an efficient photokilling of bacterial cells with shorter illumination periods as compared with irradiations performed by means of green or red light wavelengths.

As one can see in Fig. 3.12., the incubation of the *E. coli* KMY1 strain in the absence of light with TN-Et-PyP concentrations up to 3.5 μM caused no detectable decrease in cell survival.

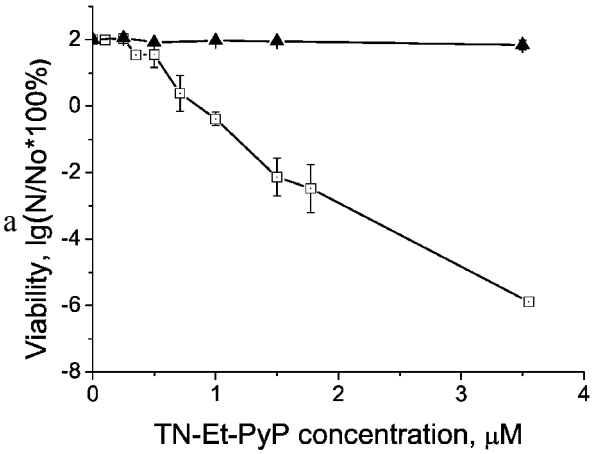

Fig. 3.12. The viability of *E. coli* KMY1 after irradiation with different TN-Et-PyP concentrations. Irradiations were performed by using LED λ = 415 nm for total light dose of 20 J/cm^2. (▲ – Cell suspension in PBS dark treated with TN-Et-PyP, □ – the same suspension irradiated with LED 415 nm.)

On the other hand, the exposure of the porphyrin-loaded bacterial cells to either 415 nm or 400 nm light from LED sources promoted a marked (*ca*. 6 log) drop in cell viability. Since no appreciable difference in the rate and extent of the photoprocess was observed between the two wavelengths, the viability of the cells irradiated with LED 400 nm was omitted in the Fig. 3.12. The determination of the amount of porphyrin taken up by the cells upon incubation for 30 min with different porphyrin concentrations showed a steady increase in the extent TN-Et-PyP binding up to at least 3.5 μM of photosensitizer (Fig. 3.13.).

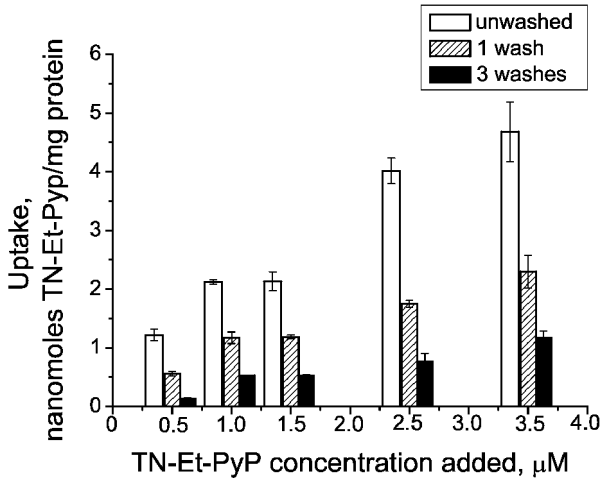

Fig. 3.13. TN-Et-PyP uptake of *E. coli* KMY1 cells incubated in the dark for 30 min with different photosensitizer concentrations

Only a fraction of the initially bound porphyrin is removed by one- or three-fold washing with PBS, indicating that a portion of the porphyrin is embedded in deeper sites of cellular envelope. This pattern of subcellular distribution could be facilitated by the structure of TN-Et-PyP molecule, where the hydrophobic contribution provided by the extended aromatic core of the molecule is counteracted by the presence of the four polar cationic moieties in the *meso* positions of the tetrapyrrolic macrocycle which may facilitate the interaction of photosensitizer with the outer membrane components such as LPS (Fig. 3.6.; 3.7. C; 3.8. C).

3.3. Morphological changes in *E. coli* KMY1 cells after photodynamic treatment

A wide range of bacterial cell districts, such as the cell envelope, cytoplasmic enzymes or DNA represent potential targets of photosensitization-induced damage, though porphyrin-mediated alterations of selected proteins in the cell envelope are reported to predominate in the initial stages of the overall photoprocess (Wainwright, 1998; Jori & Coppellotti, 2007; Salmon-Divon *et al*, 2004). As can be seen from the TEM micrographs, bacteria cells are not noticeably damaged by dark incubation with porphyrin or by the action of light alone. In all three types of the control samples the cell envelope is intact and a significant amount of bacterial cells can be seen as normally dividing (Fig. 3.3. A-C).

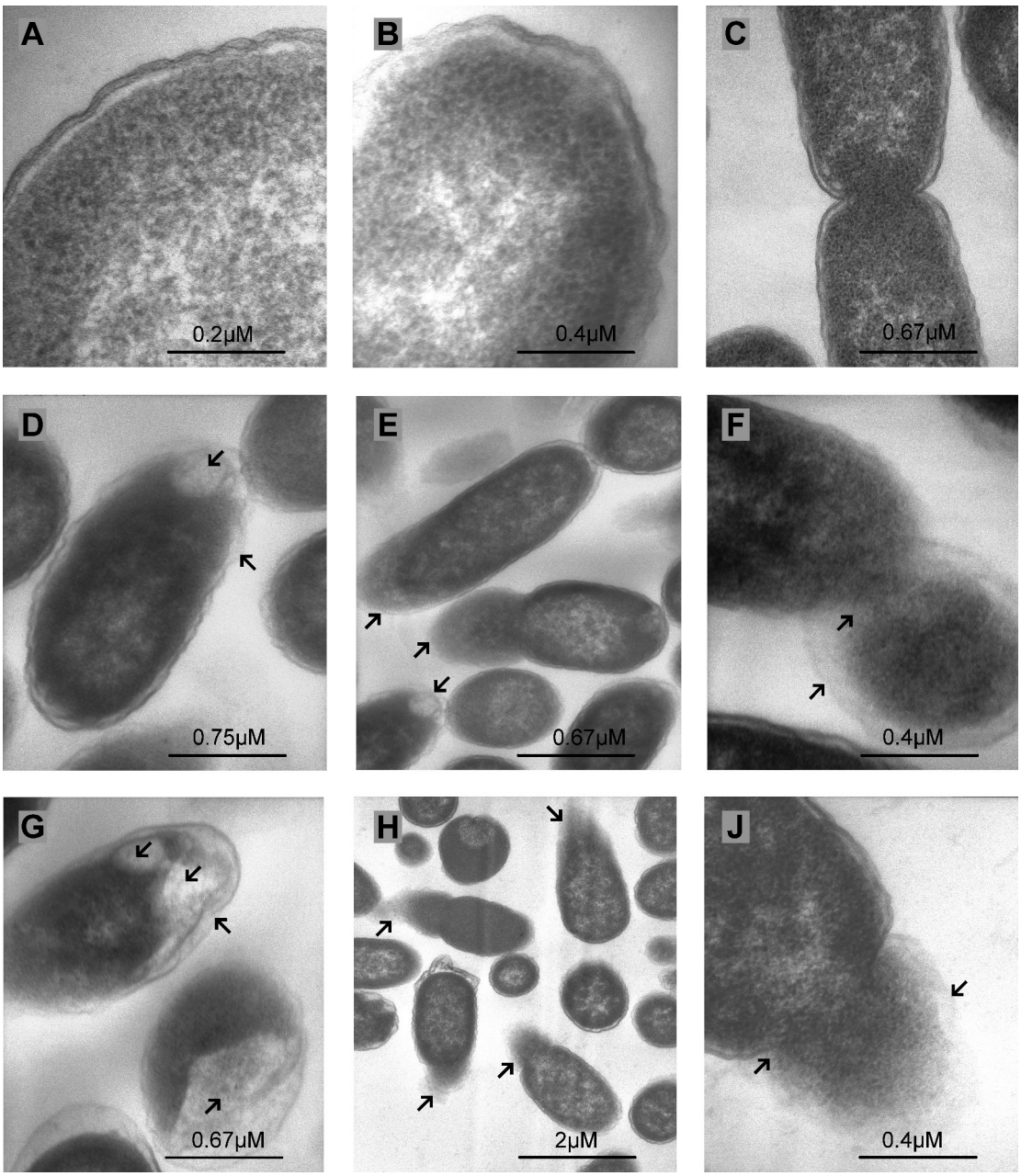

Fig. 3.14. TEM images of *E. coli* KMY1 photosensitized with TN-Et-PyP. Photosensitization was performed with $3x10^8$ cfu/ml bacteria suspended in 0.1 M PBS, pH=7.3. The bacteria suspension was incubated with TN-Et-PyP for 30 min under gentle magnetic stirring and irradiated with LED, λ=415 nm, at the dose of 20 J/cm^2. A – double control (without the dye, without irradiation); B – dark control, cells incubated in the dark with 1 μM Tn-Et-PyP; C – light control, cells irradiated without the dye; D, E, F, G – cells dark treated and irradiated with 0.25 μM photosensitizer; H, J- cells dark treated and irradiated with 1 μM photosensitizer. Small black arrows indicate damaged parts of the bacterial cell.

After irradiation with 0.25 μM TN-Et-PyP (Fig. 3.3. D-G) there is some outer membrane damage, which appears as a fuzzier image of the membrane to be compared with its pronounced margin in the control cells.

This damage is expected to increase the outer membrane permeability and allows porphyrin molecules to penetrate deeper into the cell, resulting in damage inflicted to the inner content of the bacteria that is seen as white spots abundantly occurring in the samples.

In addition, the damage of the vital plasma membrane seems to permit the leakage of the inner content, which is seen as bubble formation (Fig. 3.14. F). However, bubble-like structures are not very numerous, which corresponds with the fact that the majority of the cells are still viable (Fig. 3.12.). Irradiating bacterial cells with increasing TN-Et-PyP concentrations (up to 1 μM), results in the severe damage to both membranes in a significant number of bacteria and leakage of cell contents (Fig. 3.14. H-J). Obviously this process corresponds with decreased bacteria viability.

3.4. Permeability of inner and outer membrane

The increased permeability of membranes is usually characterised by leakage of different constituents from the cell. The presence of periplasmic alkaline phosphatase in the cell external medium can be taken as an indication of an increased permeability of the outer membrane, whereas an expulsion of β-galactosidase would reveal a damage of inner membrane compartments. Disruption of the latter compartments is often accompanied by leakage of some low molecular weight molecules, followed by DNA, RNA and other materials with strong absorbance in 260 nm region (Caminos *et al*, 2008).

It has been reported that sodium deoxycholate facilitates bacterial cell lysis if the outer membrane is damaged (Bengocheae *et al*, 1996; Rasul *et al*, 2010). The lysis could be followed by a decrease in optical density at 600 nm. However, cells coated with unimpaired outer membrane do not show any signs of lysis. According to the data presented in Fig. 3.15., cell lysis does not occur upon increasing the dye concentration when TN-Et-PyP treated bacterial cells are kept in the dark, suggesting that in this case the outer membrane is intact.

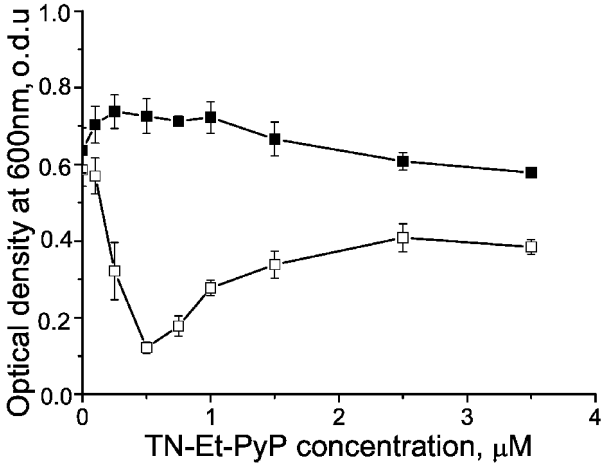

Fig. 3.15 Estimation of *E. coli* KMY1 cells outer membrane integrity by lysis with sodium deoxycholate. Outer membrane permeability was monitored according to cell lysis rate, the consequence of deoxycholate income. ■ – dark treated cells, □ – cells irradiated with TN-Et-PyP.

On the contrary, after irradiation even with dye concentrations as low as 0.5 μM, a substantial degree of lysis is seen, confirming an increased permeability of the outer membrane. Actually, almost the same amount of lysis can be achieved using 38.4 μM (or 50 μg/ml) of polymixin B sulphate, which is said to cause the extensive lysis of the cells. Unfortunately, when the TN-Et-PyP concentration reaches 0.75 μM, the lysis is shielded by release of the dye from the cells. Even six washes before applying sodium deoxycholate did not succeed in totally removing the cell component-bound dye. Since both LPS and nucleic acids were shown to interact with TN-Et-PyP (see chapter 3.1.2.) they may be attributed to the detention of the dye in the outer and, what is more important, inner regions of the cell. This finding perfectly coincides with the idea of cell envelope disruption while the bacteria are photosensitized.

In order to investigate the degree and timing of photosensitization-induced permeability in outer and inner membrane, the periplasmic alkaline phosphatase and cytoplasmic β-galactosidase assays were employed as well as monitoring of protein and 260 nm absorbing material (mostly NA) efflux from the bacterial cell. According to the data shown in Fig. 3.16. A, C an increased enzyme activity in the media was not observed, neither in the case of alkaline phosphatase nor with β-galactosidase, however both of them decreased in the cell fraction.

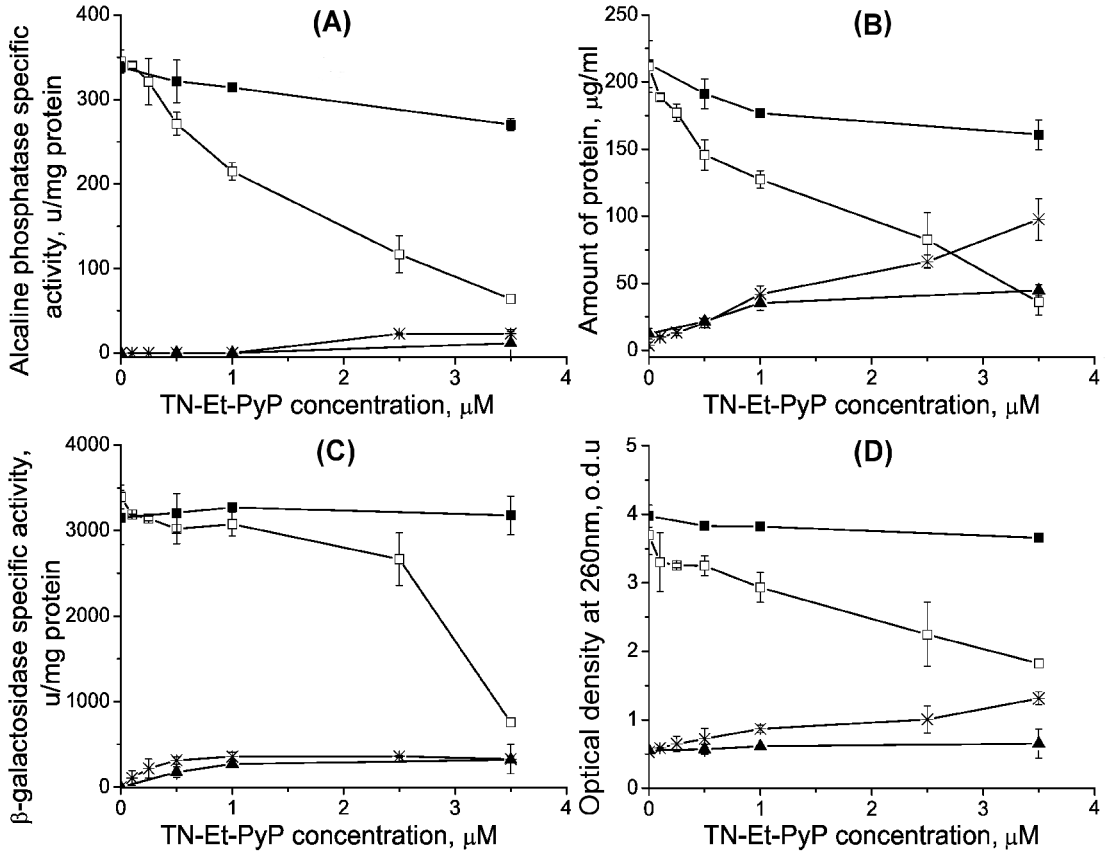

Fig. 3.16. Estimation of *E. coli* KMY1 cells outer and inner membranes integrity. Outer membrane permeability was monitored by the outcome of periplasmic alkaline phosphatase (A). Inner membrane permeability was monitored by outcome of citoplasmic β-galactosidase (C), leakage of materials absorbing at λ=260 nm (D). Protein amount changes inside and outside the cells reflect the total damage to both membranes (B). Bacteria cells were suspended in 0.1 M PBS, pH=7.3 to $3x10^8$ cfu/ml, incubated with the dye for 30 min before irradiation, which was performed with LED λ = 400 nm at the dose 20 J/cm^2. Bacteria cells were sonicated before performing enzymatic assays and measuring absorbance at λ = 260 nm. (▲ – Supernatant from non irradiated bacterial cells, * – supernatant from irradiated bacterial cells, ■ – non irradiated bacterial cells, □ – irradiated bacterial cells).

It is important to notice, that β-galactosidase activity significantly decreases only after irradiation with 2.5 μM TN-Et-PyP, while the periplasmic alkaline phosphatase is inactivated to the same extent in the presence of much lower dye concentrations. In addition, an increased amount of protein and 260 nm-absorbing compounds is observed in the media in correlation as porphyrin concentration is increased (Fig. 3.16. B, D). Naturally the amount of these molecules inside the cells is decreasing, suggesting a leakage from the bacterial cell.

3.5. Alteration of inner and outer membrane functions

The measurement of membrane voltage (Fig. 3.17.) and respiration efficiency (Fig. 3.18.) represent sensitive indications of the physiological state of inner membrane. The lipophilic nature of tetraphenylphosphonium (TPP^+) allows this compound to penetrate through hydrophobic lipid layers and this feature of the compound is widely used for estimation of membrane voltage ($\Delta\psi$, transmembrane difference of electrical potential) in objects which are negatively charged inside, such as bacteria (Rottenberg, 1986). However, the most external layer of Gram-negative bacteria outer membrane consists of negatively charged lipopolysaccharides (LPS) which form an effective barrier for the compound. Unfortunately, bacterial cells can also passively (independently of membrane voltage) bind minor amounts of TPP^+ , which is evaluated by adding polymyxin B sulfate in order to depolarize inner membrane. The barrier features of the outer membrane are bypassed by the addition of EDTA. As it has been previously shown (Vaara, 1992), EDTA removes stabilizing divalent cations from their binding sites in LPS. This results in the release of significant amount of LPS from the outer leaflet of the OM, which is changed by phospholipids, thus facilitating TPP^+ penetration. Addition of glucose contributes to increase of the membrane voltage if the inner membrane of the cell envelope is intact.

Bacterial cells treated with TN-Et-PyP in the dark show very negligible changes in membrane voltage, which could occur on account of the higher amount of porphyrin taken up by the cells, corresponding with the increased concentration of the dye added to the media (Fig. 3.17. A). This suggests that the cell inner membrane remains intact and functioning while the cells are kept in the dark. The membrane voltage loss occurs only after irradiation of bacteria in the presence of the photosensitizer, suggesting the occurrence of damage to the cell inner membrane which becomes significantly larger with increasing porphyrin concentration (Fig 3.17. B).

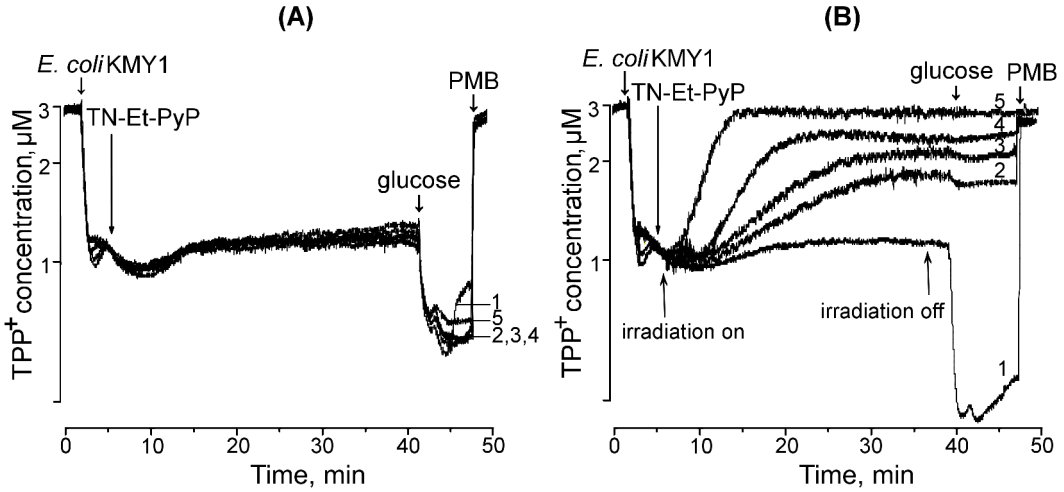

Fig. 3.17. Membrane voltage changes during irradiation with certain TN-Et-PyP concentrations (A – dark treated, B – irradiated). Bacteria were suspended in 5 ml 0.1 M Tris-HCl, (pH=8.0) placed in the vessel, thermostatted at 37°C at a concentration of $3x10^8$ cfu/ml. Irradiation was performed with LED $\lambda = 400$ nm at a dose of 20 J/cm^2. Membrane voltage was monitored as tetraphenylphosphonium ion fluxes to and from the cells. Line 1 – 0 μM TN-Et-PyP; line 2 – 0.1 μM; line 3 – 0.25 μM; line 4 – 0.5 μM; line 5 – 1 μM.

The measurements of membrane voltage can only partly elucidate the functional state of the inner membrane of bacterial cells therefore the respiration efficiency was monitored. Consumption of O_2 in bacteria treated with TN-Et-PyP in the dark does not differ significantly from the control cells that were not treated with the porphyrin. Only high concentrations that display some dark toxicity show a minor decrease of oxygen consumption (Fig. 3.18. A).

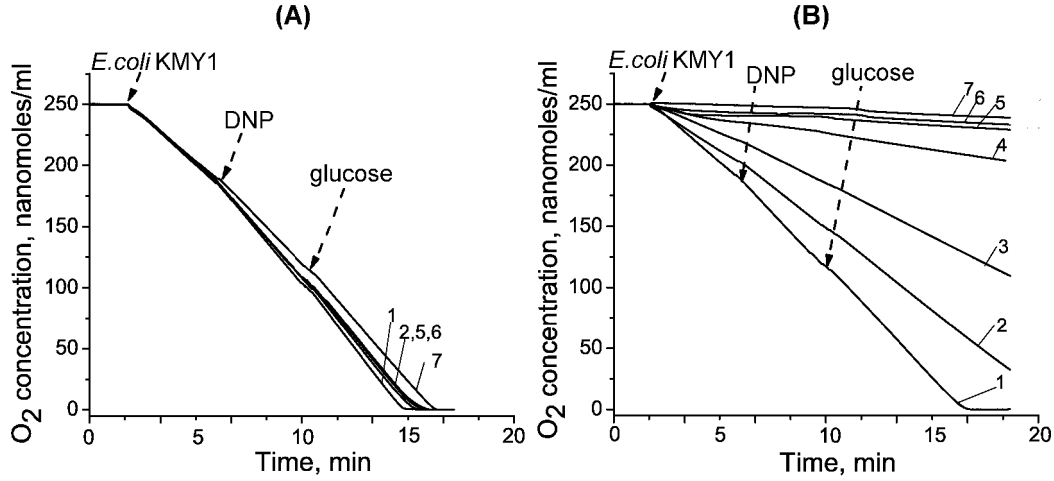

Fig. 3.18. Respiration efficiency changes in TN-Et-PyP dark treated (A) and irradiated (B) *E. coli* KMY1 cells. The samples were diluted in 0.1 M Tris-HCl, (pH=8.0) to $6x10^7$ cfu/ml before measurement. 0,002 M of DNP and 0.1 M of glucose were added to a measurement vessel. Line 1 -0 μM TN-Et-PyP; line 2 – 0.1μM; line 3 – 0.15 μM; line 4 – 0.25 μM; line 5 – 0.5 μM; line 6 – 1 μM; line 7 – 2.5 μM.

Respiration efficiency starts to diminish after irradiation with the lowest concentration used and is decreasing rapidly with increasing porphyrin concentration.

Since uncoupling effect is not seen even irradiating cells with the lowest TN-Et-PyP concentration used, it can be presumed that inactivation of the proteins residing in the membranes is the primary effect of TN-Et-PyP mediated photosensitization, whereas increased permeability is a secondary event occurring due to damage amplification in the photosensitized cell.

4. DISCUSSION

The porphyrin studied in the present investigation, namely TN-Et-PyP, belongs to the class of *meso*-substituted cationic porphyrins, which have been repeatedly shown to behave as very efficient antimicrobial photosensitizing agents (Merchat *et al*, 1996; Jori & Coppellotti, 2007; Caminos *et al*, 2008; Dai *et al*, 2009; Maish *et al*, 2010). In particular, these porphyrins are endowed with a broad spectrum of antimicrobial photodynamic activity, since they can induce an extensive killing of both Gram-positive and Gram-negative bacteria, fungi and parasitic protozoa (Merchat *et al*, 1996; Reddi *et al*, 2002; Kassab *et al*, 2002; Cormic *et al*, 2009; Smijs & Pavel, 2011). Thus, a phototherapeutic approach based on the utilization of these porphyrins could be very useful for the treatment of those infectious diseases which are characterized by the presence of a heterogeneous microbial flora or are aetiologically caused by antibiotic-resistant bacteria or fungi (Wainwright & Crossley, 2004; Maish *et al*, 2010). The results obtained in the present investigation strongly support this hypothesis and are in agreement with findings described by previous authors (Salmon-Divon *et al*, 2004; Caminos *et al*, 2008), while they allow some advancements as regards the mechanisms by which polycationic porphyrins promote the initial and eventually lethal damage of a typical representative of Gram-negative bacteria, namely *E. coli*. This bacterium was selected as a target for our studies since its sensitivity to photodynamic attacks by a number of photosensitising agents had been already assessed by different laboratories (Usatcheva *et al*, 2001; Lazzeri *et al*, 2004; Scalise & Durantini, 2005; Banfi *et al*, 2006; Hussain *et al*, 2006; Tegos *et al*, 2006b; Rossoni *et al*, 2010), moreover, the TN-Et-PyP molecule has a size and a molecular weight which prevents it from crossing the outer membrane surrounding Gram-negative bacterial cells through the porin channels, whose exclusion limit is at around 600 daltons (Nikaido, 2003).

The experiments carried out on control untreated *E. coli* cells unequivocally indicate that under our treatment conditions the observed lethal

effects can exclusively occur as a consequence of the combined action of blue light wavelengths (400 – 415 nm) and TN-Et-PyP. The incubation of the bacterial cells in the dark with the largest porphyrin concentration used in the current investigations, i.e. 3.5 μM, causes no detectable decrease in viability, as well as no appreciable change in the ultrastructural features and a variety of functional properties. On the other hand, it is apparent from the porphyrin uptake data shown in Fig. 3.13. that TN-Et-PyP displays a high affinity for some compartments of the *E. coli* external envelope, since the amount of porphyrin recovered from the bacterial cells after relatively short incubation times steadily increases with increasing porphyrin concentration in the medium, and the extent of binding does not reach a saturation value up to at least 3.5 μM TN-Et-PyP. Furthermore, about 50% or 20% of the originally bound porphyrin is still firmly associated with the *E. coli* cells after one and, respectively, three washing steps with PBS. As a consequence, it appears reasonable to suggest that a fraction of the porphyrin partitions in some districts of the outer wall, such as lipopolysaccharides. The statement is further supported by the UV-VIS absorption, fluorescence emission and excitation data, which clearly indicate the LPS – TN-Et-PyP complex formation in the model systems (Fig. 3.6., Fig 3.7. C, Fig 3.8. C). This kind of subcellular distribution pattern could be facilitated by the nature of TN-Et-PyP, where the weight of the polar contribution provided by the four positively charged quaternary nitrogen atoms in the peripheral pyridyl rings is counterbalanced by the hydrophobic contribution due to the four N-bound ethyl chains and, most of all, the flat aromatic tetrapyrrolic macrocycle. The interpretation of results obtained from studies of interaction between TN-Et-PyP and components of bacterial envelope are much more complicated, since every model system only partially reflects the situation occurring in an intact bacterial cell. Although, we were not able to perceive any significant interaction between three types of lipid molecules, prevailing in *E. coli* cells and TN-Et-PyP (Fig. 3.6.-3.9.), such events cannot be completely excluded when the living systems are concerned,

since transmembrane electrochemical gradient may play a significant role and contribute to increased porphyrin binding at least to some extent as have been reported previously (Engelman *et al*, 2007). Additionally, our studies intended to explore the possibility of TN-Et-PyP molecules to bind proteins (particularly BSA) revealed very negligible interaction (Fig. 3.6.-3.8.). However, the real situation appearing in photosensitized bacterial cell may differ, since BSA may not be the best representative of the protein, when Gram-negative bacteria are concerned. Consequently, plausible photosensitizer interaction of the porphyrin with some outer membrane proteins (particularly porins containing charged amino acids) may occur in the cells.

On the basis of these considerations, it is to be expected that the earliest targets affected by the TN-Et-PyP-photosensitized processes are localized in correspondence of the outer membrane. Since it is generally accepted that *meso*-substituted porphyrins largely act *via* the intermediacy of singlet oxygen (Moan, 1990; Foote, 1991) the photoinduced damage is likely to be confined in the microenvironment of the cell-associated photosensitizer given the circumstance that the very short lifetime of this highly reactive oxygen species generally restricts its action within an about 0.1 μm range around its generation site (Moan, 1990). Actually, TEM observations (Fig. 3.14.) clearly point out that the primary detectable modifications caused by 415 nm irradiation of TN-Et-PyP–loaded *E. coli* cells predominantly involve the external cell envelope. Thus, upon mild irradiation conditions, such as short time exposure to light in the presence of photosensitizer concentrations as low as 0.25 μM, the main morphological alterations are represented by a pronounced loss of the outlining of the outer membrane (Fig. 3.14. E); this event is indicative of a leakier three-dimensional organization of this structure. The finding is in agreement with previous reports (Nitzan *et al*, 1992; Spesia *et al*, 2009) pointing out that the photosensitized damage of *E. coli* initially involves the rupture of the outer envelope. Some authors additionally noticed (Spesia *et al*, 2009) the formation of small bubbles at the cell surface upon

irradiation of *E. coli* with a tetracationic Zn(II)-phthalocyanine, which were interpreted as arising from an oxidative stress response of outer membrane proteins to the photodynamic attack. The formation of serious photoinduced structural alterations localized in inner cellular compartments including the development of a large vesicle in close proximity of one cell pole is evident from a careful observation of the micrograph in Fig. 3.14. E-G. The vesicle is full of a significant amount of endocytoplasmic and inner membrane material. When greater porphyrin doses, such as 1 μM, were used in order to promote more extensive cell damage, TEM images (see Fig. 3.14. H-J) demonstrated the rupture of the large vesicle and consequent leakage of the inner material from the bacteria cell. Hence, it appears that the initially photoinduced increased porosity of the outer membrane prompts the penetration of the photosensitizing agent to deeper sites in the cell, so that significant amounts of porphyrin can reach the periplasmic space and the cytoplasm. The correlation between the kinetic data for the photosensitized killing of *E. coli* and the sequence of the changes in the cell ultrastructural features would indicate that the collapse of the above mentioned large vesicle has fatal consequences for the *E. coli* cells.

It is probable that the cell death is the end result of the initial enhanced degree of permeability of the outer membrane, which is possibly further amplified owing to the photooxidatively altered intracellular interactions stabilizing the tight native architecture of the inner membrane and the cytoplasm. According to the studies describing the rate and extent of photoinduced cell lysis, molecules with a molecular weight ranging from 420 (sodium deoxycholate) to 1420 (TN-Et-PyP porphyrin) can diffuse across the outer membrane after the photodamage which has been originally achieved by irradiation using a 0.25 μM porphyrin concentration (Fig. 3.15.). The redistribution of the porphyrin among the various subcellular regions should bring about additional types of damage in the new surroundings of the photosensitizing agent. This statement is supported by the observed decrease in

specific enzymatic activities, such as alkaline phosphatase and β-galactosidase (Fig. 3.16. A and C), which are known marker enzymes for testing the permeability of outer and inner membranes, as well as by the changes occurring in the membrane voltage already observed after short irradiation times (Fig. 3.17.). The membrane voltage represents a very sensitive indicator of the inner membrane integrity and its impairment could reflect alterations of the functional state of $\Delta\psi$ generators, e.g. members of the respiratory chain and ATPase which are situated in the inner membrane. It has been previously shown that different components of the oxidative phosphorylation system are inactivated during photodynamic treatment with *meso*-tetra(N-methyl-4-pyridyl)porphine, even though ATPase appears to be less susceptible than other enzymes, such as NADH dehydrogenase, since the transmembrane segments of ATPase are partially protected by inner membrane lipids (Valduga *et al*, 1999). In the case of TN-Et-PyP, *E. coli* cells show a decreased respiratory efficiency upon irradiation with increasing porphyrin concentrations (Fig. 3.18. B), which suggests the occurrence of damage to $\Delta\psi$ generators. Most importantly, as one can deduce from the plots in Fig. 3.18. B, when low porphyrin doses are used, no uncoupling effect, namely an increase in respiratory efficiency to compensate for minor lesions to the integrity of the inner membrane, is observed. This indicates that the respiratory function has been lost earlier than the alteration of the inner membrane integrity.

The concerted effect of such different types of damage to a number of subcellular compartments or constituents can markedly propagate the initial damage of the cell envelope permeability leading to the formation of gaps large enough to promote the release of an appreciable amount of 260 nm – absorbing material from the cell (Fig. 3.16. D). Such material probably comprises nucleic acids and/or proteins, and its diffusion out of the cells should represent the final step of the photoprocess. It is actually supported by spectroscopic data presented in Fig. 3.6. A – 3.8. A. The data suggest the gradual cell destruction and nucleic acid leakage from the cell, which results in

increasing amount of complex formed between negatively charged nucleic acids backbone and tetracationic porphyrin, which is exhibited by the gradually occurring Soret band shift up to 17 nm to the longer wavelength of the absorption spectra. According to the generally accepted rules for estimation of the photosensitizer – DNA interaction mode (Pasternack *et al*, 1983a,b; Mettath *et al*, 1999; Kang *et al*, 2005), the bathochromic shift (> 15 nm) in concert with strong hypochromic effect (> 35%) presumes the intercalating character of the TN-Et-PyP interaction with nucleic acids in model system. This finding is in good agreement with the previously reported results concerning intercalating mode of binding to DNA demonstrated for closely related porphyrinic photosensitizer TMPyP (Sari *et al*, 1990; Munson & Fiel, 1992). However, the absence of isobestic point in the absorption spectra of the porphyrin in model system may imply the existence of different binding complexes (for example with residual RNA) and/or the more complicated binding process because of plasmid DNA initial superspiralization. Therefore further research, particularly study of circular dichroism, are needed for final confirmation of the intercalating mode of TN-Et-PyP binding to DNA.

In conclusion, the data presented in this work allow us to propose a stepwise pathway for the killing of *E. coli* cells caused by blue light-photo activated TN-Et-PyP, thus:

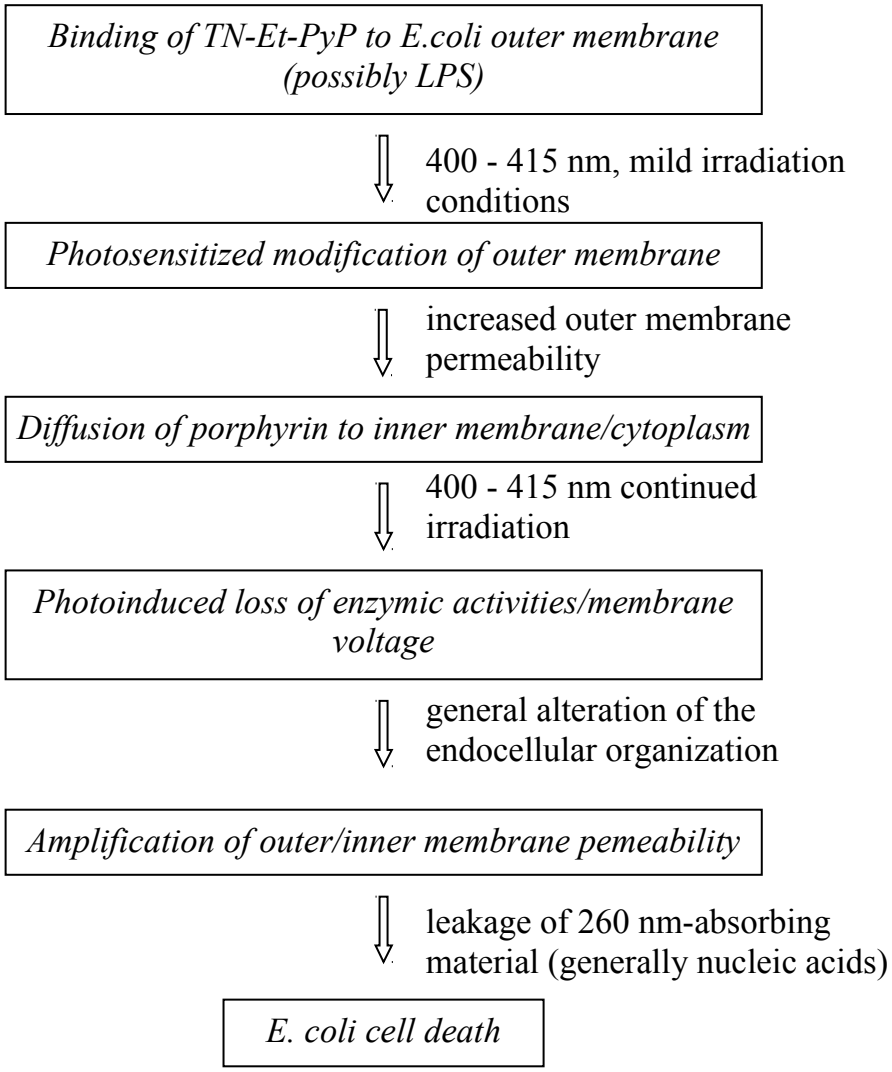
Binding of TN-Et-PyP to E.coli outer membrane (possibly LPS)
400 - 415 nm, mild irradiation conditions
Photosensitized modification of outer membrane
increased outer membrane permeability
Diffusion of porphyrin to inner membrane/cytoplasm
400 - 415 nm continued irradiation
Photoinduced loss of enzymic activities/membrane voltage
general alteration of the endocellular organization
Amplification of outer/inner membrane pemeability
leakage of 260 nm-absorbing material (generally nucleic acids)
E. coli cell death

CONCLUSIONS

1. The state of symmetry of TN-Et-PyP molecule is changing from D2b to D4b in buffered and ethanol solutions, though the time needed for conversion increases with decreasing polarity of the solvent.

2. Tetra-cationic TN-Et-PyP forms complexes with nucleic acids and lipopolysaccharides in buffer solution, the interaction being of electrostatic nature.

3. TN-Et-PyP targets *E. coli* KMY1 envelope and permeabilizes it upon irradiation with blue light.

4. The periplasmic and cytoplasmic marker enzymes alkaline phosphatase and β-galactosidase are inactivated inside the cells upon irradiation with TN-Et-PyP, though the latter loses activity after treatment with considerably larger concentration of TN-Et-PyP.

5. The membrane voltage and respiration efficiency are impaired due to photosensitized inactivation of inner membrane proteins.

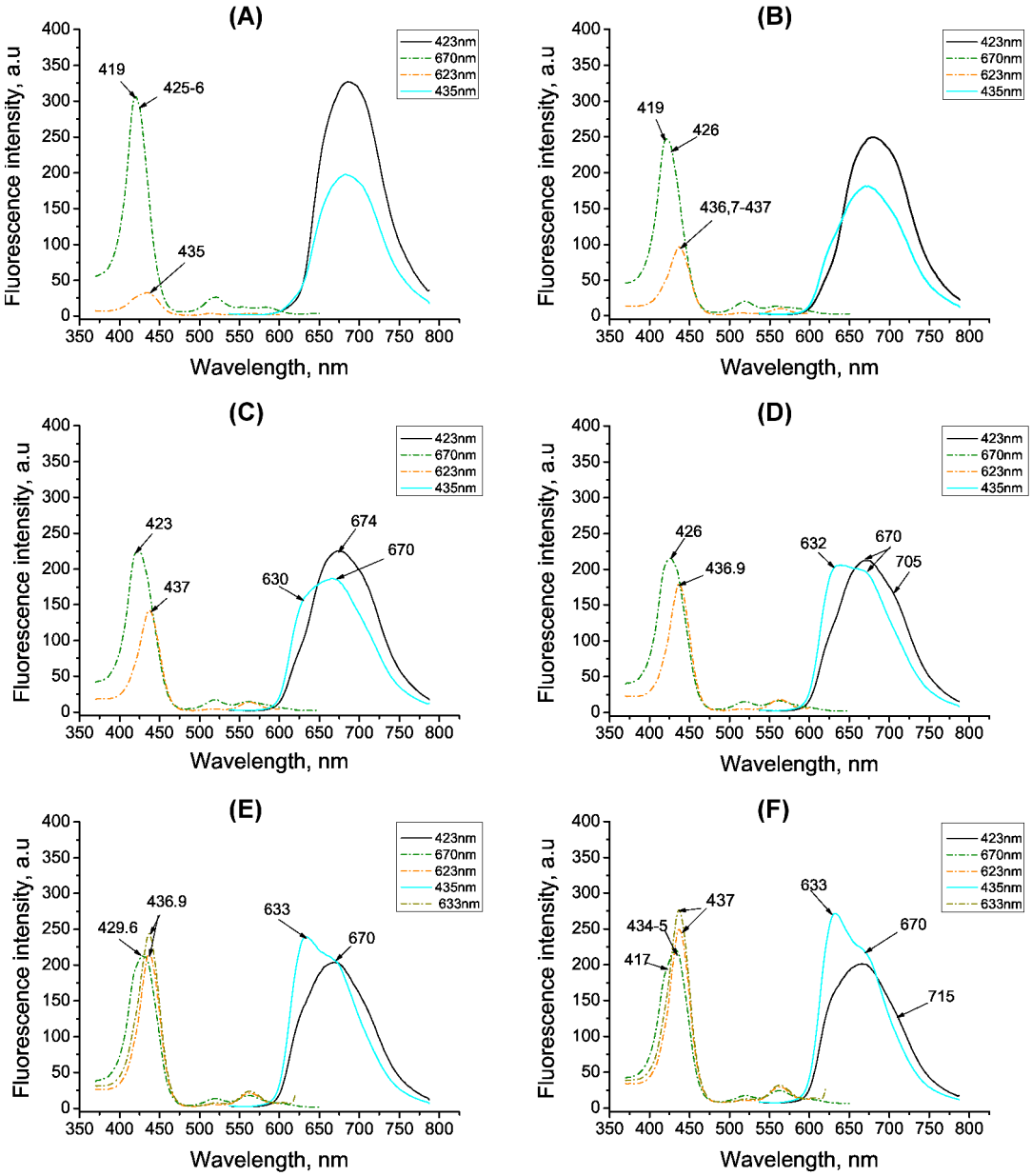

Fig. 3.19. The variation of TN-Et-PyP fluorescence emission and excitation spectra in PBS solution in time course. TN-Et-PyP solution in PBS (pH=7.3) with OD_{423nm} = 0.1 was kept in dark for 0 h (A); 1 h (B); 2 h (C); 3 h (D); 4 h (E); 5 h (F). Wavelengths of excitation and registering denoted in the legend.

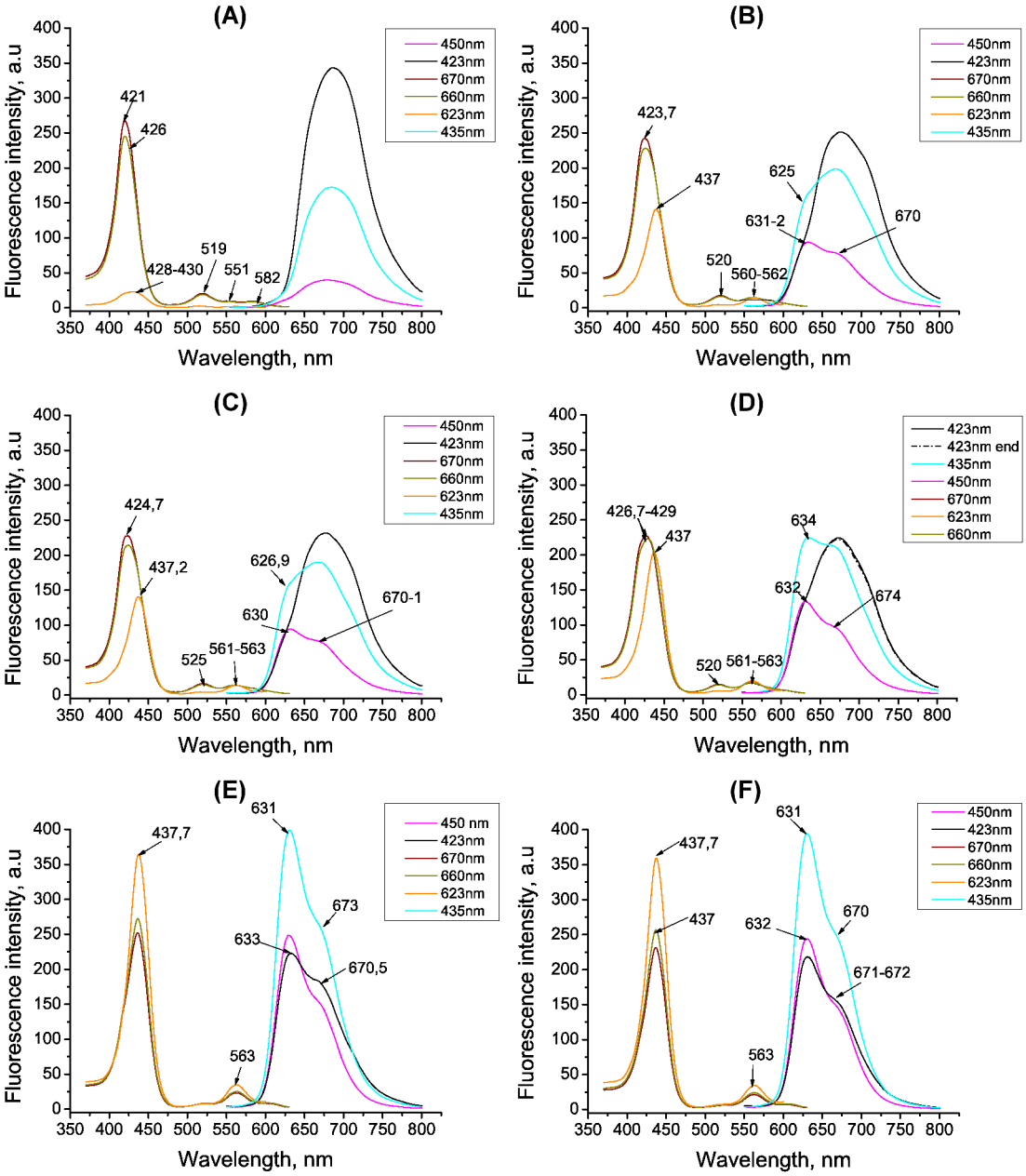

Fig. 3.20. The variation of TN-Et-PyP fluorescence emission and excitation spectra in PBS solution depending on the temperature and the time. TN-Et-PyP solution in PBS (pH=7.3) with OD_{423nm} = 0.1 (A) was heated up to 60ºC (B) cooled to room temperature (C), afterwords cooled to +4ºC (D), kept at +4ºC for 3 days (E); kept at +4ºC for 5 days (F). Wavelengths of excitation and registering denoted in the legend.

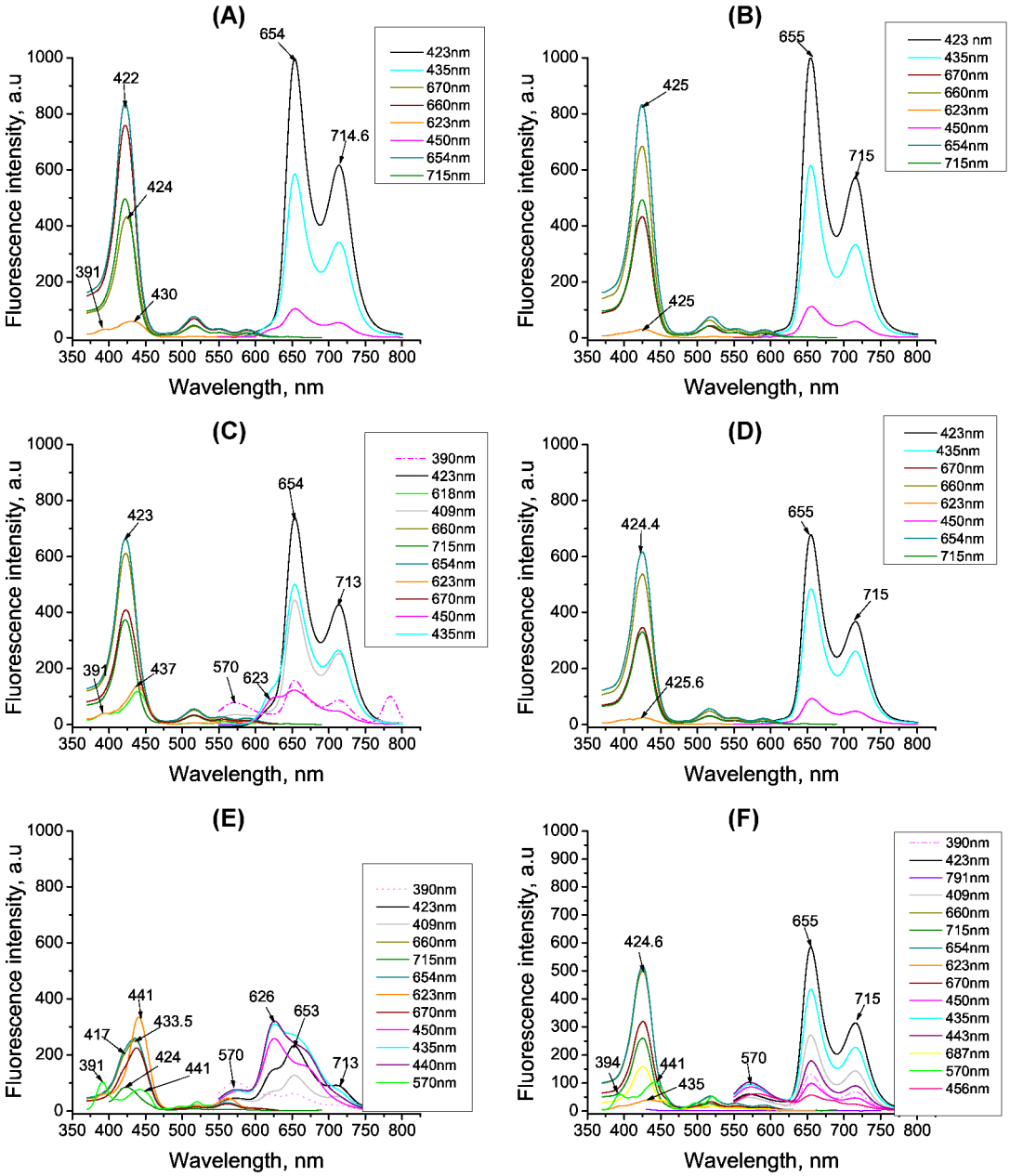

Fig. 3.21. TN-Et-PyP fluorescence emission and excitation spectra in 50% (A, C, E) and 96% (B, D, F) ethanol solutions. TN-Et-PyP was diluted to OD = 0.1 o.u with appropriate concentration of ethanol. (A) and (B) immediately after preparation; (C) and (D) – the samples were kept at +4ºC for 24h; (E) and (F) – the samples were kept at +4ºC for 3days. Wavelengths of excitation and registering denoted in the legend.

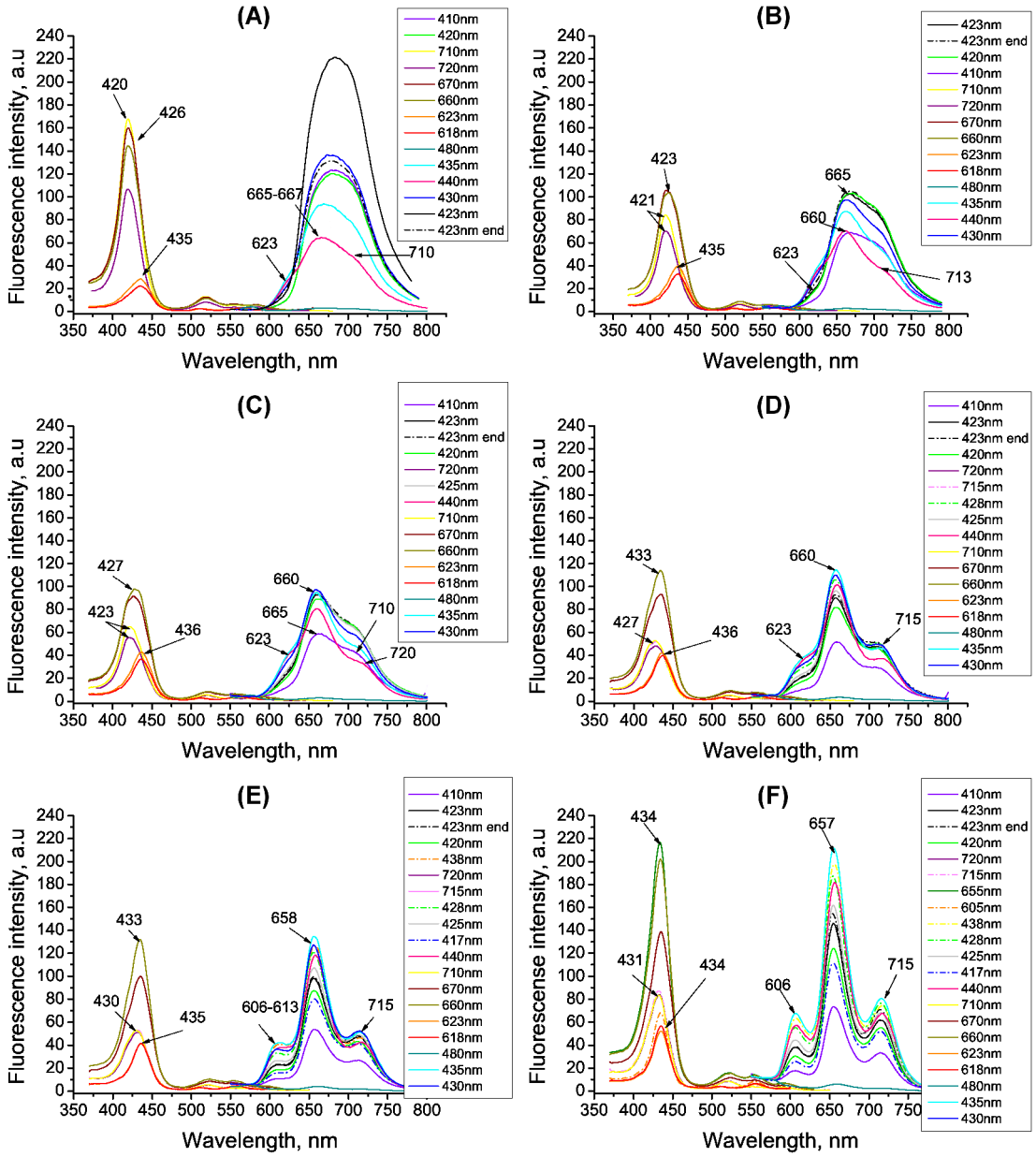

Fig. 3.22. The variation of TN-Et-PyP fluorescence emission and excitation spectra upon titration with gradually increasing NA concentration. TN-Et-PyP solution in PBS (pH=7.3) with OD_{423nm} = 0.1 was titrated with NA in molar ratio Dye:NA = 1:0 (A); Dye:NA = 1:5 (B); Dye:NA = 1:10 (C); Dye:NA = 1:25 (D); Dye:NA = 1:50 (E); Dye:NA = 1:250 (F). Wavelengths of excitation and registering denoted in the legend.

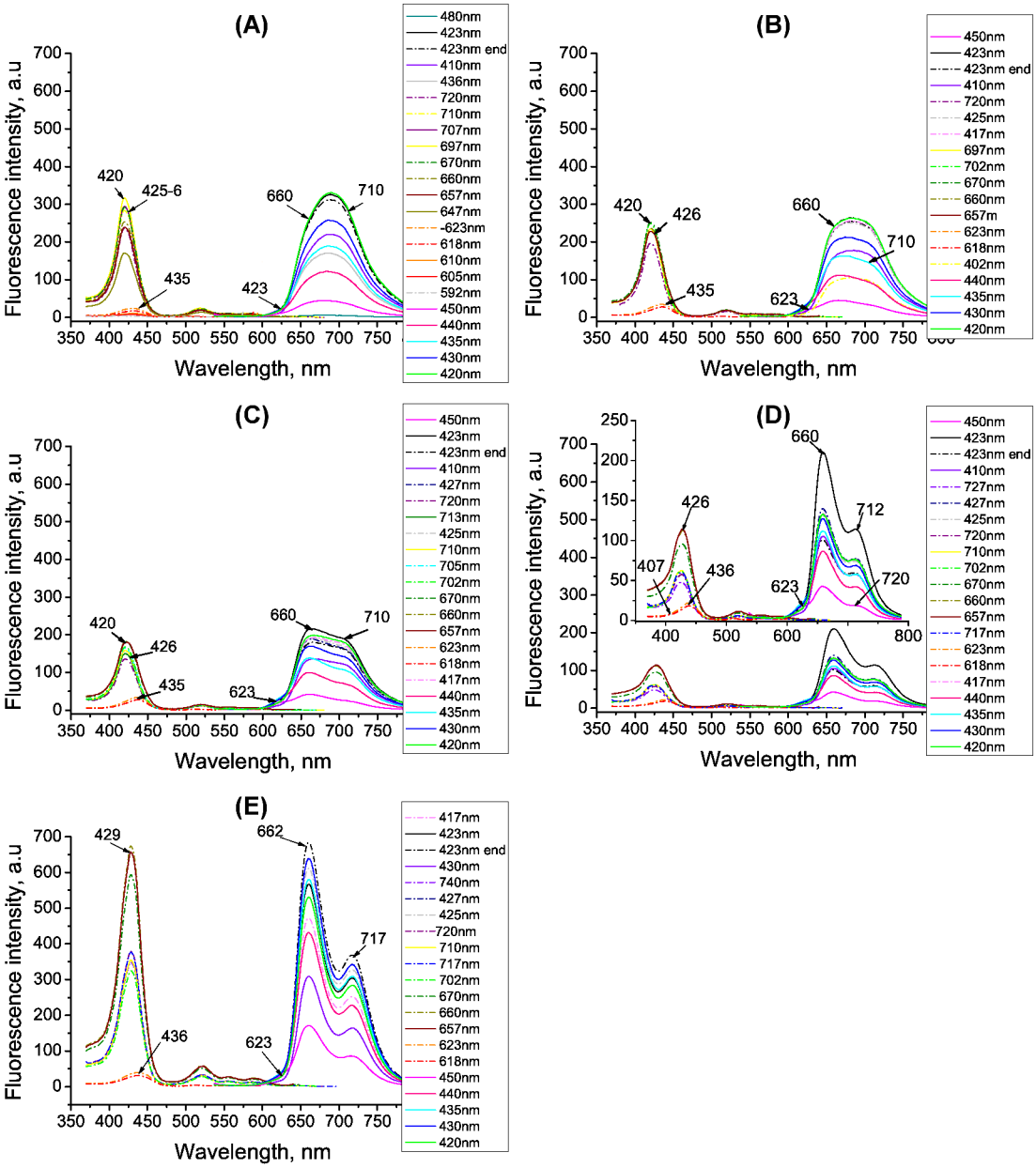

Fig. 3.23. The variation of TN-Et-PyP fluorescence emission and excitation spectra upon titration with gradually increasing SDS concentration. TN-Et-PyP solution in PBS (pH=7.3) with OD_{423nm} = 0.1 was titrated with SDS in molar ratio Dye:SDS = 1:0 (A); Dye:SDS = 1:50 (B); Dye:SDS = 1:100 (C); Dye:SDS = 1:250 (D); Dye:SDS = 1:500 (E). Wavelengths of excitation and registering denoted in the legend.

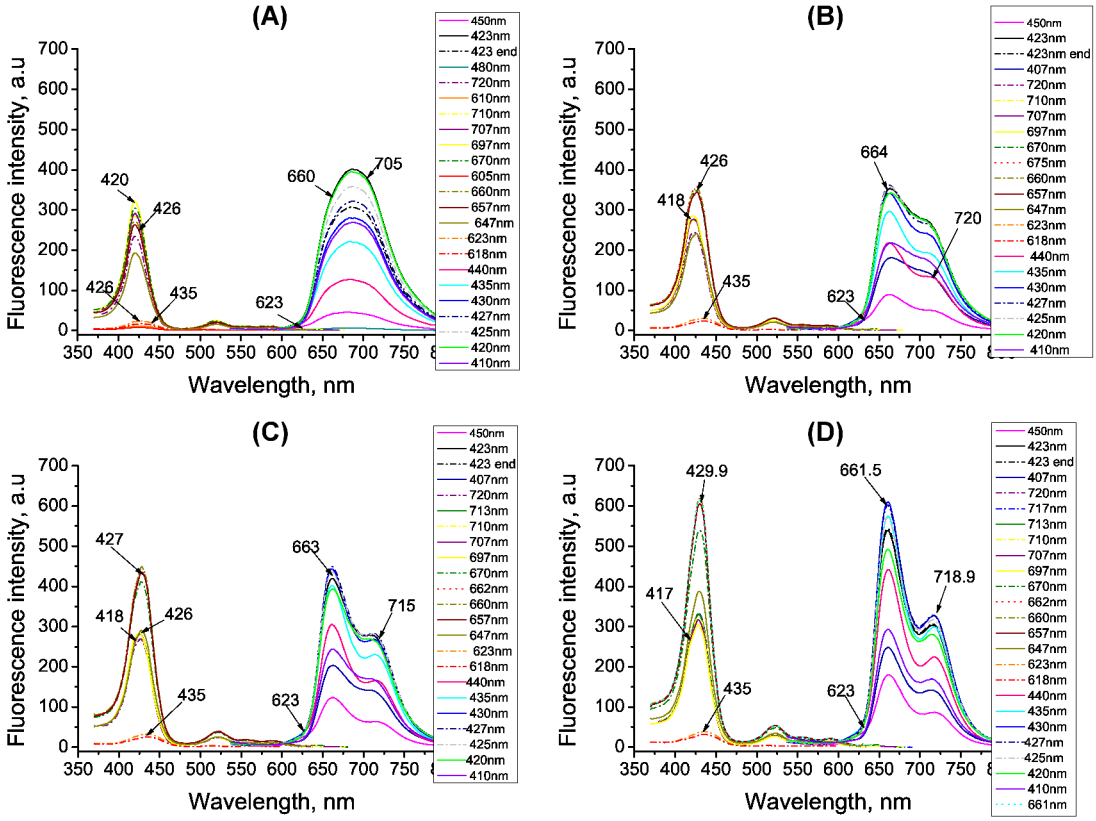

Fig. 3.24. The variation of TN-Et-PyP fluorescence emission and excitation spectra upon titration with gradually increasing LPS concentration. TN-Et-PyP solution in PBS (pH=7.3) with OD_{423nm} = 0.1 was titrated with LPS in molar ratio Dye:LPS = 1:0 (A); Dye:LPS = 1:5 (B); Dye:LPS = 1:10 (C); Dye:LPS = 1:25 (D); Wavelengths of excitation and registering denoted in the legend.

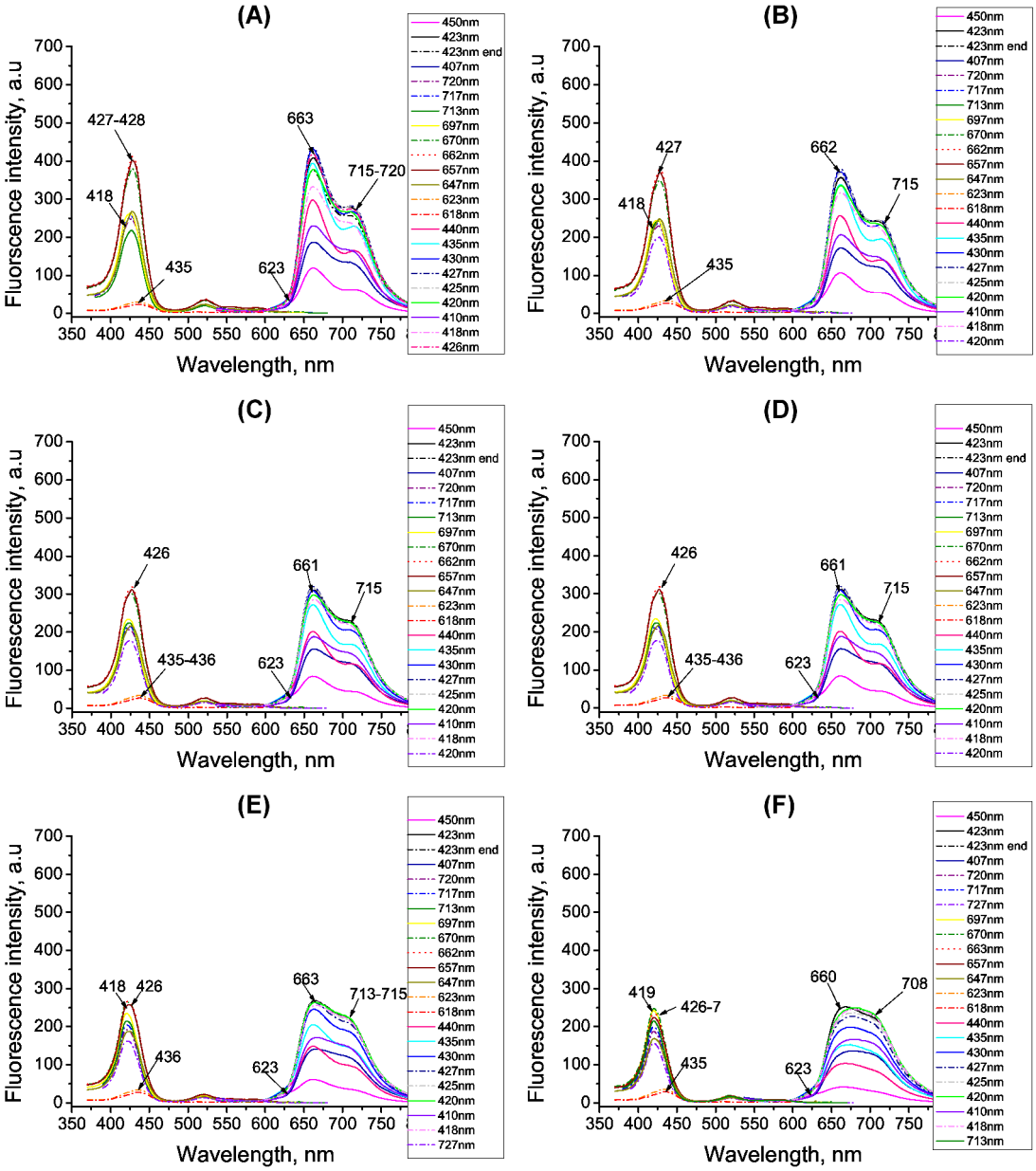

Fig. 3.25. The variation of TN-Et-PyP fluorescence emission and excitation spectra upon addition of LPS in molar ratio Dye:LPS = 1:10 and afterwards titration with gradually increasing $MgCl_2$ concentration: (A) – molar ratio Dye:LPS:$MgCl_2$ = 1:10:0; (B) – Dye:LPS:$MgCl_2$ = 1:10:0.05; (C) – Dye:LPS:$MgCl_2$ = 1:10:0.5; (D) – Dye:LPS:$MgCl_2$ = 1:10:1; (E) – Dye:LPS:$MgCl_2$ = 1:10:5; (F) – Dye:LPS:$MgCl_2$ = 1:10:10. Wavelengths of excitation and registering denoted in the legend.

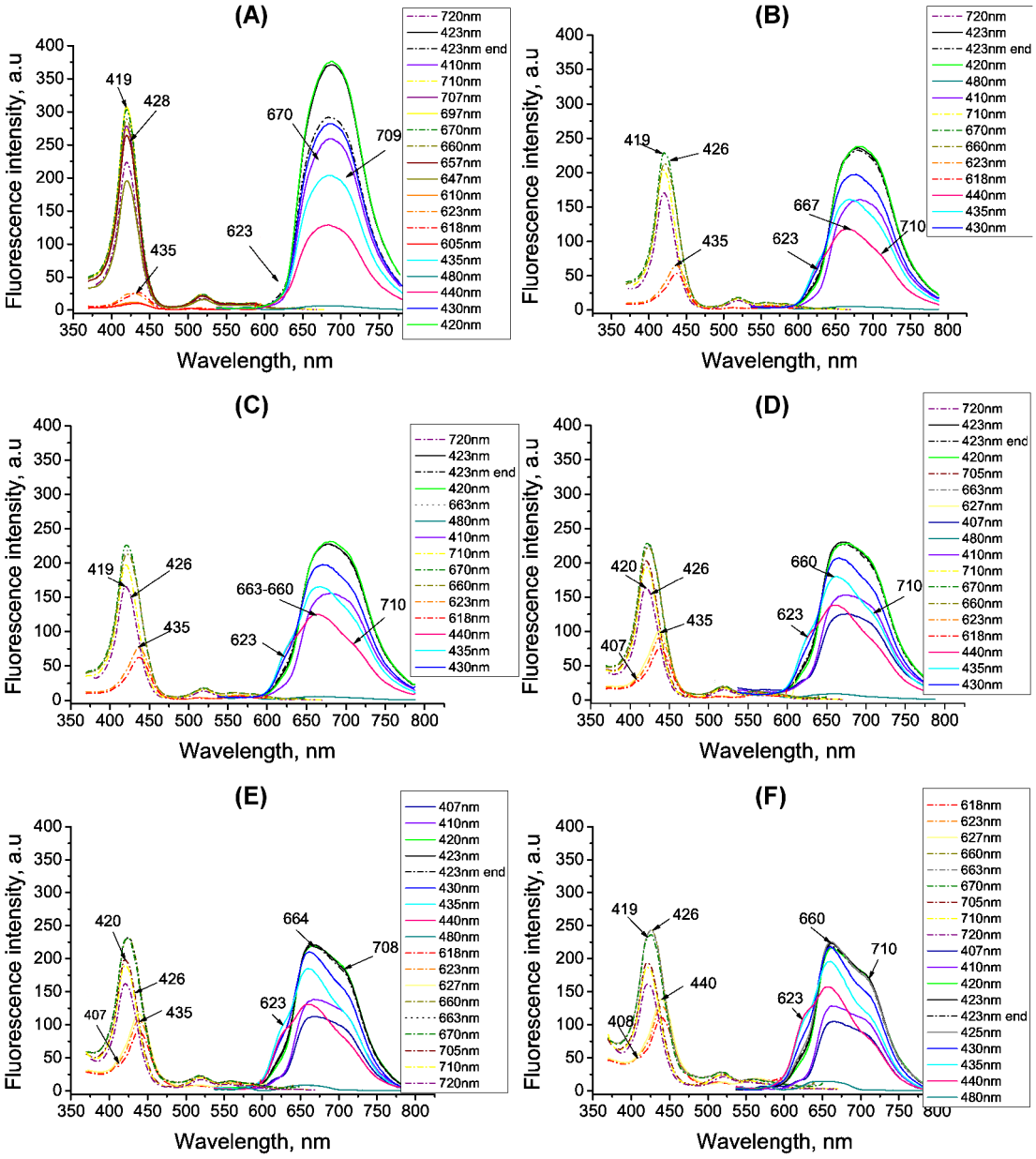

Fig. 3.26. The variation of TN-Et-PyP fluorescence emission and excitation spectra upon titration with gradually increasing lipid concentration. TN-Et-PyP solution in PBS (pH=7.3) with OD_{423nm} = 0.1 was titrated with lipids in molar ratio Dye:lipids = 1:0 (A); Dye:lipids = 1:22 (B); Dye:lipids = 1:50 (C); Dye:lipids = 1:250 (D); Dye:lipids = 1:500 (E); Dye:lipids = 1:1500 (F). Wavelengths of excitation and registering denoted in the legend.

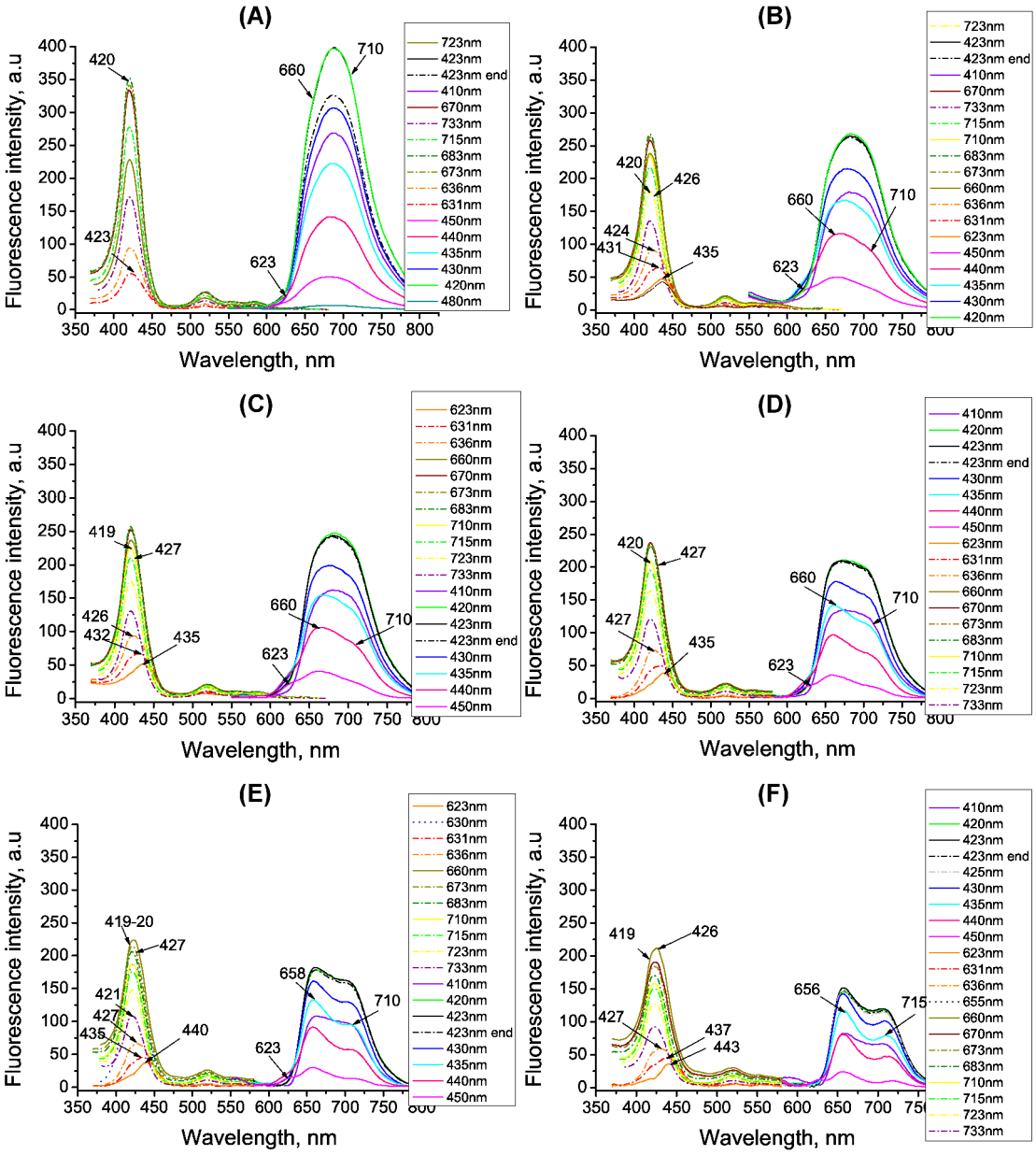

Fig. 3.27. The variation of TN-Et-PyP fluorescence emission and excitation spectra upon titration with gradually increasing BSA concentration. TN-Et-PyP solution in PBS (pH=7.3) with OD_{423nm} = 0.1 was titrated with BSA in molar ratio Dye:BSA = 1:0 (A); Dye:BSA = 1:50 (B); Dye:BSA = 1:100 (C); Dye:BSA = 1:250 (D); Dye:BSA = 1:500 (E); Dye:BSA = 1:1000 (F). Wavelengths of excitation and registering denoted in the legend.

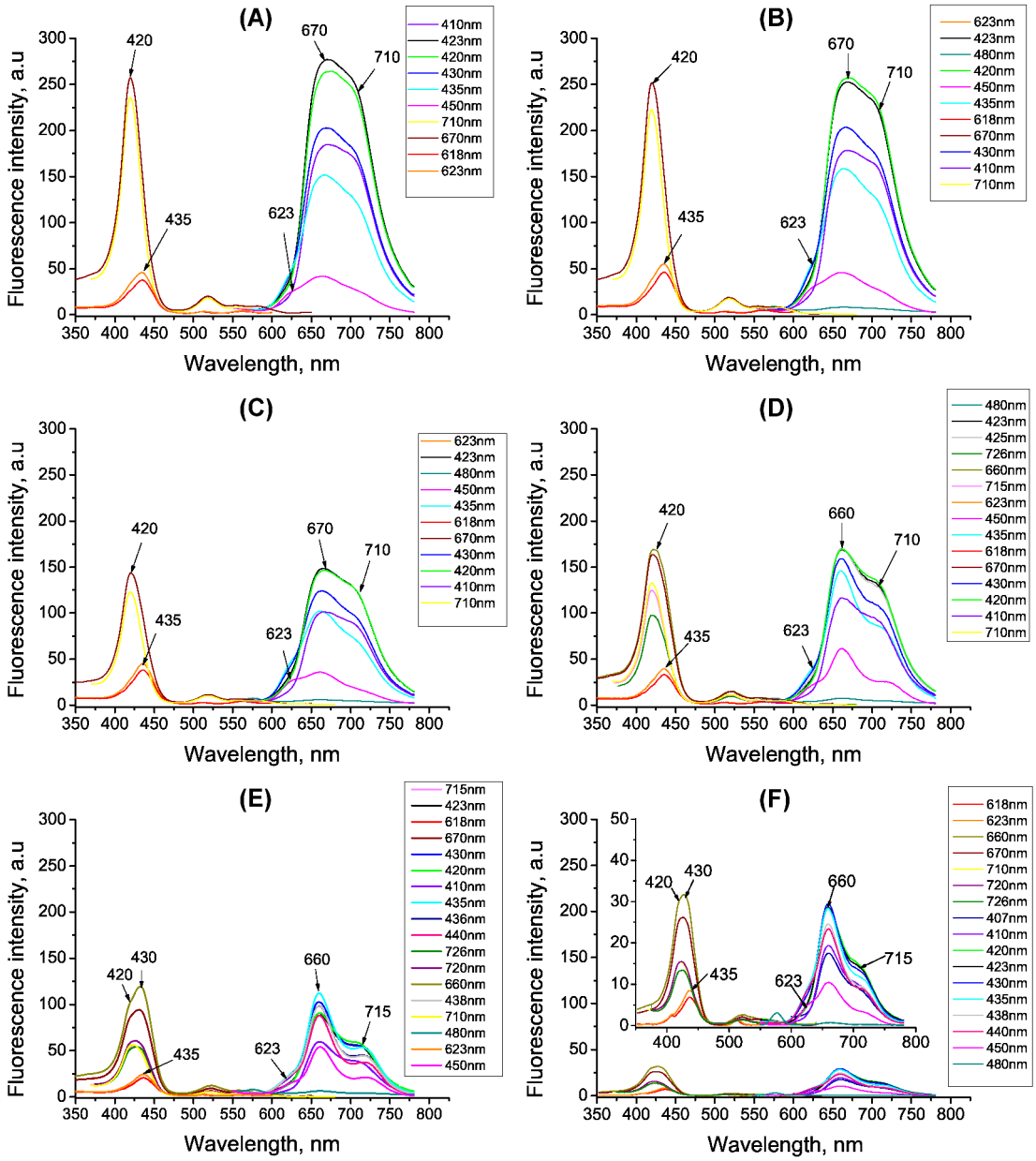

Fig. 3.28. The variation of TN-Et-PyP fluorescence emission and excitation spectra in the supernatant left after harvesting *E. coli* KMY1 cells treated with the porphyrin. *E. coli* KMY1 suspension was mixed with TN-Et-PyP at total OD_{423nm} = 0.1. The suspension was irradiated with increasing light dose (6 J/cm^2, 18 J/cm^2, 36 J/cm^2, 72 J/cm^2) or kept in the dark for the time periods equal to irradiation time. Afterwards the cells were harvested by centrifugation. The fluorescence excitation and emission spectra of the porphyrin left in the supernatant were recorded. (A) – the porphyrin in supernatant from non irradiated cells; (B) – the porphyrin in supernatant from non irradiated cells kept in the dark for the time equal to irradiation with 72 J/cm^2; (C) – the porphyrin in supernatant from cells irradiated with 6 J/cm^2; (D) – the porphyrin in supernatant from cells irradiated with 18 J/cm^2; (E) – the porphyrin in supernatant from cells irradiated with 36 J/cm^2; (F) – the porphyrin in supernatant from cells irradiated with 72 J/cm^2.

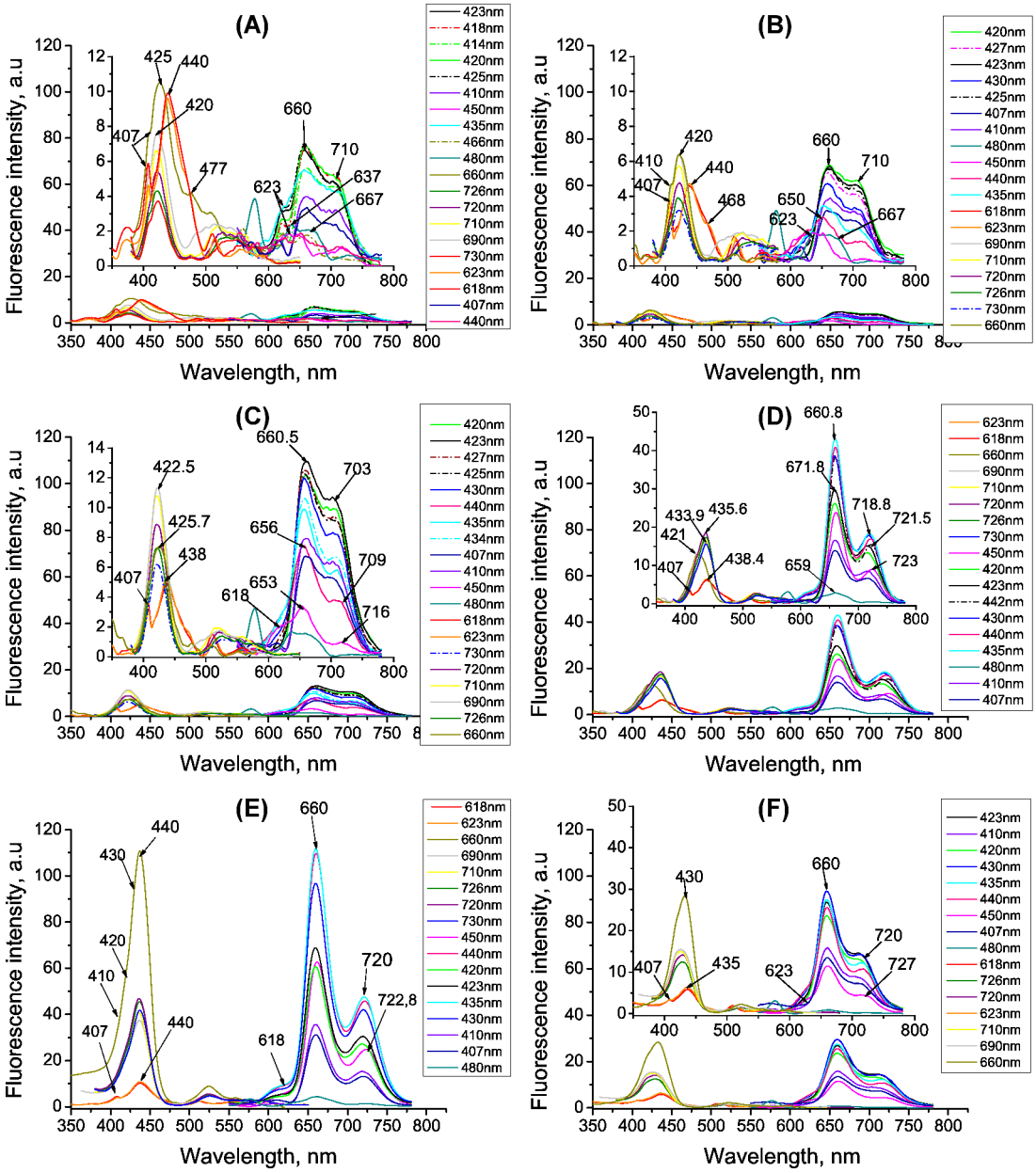

Fig. 3.29. The variation of TN-Et-PyP fluorescence emission and excitation spectra in the supernatant left after harvesting *E. coli* KMY1 cells treated with the porphyrin. *E. coli* KMY1 suspension was mixed with TN-Et-PyP at total OD_{423nm} = 0.1. The suspension was irradiated with increasing light dose (6 J/cm^2, 18 J/cm^2, 36 J/cm^2, 72 J/cm^2) or kept in the dark for the time periods equal to irradiation time. Afterwards the cells were harvested by centrifugation and resuspended in sterile PBS (pH = 7.3). The fluorescence excitation and emission spectra of the porphyrin left in the bacterial cell fraction were recorded. (A) – the porphyrin in non irradiated cell suspension; (B) – the porphyrin in non irradiated cell suspension kept in the dark for the time equal to irradiation with 72 J/cm^2; (C) – the porphyrin in cell suspension irradiated with 6 J/cm^2; (D) – the porphyrin in cell suspension irradiated with 18 J/cm^2 ; (E) – the porphyrin in cell suspension irradiated with 36 J/cm^2; (F) – the porphyrin in cell suspension irradiated with 72 J/cm^2.

Acknowledgements

I would like to express gratitude to all the people who supported and helped me during the work on the thesis:

Vida Kirvelienė for the ability of doctoral studies.

My supervisor Elenutė Bakienė for tolerance and freedom to implement some of my own ideas into the work, for enormous help with the scientific literature, critical reading of the dissertation manuscript, the immense warmth and care I received working together.

My scientific advisor Saulius Bagdonas for excellent guidance in spectroscopy and the infinity of patience in explaining my stupid questions, for the feeling of being a welcome guest in your lab.

Prof. Giulio Jori and his group (Michy, Clara and Monica) for showing me the world of photobiology, for generously sharing their experience, for patience and enormous help in work and in preparing the article, for two unforgettable summers in Padova and Bressannone.

Jurgis Kadziauskas for critical reading the manuscript of the dissertation, valuable suggestions and asking the right questions that made me see my work in another light.

Ramutė Pagalytė, Arvydas Markuckas, Julija Armalytė, Vaida Šeputienė, Daiva Dabkevičienė for advices, sharing the reagents and experience. My warmest appreciation for all of you.

Special thanks for all the other people in the department, who helped with the equipment, were friendly and welcoming, while I was working in their labs.

My special gratitude to Justina Šileikytė and Saulius Bagdonas for the help in connecting Prof. G. Jori.

Sandra Stukaitė, Simona Gliebutė, Ana Solopova, Silvija Zulgytė, Lina Jakutytė, Andrius Buivydas, Natalija Ciurkaniuk, Tadas Misiūnas for being perfect colleagues and encouraging friends..

My Parents for their love, support and always believing in me.

REFERENCES

1. **Abe H., Wagner S. J. (1995).** Analysis of viral DNA, protein and envelope damage after methylene blue, phthalocyanine derivative or merocyanine 540 photosensitization, *Photochem Photobiol*, 61, 402–9.

2. **Allaker R. P. (2010).** The use of nanoparticles to control oral biofilm formation, *J Dent Res*, 89, 11, 1175-1186.

3. **Alves E., Costa L., Carvalho C. M. B., Tome J. P. C., Faustino M. A., Neves M. G. P. M. S., Tome A. C., Cavaleiro J. A. S., Cunha A., Almeida A. (2009)** Charge effect on the photoinactivation of Gram-negative and Gram-positive bacteria by cationic meso-substituted porphyrins, *BMC Microbiology*, 9,70, doi:10.1186/1471-2180-9-70.

4. **Allen M. C., Weber J. M., van Lier J. E. (1995).** Sulphophthalocyanines for photodynamic inactivation of viruses in blood products-effects of structural modifications, *Photochem Photobiol*, 62, 184-189.

5. **Atsay A., Koca A., Koçak M. B., (2009)**. Synthesis, electrochemistry and in situ spectroelectrochemistry of water-soluble phthalocyanines, *Transition Met Chem*, 34, 877-890.

6. **Arbogast J. W., Darmanyan A. P., Foote C. H. S., Rubin Y., Diederich F. N., Alvarez M. M., Anz S. J., Whetten R. L. (1991)** Photophyslcal Properties of C60, *J Phys Chem*, 95*,* 11-17.

7. **Aveline B. M. (2001)** ch 2 Primary processes in photosensitization mechanisms in book; Photodynamic therapy and fluorescence diagnosis in dermatology ed. by Calvazara-Pinton P., Szeimes R. M., Ortel B, 1st ed, Elsevier science BV, Netherlands, 17-39.

8. **Bachmann B., Knüver-Hopf J., Lambrecht B., Mohr, H. (1995).** Target structures for HIV-1 inactivation by methylene blue and light, *J Med Virol*, 47, 172–178.

9. **Bauman N. M., Smith R. J. H. (1996).** Recurrent respiratorypapillomatosis, *Pediatr Clin North Am*, 43, 1385-1401.

10. **Banfi S., Caruso E., Buccafurni L., Battini V., Zazzaron S., Barbieri P., Orlandi V. (2006)**. Antibacterial activity of tetraaryl-porphyrin photosensitizers: An in vitro study on Gram negative and Gram positive bacteria, *J Photochem Photobiol B,* 85, 28-38.

11. **Bellin J.S., Grossman L.I. (1965).** Photodynamic degradation of nucleic acids, *Photochem Photobiol*, 4, 45-58.

12. **Bengoecheae J. A., Diaz R., Moriyon I. (1996).** Outer membrane differences between pathogenic and environmental *Yersinia enterocolitica* probed with

hydrophobic permeants and polycationic peptides, *Infect Immun*, 64, 12, 4891–4899.

13. **Ben-Hur E., Horowitz B. (1996)** Virus inactivation in blood, *AIDS*, 10, 1183-1190.

14. **Benkoski J. J., Jesorka A., Edvardsson M., Hook F. (2006).** Light-regulated release of liposomes from phospholipid membranes via photoresponsive polymer-DNA conjugates, *Soft Matter* 2, 710–715.

15. **Bertiaume F., Reiken S., Toner M., Tompkins R., Yarmush M. (1994).** Antibody targeted photolysis in bacteria in vivo, *Biotechnology*, 12, 703-706.

16. **Berlett B. S. & Stadtman E. R. (1997).** Protein oxidation in aging, disease and oxidative stress, *J Biol Chem*, 272, 33, 20323-20316.

17. **Bertoloni G., Salvato B., Dall'Acqua M., Vazzoler M., Jori G. (1984).** Hematoporphyrin – sensitized photoinactivation of *Streptococcus faecalis, Photochem Photobiol*, 39, 6, 811-816.

18. **Bertoloni G., Rossi F., Valduga G., Jori G., van Lier J. E. (1990)** Photosensitizing activity of water- and lipid-soluble phthalocyanines on *Escherichia coli, FEMS Microbiol Lett*, 59, 149-155.

19. **Bhatti M., MacRobert A., Meghji S., Henderson B., Wilson M. (1998)** A study of the uptake of toluidine blue O by Porphyromonas gingivalis and the mechanism of lethal photosensitization, *Photochem Photobiol*, 68, 370-376.

20. **Bhatti M., MacRoberts A., Henderson B., Sheperd P., Crindland J., Wilson M. (2000).** Antibody – targeted lethal photosensitization of *Porphyromonas gingivalis*, *Antimicrob Agents Chemother*, 44, 10, 2615-2618.

21. **Biel M. A. (2010)** Photodynamic therapy of bacterial and fungal biofilm infections, *Methods Mol Biol*, 635, 175-194.

22. **Bombelli C., Bordi F., Ferro S., Giansanti L., Jori G., Mancini G., Mazzuca C, Monti D, Ricchelli F., Sennato S, Venanzi M. (2008)**. New cationic liposomes as vehicles of m-tetrahydroxyphenylchlorin in photodynamic therapy of infectious diseases, *Mol Pharm*, 5, 4, 672-679.

23. **Bozzola J. J., Russell L. D. (1999).** Electron microscopy, ch. 2 Specimen preparation for transmission electron microscopy, ch.4 Ultramicrotomy, 18-46; 74-109 2nd ed, Jones & Bartlett Publishers, Sudbury, Mass.

24. **Bronshtein I., Smith K. M., Ehrenberg B. (2005).** The effect of pH on the topography of porphyrins in lipid membranes, *Photochem Photobiol*, 81, 446-451.

25. **Burns T., Wilson M., Pearson G. J. (1994).** Killing the cariogenic bacteria by light from gallium aluminum arsenide diode laser, *J Dent*, 22, 273-278.

26. **Calin M. A., Parasca S.V. (2009)**. Light sources for photodynamic inactivation of bacteria, *Lasers Med Sci*, 24, 3, 453-460.

27. **Caminos D. A., Spesia M. B., Durantini E. N. (2006).** Photodynamic inactivation of *Escherichia coli* by novel meso-substituted porphyrins by 4-(3-N,N,N-trimethylammoniumpropoxy)phenyl and 4-(trifluoromethyl)phenyl groups, *Photochem Photobiol Sci*, 5 (I), 56-65.

28. **Caminos D. C., Spesia M. B., Pons P., Durantini E. N. (2008).** Mechanisms of *Escherichia coli* photodynamic inactivation by an amphiphylic tricationic 5,10,15,20-tetr(4-N,N,N-trimethylamoniumphenyl) porphyrin, *Photochem Photobiol Sci,* 7, 1071-1078.

29. **Carlton N. M. (1999).** Phage therapy: past history and future prospects, *Arch Immunol Ther Exp*, 47, 5, 267-274.

30. **Cassidy C. M., Donnelly R. F., Tunney M. M. (2010)** Effect of sub-lethal challenge with Photodynamic Antibacterial Chemotherapy (PACT) on the antibiotic susceptibility of clinical bacterial isolates, *J Photochem Photobiol B*, 99, 1, 62-66.

31. **Cassidy C. M., Tunney M. M., Magee N. D., Elborn J. S., Bell S., Singh T. R., Donnelly R. F. (2011)**. Drug and light delivery strategies for photodynamic antimicrobial chemotherapy (PACT) of pulmonary pathogens: a pilot study, *Photodiagnosis Photodyn Ther*, 8, 1, 1-6.

32. **Castano A. P., Demidova T. N., Hamblin M.R. (2004).** Mechanisms in photodynamic therapy: part one——photosensitizers, photochemistry and cellular localization**.** *Photodiagnosis and Photodynamic Therapy,* 1, 279—293.

33. **Castano A. P., Demidova T. N., Hamblin M.R. (2005).** Mechanisms in photodynamic therapy: part two——cellular signaling, cell metabolism and modes of cell deat,. *Photodiagnosis and Photodynamic Therapy,* 2, 1—23.

34. **Cavalcante A. C. D., Martinez G. R., Di Mascio P., Menck C. F. M., Agnez-Lima L. F. (2002)** Cytotoxicity and mutagenesis induced by singlet oxygen in wild type and DNA repair deficient *Escherichia coli* strains, *DNA Repair I*, 1051-1056.

35. **Chatterjee S. R., Shetty S. J., Devasagayam T. P. A., Srivastava T. S. (1997).** Photocleavage of plasmid DNA by the prophyrin *meso-tetralds* [4-(carboxymethyleneoxy) phenyl] porphyrin**,** *J Photochem Photobiol B*, 41, 128—135.

36. **Choi S. S., Lee H. K., Chae H. S. (2010)** In vitro photodynamic antimicrobial activity of methylene blue and endoscopic white light against Helicobacter pylori 26695, *J Photochem Photobiol B*, 101, 3, 206-209.

37. **Chopra I. (2002).** Encyclopedia of Life Sciences, ch. Antibiotics, John Wiley and Sons Ltd., www.els.net.

38. **Cohen S. N., Chang A. C. Y., Hsu L. (1972).** Nonchromosaomal antibiotic resistance in bacteria: Genetic transformation of *Escherichia coli* by R-factor DNA, *PNAS*, 69, 2110-2114.

39. **Collins T. L., Markus E. A., Hassett D. J., Robinson J. B. (2010)**. The effect of a cationic porphyrin on *Pseudomonas aeruginosa* biofilms, *Curr Microbiol*, 61, 5, 411-416.

40. **Cormic M. P., Alvarez M. G., Rovera M., Durantini E. N. (2009).** Photodynamic inactivation of Candida albicans sensitized by tri- and tetracationic porphyrin derivatives, *Eur J Med Chem*, 44, 4, 1592-1599.

41. **Croke D. T., Perrouault L., Sari M. A., Battioni J. P., Mansuy D., Helene C., Le Doan T. (1993)**. Structure-activity relationships for DNA photocleavage by cationic porphyrins, *J Photochem Photobiol B*, 18, 41-50.

42. **Cvirkaitė-Krupovič V., Poranen M., Bamford D. H. (2010).** Phospholipids act as a secondary receptor during the entry of enveloped dsRNA bacteriophage phi6, *J Gen Virol*, Pt 8, 2116-2120.

43. **Dai T., Huang Y. Y., Hamblin M. R. (2009).** Photodynamic therapy for localized infections – State of the art, *Photodiagnosis and Photodynamic Therapy*, 6, 170-188.

44. **Dai T., Huang Y. Y., Sharma S. K., Hashmi J. T., Kurup D. B., Hamblin M. R. (2010).** Topical antimicrobials for burn wound infections, *Recent patents on Anti-Infective Drug Discovery*, 5, 124-151.

45. **Dean R. L. (2002).** Kinetic studies with alkaline phosphatase in the presence and absence of inhibitors and divalent cations, *Biochem Mol Bio. Educ*, 30**,** 6, 401–407.

46. **DeFedericis H-C., Patrzyc H. B., Rajecki M. J., Budzinski E. E., Iijima H., Dawidzik J. B., Evams M. S., Greene K. F., Box H. C. (2006).** Singlet oxygen induced DNA damage, *Radiation Research*, 165, 4, 445-451.

47. **Demidova T. N., Hamblin M. R. (2005)**. Photodynamic inactivation of *Bacillus* spores, mediated by phenothiazinium dyes, *Appl Environ Microbiol*, 71, 11, 6918-6925.

48. **De Rosa M.C., Crutchley R. J. (2002)** Photosensitized singlet oxygen and its applications, *Coord Chem Rev,* 233-234, 351-371.

49. **Dougherty T. J., Potter W. R., Weishaupt K. R. (1984)**. The structure of the active component of hematoporphyrin derivative, *Progress in Clinical and Biological Research*, 170, 301-314.

50. **Egushi Y., Oshima T., Mori H., Aono R., Yamamoto K., Ishihama A., Utsumi R. (2003).** Transcriptional regulation of drug efflux genes by EvgAS, a two-component system *Escherichia coli*, *Microbiology*, 149, 2819–2828.

51. **Ehrenberg B., Malik Z., Nitzan Y. (1985).** Fluorescent spectral changes of hematoporphyrin derivative upon binding to lipid vesicles, *S. aureus* and *E. coli* cells, *Photochem Photobiol*, **41**, 429-435.

52. **Embleton M. L., Nair S. P., Cookson B. D., Wilson M. (2002).** Selective lethal photosensitization of methicillin-resistant *Staphylococcus aureus* using an IgG-tin(IV) chlorine e6 conjugate, *J. Antimicrob Chemother*, 50, 857-864.

53. **Engelhardt V, Krammer B, Plaetzer K. (2010).** Antibacterial photodynamic therapy using water- soluble formulations of hypericin or mTHPC is effective in inactivation of Staphylococcus aureus, *Photochem Photobiol Sci*, 9, 3, 365-369.

54. **Engelmann F. M., Mayer I., Gabrielli D. S., Toma H. E., Kowaltowski A. J., Araki K., Baptista M. S. (2007)**. Interaction of cationic *meso*-porphyrins with liposomes, mitochondria and erythrocytes, *J Bioenerg Biomembr*, 39, 175-185.

55. **Evans M. D., Dizdaroglu M., Cooke M. S. (2004)**. Oxidative DNA damage and disease: induction, repair and significance, *Mut Res*, 567, 1-61.

56. **Farr S. B., Kogoma T. (1991).** Oxidative stress responses in *Escherichia coli* and *Salonella typhimurium*, *Microbiol Mol Biol Rev*, 55, 4, 561-585.

57. **Fernandes P. (2006).** Antibacterial discovery and development- the failure of success, *Nature Biotechnology*, 24, 12, 1497-1503.

58. **Fernebro J. (2011)**. Fighting bacterial infections – future treatment options, *Drug Resistance Updates*, 14, 125-139.

59. **Ferro S., Ricchelli F., Monti D., Mancini G., Jori G. (2007).** Efficient photoinactivation of methicillin-resistant *Staphylococcus aureus* by a novel porphyrin incorporated into a poly-cationic liposome, *Int J Biochem & Cell Biol* 39, 1026–1034.

60. **Fotinos N., Convert M., Piffaretti J. C., Gurny R., Lange N. (2008)** 5-aminolevulinic acid and 5-aminolevulinic acid derivatives mediated effects on gram-negative and gram-positive bacteria, *Antimicrob Agents Chemother*, 52, 4, 1366-1373.

61. **Ford K., Fox K. R., Neidle S., Waring M. J. (1987).** DNA sequence preferences for an intercalating porphyrin compound revealed by footprinting, *NAR*, 15, 5, 2221-2234.

62. **Foote C. S. (1968).** Mechanisms of photosensitized oxidation, *Science*, 162, 3857, 963-969.

63. **Foote C. F. (1991).** Definition of Type I and Type II photosensitized oxidation, *Photochem Photobiol*, 54, 5, 569.

64. **Freire S., Bordello J., Granadero D., Al-Soufi W., Novo M. (2010).** Role of electrostatic and hydrophobic forces in the interaction of ionic dyes with charged micelles, *Photochem Photobiol Sci*, 9, 687-696.

65. **French G. L. (2010).** The continuinig crisis in antibiotic resistance, *Int J Antimicrob Agents*, 3653, 53-57.

66. **Friedrich C.L., Moyles D., Beverige T.J., Hancock R.E. (2000).** Antibacterial action of structurally diverse cationic peptides of gram-positive bacteria, *Antimicrob Agents Chemother*, 44, 2086-2092.

67. **Gad F., Zahra T., Francis K. P., Hasan T., Hamblin M. R. (2004).** Targeted photodynamic therapy of established soft-tissue infections in mice, *Photochem Photobiol Sci*, 3, 451-458.

68. **George S., Hamblin M.R., Kishen A. (2009)** Uptake pathways of anionic and cationic photosensitizers into bacteria, *Photochem Photobiol Sci*, 8, 788-795.

69. **Gold M.H. (2007).** Acne and PDT: a new techniques with lasers and light sources, *Lasers Med Sci*, 25, 434-442.

70. **Goldstein E., Citron D. M., Geffen D. (2011)**. Resistance trends in antimicrobial susceptibility of anaerobic bacteria, part I, *Clinical Microbiology Newsletter*, 33,1, 1-8.

71. **Goldstein E., Citron D. M., Geffen D. (2011).** Resistance trends in antimicrobial susceptibility of anaerobic bacteria part II, *Clinical Microbiology Newsletter*, 33, 2, 9-15.

72. **Grandadam M., Ingrad D., Huraux J. M., Avelyne B., Delgado O., Vever-Bizet C., Brault D. (1995)**. Photodynamic inactivation of cell free HIV strains by a red absorbing chlorin –type photosensitizer, *J. Photochem Photobiol B*, 31, 171-177.

73. **Griffiths, J., Schofield, J., Wainwright M., Brown, S. B. (1997)**. Some observations on the synthesis of polysubstituted zinc phthalocyanine sensitisers for photodynamic therapy, *Dyes and Pigments* 33, 65–78.

74. **Guo H., Pan X., Mao R., Zhang X., Wang L., Lu X., Chang J., Guo J. T., Passic S., Krebs F. C., Wigdahl B., Warren T. K., Retterer C. J., Bavari S., Xu X., Cuconati A., Block T. M. (2011)**. Alkylated porphyrins have

broad antiviral activity against hepadnaviruses, flaviviruses, filoviruses and arenaviruses, *Antimicrob Agents Chemother*, 55, 2, 478-486.

75. **Haddon R. C., Brus L. E., Raghavachari K. (1986).** Electronic structure and bonding in icosahedral C60, *Chem Phys Lett*, 125, 5.6**,** 459-464.

76. **Hamblin M.R., O'Donnell D.A., Murthy N., Rajagopalan K., Michaud N., Sherwood M.E., Hasan T. (2002).** Polycationic photosensitizer conjugates: effects of chain length and gram classification on the photodynamic inactivation of bacteria, *J Antimicrob Chemother*, 49, 941-951.

77. **Hamblin M. R., Zahra T., Contag C. H., McManus A. T., Hasan T. (2003).** Optical monitoring and treating of potentially lethal wound infections in vivo, *J Infect Dis*, 187, 1717-1725.

78. **Hamblin M. R., Hasan T. (2004).** Photodynamic therapy: a new antimicrobial approach to infectious disease? *Photochem Photobiol Sci*, 3, 436-450.

79. **Hamblin M. R. (2010)** Innovative cationic fullerenes as broad-spectrum light-activated antimicrobials, *Nanomedicine*, 6, 3, 442-452.

80. **Horiuchi H., Takagi M., Yano K. (1984).** Relaxation of supercoiled plasmid DNA by oxidative stress in *Escherichia coli*, *J Bacteriol*, 160, 3, 1017-1021.

81. **Hörfelt C., Stenquist B., Halldin C. B., Ericson M. B., Wennberg A. M. (2009)**. Single low-dose red light is an efficacious as methyl-aminolevulinate –photodynamic therapy for treatment of acne: clinical assesment and fluorescence monitoring, *Acta Derm Venereol*, 89, 4, 372-378.

82. **Huang L., Terakawa M., Zhiyentayev T., Huang Y. Y., Sawayama Y., Jahnke A., Tegos G. P., Wharton T., Immordino M. L., Dosio F., Cattel L. (2006).** Stealth liposomes: review of the basic science, rationale, and clinical applications, existing and potential, *Int J Nanomedicine* 1, 3, 297–315.

83. **Hussain S., Harris F., Phoenix D. A. (2006).** The phototoxicity of phenothiazinium-based photosensitiers to bacterial membranes, *FEMS Immunol Med Microbiol*, 46, 1, 124-130.

84. **Isturiz R. E. (2010)**. Optimising antimicrobial prescribing, *Int J Antimicrob Agents*, 3653, 519-522.

85. **Yacoby I., Benhar I. (2007).** Targeted bacterial therapy, *Infectious Disorders- Drug Targets,* 7, 221-229.

86. **Yacoby I., Shamis M., Bar H., Shabat D., Benhar I. (2006).** Targeting antibacterial agents by using drug-carrying filamentous bacteriophages, *Antimicrob Agents Chemother*, 50, 6, 2087-2097**.**

87. **Jesorka A., Orvar O. (2008).** Liposomes: technologies and analytical applications, *Ann Rev Analytical Chem*, 1, 801-832.

88. **Jori G. (2003)** ch. 146 Photodynamic therapy: basic and preclinical aspects in: CRC Handbook of Organic Photochemistry and Photobiology, edd. by Horspool W and Lenci F., CRC Press, Boca Raton, 146-1 – 146-10.

89. **Jori G., Roncucci G. (2006).** Photodynamic therapy in microbial infections, *Adv Clin Exp Med*, 15, 3, 421-426.

90. **Jori G., Fabris C., Soncin M., Ferro S., Coppellotti O., Dei D., Fantetti L., Chiti G., Roncucci G. (2006).** Photodynamic therapy in the treatment of microbial infections: basic principles and perspective applications, *Lasers in Surgery and Medicine*, 38, 468-481.

91. **Jori G., Coppellotti O. (2007)**. Inactivation of Pathogenic Microorganisms by photodynamic techniques: mechanistic aspects and perspective applications, *Anti-Infect Agents Med Chem,* 6, 119-131.

92. **Kang J., Wu H., Lu X., Wang Y, Zhou L. (2005).** Study on the interaction of new water-soluble porphyrin with DNA, *Spectrochimica Acta* Part A 61, 2041-2047.

93. **Kassab K., Ben-Amor T., Jori G., Coppellotti O. (2002).** Photosensitization of *Colpoda inflate* cysts by meso-substituted cationic porphyrins, *Photochem Photobiol Sci*, 1, 560-564.

94. **Kato A., Ohnishi H., Yamamoto K., Furuta E., Tanabe H., Utsumi R. (2000).** Transcription of *emrKY* is regulated by the EvgA-EvgS two-component system in *Escherichia coli* K12, *Biosci Biotechnol Biochem*, 64, 1203–1209.

95. **Kroto H. W., Heath J. R., O'Brien S. C., Curl F., Smalley R. E. (1985)** Buckminsterfullerene, *Nature*, 318. 6042, 162-163.

96. **Kussovski V., Montareva V., Angelov I., Orozova P., Wöhrle D., Schnurpfeil G., Borisova E., Avramov L. (2009).** Photodynamic inactivation of Aeromonas hydrophila bycationic phthalocyanines with different hydrophobicity, *FEMS Microbiol Lett*, 294, 2, 133-140.

97. **Lambrecht, B., Norley, S. G., Kurth, R., Mohr, H. (1994).** Rapid inactivation of HIV-1 in single donor preparations of human fresh frozen plasma by methylene blue/light treatment, *Biologicals* 22, 227–231.

98. **Lambrechts S. A., Aalders M. C., Verbraak F. D., Lagerberg J. W., Dankert J. B., Schuitmaker J. J. (2005).** Effect of albumin on the photodynamic inactivation of microorganisms by a cationic porphyrin, *J Photochem Photobiol B*, 79, 51-57.

99. **Lazzeri D., Rovera L., Pascual L., Durantini E. N. (2004).** Photodynamic studies and photoinactivation of *Escherichia coli* using *meso*-substituted cationic porphyrins with asymmetric charge distribution, *Photochem Photobiol*, 80, 2, 286-293.

100. **Levin B. R., Bull J. J. (2004)**. Population and evolutionary dynamics of phage therapy, *Nature Rev, Microbiology*, 2, 166-173.

101. **Maish T., Szeimies R. M., Jori G., Abels C. (2004).** Antibacterial photodynamic therapy in dermathology, *Photochem Photobiol Sci*, 3, 907-917.

102. **Maish T. (2009)**. A new strategy to destroy antibiotic resistant microorganisms: antimicrobial photodynamic treatment, *Mini Rev Med Chem*, 9, 8, 974-983.

103. **Maish T., Hackbarth S., Regensburger J., Felgenträger A., Baumler W., Landthaler M., Röder B. (2010)** Photodynamic inactivation of multiresistant bacteria (PIB) – a new approach to treat superficial infections in the 21st century, *J Dtsch Dermatol Ges* (*Journal of the German Society of Dermatology),* 8, DOI:10.1111/j.1610-0387.2010.07577.x.

104. **Malik Z., Ladan H., Nitzan Y. (1992).** Photodynamic inactivation of Gram-negative bacteria: problems and possible solutions, *J Photochem Photobiol, B*., 14, 262-266.

105. **Malik Z., Babushkin T., Sher S., Hanania J., Ladan H., Nitzan Y., Salzberg S. (1993)** Collapse of K+ and ionic balance during photodynamic inactivation of leucemic cells, erythrocytes and *Staphylococcus aureus*, *Int J Biochem*, 25, 10, 1399-1406.

106. **Mantareva V., Kussovski V., Angelov I., Borisova E., Avramov L., Schnurpfeil G., Wöhrle D. (2007)** Photodynamic activity of water-soluble phthalocyanine zinc (II) complexes against pathogenic microorganisms, *Bioorg Med Chem*, 15, 4829-4835.

107. **Mantareva V., Kussovski V., Angelov I., Wöhrle D., Dimitrov R., Popova E., Dimitrov S. (2010)** Non-aggregated Ga(III)-phthalocyanines in the photodynamic inactivation of planctonic and biofilm cultures of pathogenic microorganisms, *Photochem Photobiol Sci*, 10, 1, 91-102.

108. **Martin J. P., Logsdon N. (1987)**. The role of oxygen radicals in dye mediated photodynamic effects in *Escherichia coli* B, *J Biol Chem*, 262, 7213-7219.

109. **Meisel P., Kocher T. (2005).** Photodynamic therapy for periodontal diseases: state of the art, *J Photochem Photobiol B*, 79, 159-170.

110. **Merchat M., Bertolini G., Giacomini P., Villanueva A., Jori, G. (1996).** Meso-substituted cationic porphyrins as efficient photosensitizers of Gram-positive and Gram-negative bacteria, *J Photochem Photobiol B,* 32, 153–157.

111. **Meisel P., Kocher T. (2005).** Photodynamic therapy for periodontal diseases: state of art, *J Photochem Photobiol B*, 79, 159-170.

112. **Mettath S., Munson B. R., Pandey R. K. (1999)**. DNA interaction and photocleavage properties of porphyrins containing cationic substituents at the peripheral position, *Bioconjugate Chem*, 10, 94-102.

113. **Merril C. R., Scholl D., Adhya S. L. (2003)** The prospect for bacteriophage therapy in western medicine, *Nature Rev Drug discovery*, 2, 489-497.

114. **Миллер Дж. (1976).** Эксперименты в молекулярной генетике. – М: Мир, 365-371.

115. **Millson, C. E., Wilson, M., MacRobert, A. J., Bedwell, G., Bown, S. G. (1996)**. The killing of *Helicobacter pylori* by low-power laser light in the presence of photosensitizer, *J Med Microbiol*, 44, 245-252.

116. **Moan J. (1990).** Properties for optimal PDT sensitizers, *J Photochem Photobiol B,* 5, 521–524.

117. **Moan J., Berg K. (1991)**. The photodegradation of porphyrins in cells can be used to estimate the lifetime of singlet oxygen, *Photochem Photobiol*, 53, 549–553.

118. **Moellering R.C. (2011)**. Discovering new antimicrobial agents, *Int J Antimicrob Agents*, 37, 2-9.

119. **Munson B. R., Fiel R. J. (1992).** DNA intercalation and photosensitization by cationic *meso*-substituted porphyrins, *NAR*, 20, 6, 1315-1319.

120. **Nastri L., Donnarumma G., Porzio C., De Gregorio V., Tufano M. A., Caruso F., Mazza C., Serpico R. (2010)**. Effects of toluidine mediated photodynamic therapy on periopathogens and periodontal biofilm: in vitro evaluation, *Int J Immunopathol Pharmacol*, 23, 4, 1125-1132.

121. **Nikaido H. (2003).** Molecular basis of bacterial outer membrane permeability revisited, *Microbiol. Mol. Biol. Rev.* 67, 593–656.

122. **Nikaido H. (2009).** Multidrug resistance in bacteria, *Annu Rev Biochem*, 78, 119-146.

123. **Nisnevitch M., Nakonechny F., Nitzan Y. (2010)**. Photodynamic antimicrobial chemotherapy by liposome – encapsulated water soluble photosensitizers, *Bioorg Khim*, 36, 3, 396-402.

124. **Nitzan Y., Shainberg B., Malik Z. (1987).** Photodynamic effects of deuteroporphyrin on gram-positive bacteria, *Curr Microbiology*, 15, 251-258.

125. **Nitzan Y., Gutterman M., Malik Z., Ehrenberg B. (1992).** Inactivation of gram-negative bacteria by photosensitized porphyrins, *Photochem Photobiol*, 55, 1, 89-96.

126. **Nitzan Y., Dror R., Ladan H., Malik Z., Kibel S., Gottfried V. (1995).** Structure – activity relationship of porphines for photoinactivation of bacteria, *Photochem. Photobiol*, 62, 2, 342-347.

127. **Nitzan Y., Ashkenazi H. (1999).** Photoinactivation of *Deinococcus radiodurans*: an unusual gram-positive microorganism, *Photochem Photobiol*, 69, 4, 505-510.

128. **Nitzan Y., Salmon –Divon M., Shporen E., Malik Z. (2004)** ALA induced photodynamic effects on Gram positive and negative bacteria, *Photochem. Photobiol. Sci.,* 3, 430-435.

129. **Nitzan Y., Ashkenazi H. (2001)**. Photoinactivation of *Acinetobacter baumannii* and *Escherichia coli B* by cationic hydrophilic porphyrin at various light wavelengths, *Curr Microbiol*, 42, 408-414.

130. **North J., Neyndorff H., Levy J. G. (1993).** Photosensitizers as virucidal agents, *J Photochem Photobiol B.* 17, 99–108.

131. **Orenstein A., Klein D., Kopolovic J., Winkler E., Malik Z., Keller N., Nitzan Y. (1998).** The use of porphyrins for eradication of *Staphylococcus aureus* in burn wound infections*, FEMS Immunology and Medical Microbiology*, 19, 307-314.

132. **OhUigin C., McConnell D. J., Kelly J. M., van der Putten W. J. M. (1987).** Methylene blue photosensitized strand cleavage of DNA: effects of the dye binding and oxygen, *NAR*, 15, 7411-7427.

133. **O'Riordan K., Akilov O. E., Hasan T. (2005).** The potential for photodynamic therapy in the treatment of localized infections, *Photodiagnosis and Photodynamic Therapy*, 2, 247-262.

134. **Pagonis T. C., Chen J., Fontana C. R., Devalapally H., Ruggiero K., Song X, Foshi F, Dunham J, Skobe Z., Yamazaki H., Kent R., Tanner A. C., Amiji M. M., Soukos N. S. (2010)** Nanoparticle based endodontic antimicrobial photodynamic therapy, *J Endod*, 36, 2, 322-328.

135. **Pasternack R. F., Huber P. R., Boyd P., Engasser G., Francesconi L., Gibbs E., Fasella P., Cerio Venturo G., Hinds L. (1972)**. On the aggregation of meso-substituted water soluble porphyrins, *J Am Chem Soc*, 94, 13, 4511–4517.

136. **Pasternack R. P., Gibs E. J., Villafranca J. J. (1983a).** Interaction of porphyrins with nucleic acids, *Biochemistry*, 22, 10, 2406-2414.

137. **Pasternack R. P., Gibs E. J., Villafranca J. J. (1983b).** Interaction of porphyrins with nucleic acids, *Biochemistry*, 22, 23, 5409-5417.

138. **Perni S., Prokopovich P., Pratten J., Parkin I. P., Wilson M. (2011)**. Nanoparticles: their potential use in antibacterial photodynamic therapy, *Photochem Photobiol Sci*, DOI: 10.1039/c0pp00360c.

139. **Phoenix D. A., Harris F. (2006)** Light activated compounds as antimicrobial agents- patently obvious?, *Recent Patents on Anti-Infective Drug Discovery*, 1, 181-199.

140. **Prasad P. N. (2003)**. Introduction to biophotonics, ch. 2 Fundamentals of light and matter, ch 12 Light-activated therapy: Photodynamic therapy, John Wiley & Sons, Inc, New Jersey, 11-46, 433-460.

141. **Praseuth D., Gaudemer A., Verlhac J. B., Kraljic I., Sissoëff I., Guille E. (1986).** Photocleavage of DNA in the presence of synthetic water-soluble porphyrins, Photochem Photobiol, 44, 6, 717-724.

142. **Pushpan S. K., Vencatraman S., Anand V. G., Sancar J., Parmeswaran D., Ganesan S., Chandrashekar T. K. (2002)** Porphyrin in photodynamic therapy – a search for ideal photosensitizers, *Curr Med Chem-Anti-Cancer Agents*, 2, 187-207.

143. **Quiroga E. D., Alvarez M. G., Durantini E. N. (2010)** Susceptibility of Candida albicans to photodynamic action of 5,10,15,20-tetra(4-N-methylpyridyl)porphyrin in different media, *FEMS Immunology and Medical microbiology*, 1-9.

144. **Raghavendra M., Koregol A., Bhola S. (2009).** Photodynamic therapy: a targeted therapy in periodontics, *Australian Dental Journal*, 54, (1 Suppl), S102–S109.

145. **Rasko D. A., Sperandio V. (2010).** Anti-virulence strategies to combat bacterial mediated disease, *Nature Rewievs, Drug Discovery*, 9, 117-128.

146. **Rasul R., Cole N., Balasubramanian D., Chen R., Kumar N., Willcox M. P. D. (2010).** Interaction of the antimicrobial peptide melamine with bacterial membranes, *Int J Antimicrob Agents*, 35, 566–572.

147. **Reddi E., Jori G. (1998).** Steady-state and time-resolved spectroscopic studies of photodynamic sensitizers: porphyrins and phthalocyanines, *Rev Chem Interm*., 10, 241-268.

148. **Reddi E., Ceccon M., Valduga G, Jori G., Bommer J. C., Elisei F., Latterini L., Mazzucato U. (2002).** Photophysical properties and antibacterial activity of meso-substituted cationic porphyrins, *Photochem Photobiol*, 75, 5, 462-470.

149. **Ricchelli F., Jori G. (1990)** Factors influencing the distribution pattern of porphyrins in cell membranes, *Photochem Photobiol B*, 6, 69-77.

150. **Ricchelli F. (1995).** New Trends in Photobiology (Invited Review) Photophysical properties of porphyrins in biological membranes, *J Photochem Photobiol B*, 29, 109-118.

151. **O' Riordan K., Akilov O. E., Hasan T. (2005)**. The potential for photodynamic therapy in the treatment of localized infections, *Photodyagn Photodynam Ther*, 2, 247-262.

152. **Rossoni R. D., Junqueira E. L., Santos E. L. S., Costa A. C. B., Jorge A. O. C. (2010).** Comparison of the efficacy of Rose Bengal and erythrosine in photodynamic therapy against *Enterobacteriaceae*, *Lasers Med Sci*, 25, 581-58.

153. **Rottenberg H. (1989).** Proton electrochemical potential gradient in vesicles, organelles and prokaryotic cells, *Methods Enzymol*, 172, 63–84.

154. **Rotomskis R., Streckytė G, Griciūtė L. (2002).** Fotosensibilizuota navikų terapija: pirminiai vyksmai, sk. 4 Fotosensibilizatoriai, sk. 5 Fotosensibilizuoti procesai navikų terapijoje, sk. 6 Sensibilizatorių fotostabilumas bei fototransformacijos ir jų reikšmė fototerapinėms dozėms, sk. 7 Endogeniniai fotosensibilizatoriai „Lietuvos mokslas" 73-97, 139-152, 161-174, 201-210.

155. **Rotomskis R., Bagdonas S., Valančiūnaitė J. (2007).** Biofotonika, sk1 Šviesos srauto charakteristikos, sk2 Biologinių objektų liuminescencija, VU leidykla, 1-48, 49-77.

156. **Rovaldi C. R., Pievsky A., Sole N. A., Friden P. M., Rothstein D. M., Spacciapoli P. (2000).** Photoactive porphyrin derivative with broad spectral activity against oral pathogens in vitro, *Antimicrob Agents Chemother*, 44, 12, 3364-3367.

157. **Ruiz N., Kahne D., Silhavy T.J. (2006).** Advances in understanding bacterial outer-membrane biogenesis, *Nature Rev Microbiol*, 4, 57-66.

158. **Salmon-Divon M., Nitzan Y., Malik Z. (2004)**. Mechanistic aspects of *Escherichia coli* photodynamic inactivation by cationic tetra-meso(N-methylpyridyl)porphine, *Photochem Photobio. Sci*, 3, 423-429.

159. **Samad A., Sultana Y., Aqil M. (2007).** Liposomal drug delivery systems: an update review, *Curr Drug Delivery 4,* 297-305.

160. **Sambrook J., Russell D. W. (2001).** Molecular cloning. A laboratory manual, 3rd ed, I ch. Plasmids and their usefulness in molecular cloning; Appendix 1 Preparation of buffers and stock solutions for use in molecular biology; Appendix 8 Commonly used technique in molecular cloning, 1.24, 1.31-1.42; A1-7-1.16; A8.12-8.16 Cold Spring Harbor Laboratory Press, NY.

161. **Santus R., Reyftmann J. P. (1986).** Photosensitization of membrane components, *Biochimie,* 68, 843-848.

162. **Salyers A. A., Whitt D. D. (2001).** Microbiology, ch 4, Structural features of prokaryotes, Fitzgerald Science Press, Maryland, USA, 51-61.

163. **Sari M. A., Battioni J. P., Dupre D., Mansuy D., Le Pecq J. B. (1990).** Interaction of cationic porphyrins with DNA: Importance of the number and position of charges and minimum structural requirements for intercalation, *Biochemistry*, 29, 4205-4215.

164. **Scalise I., Durantini E. N. (2005).** Synthesis, properties and photodynamic inactivation of *Escherichia coli* using a cationic and noncharged Zn(II)pyridyloxypthalocyanine derivatives, *Bioorg Med Chem*, 13, 8, 3037-3045.

165. **Seah L. H., Burgoyne L.A. (2001).** Photosensitizer initiated attacks on DNA under dry conditions and their inhibition: a DNA archiving issue, *J Photochem Photobiol B*, 61, 10–20.

166. **Segalla A., Borsarelli C. D., Braslavsky S. E., Spikes J. D., Roncucci G., Dei D., Chiti G., Jori G., Reddi E. (2002).** Photophysical, photochemical and antibacterial photosensitizing properties of a novel actacationic Zn(II)-phthalocyanine, *Photochem Photobiol Sci*, 1, 641-648.

167. **Sies H., Menck C. F. M. (1992)**. Singlet oxygen induced damage, *Mut Res/DNAging*, 275, 3-6, 367-375.

168. **Shih M. H., Huang F. C. (2011)**. Effects of photodynamic therapy of rapidly growing nontuberculous mycobacteria keratitis, *Invest Ophthalmol Vis Sci*, 52, 1, 223-229.

169. **Skripchenko A. A., Wagner S. J. (2000)**. Inactivation of WBCs in RBC suspensions by photoactive phenothiazine dyes: comparison of dimethylmethylene blue and MB, *Transfusion*, 40, 968–975.

170. **Smetana Z, Ben-Hur E, Mendelson E., Salzberg S., Wagner P., Malik Z.(1998)**. Herpes simplex virus proteins are damaged following photodynamic inactivation with phthalocyanines, *J Photochem Photobiol B*, 44, 1, 77-83.

171. **Smijs T. G. M., Pavel S. (2011).** The susceptibility of dermatophytes to photodynamic treatment with special focus on *Trychophiton rubrum*, *Photochem Photobiol*, 87, 1, 2-13.

172. **Soukos N.S., Ximenez-Fyvie L. A., Hamblin M. R., Socransky S. S., Hasan T. (1998).** Targeted Antimicrobial photochemotherapy, *Antimicrob Agents Chemother*, 42, 10, 2595-2601.

173. **Soukos N. S., Goodson J. M. (2011)**. Photodynamic therapy in the control of oral biofilms, *Periodontol 2000*, 55, 1, 143-166.

174. **Spesia M .B., Milanesio M. E., Durantini E. N. (2008)**. Synthesis, properties and photodynamic inactivation of Escherichia coli by novel cationic fullerene C60 derivative, *Eur J Med Chem,* 43, 853-861.

175. **Spesia M. B., Caminos D. A., Pons P., Durantini E. N. (2009).** Mechanistic insight of the photodynamic inactivation of *Escherichia coli* by a tetracationic zinc(II)phthalocyanine derivative, *Photodiagnosis and Photodynamic Therapy*, 6, 52-61.

176. **Stadtman E. R., Levine R. L. (2003)**. Free radical-mediated oxidation of free amino acids and amino acid residues in proteins, *Amino acids*, 25, 3-4, 207-218.

177. **Sternberg E. D., Dolphin D., Brucner C. (1998)**. Porphyrin based photosensitizers for use in photodynamic therapy, *Tetrahedron*, 54, 4151-4202.

178. **Streckytė G., Didžiapetrienė J., Kirvelienė V., Bagdonas S., Rotomskis R. (2008)**. Fotosensibilizacija biosistemose: taikymas ir perspektyvos, sk. 4 Pirminiai fotosensibilizuoti vyksmai, sk. 6 Fotosensibilizatoriai, „Progretus“ poligrafijos centras, 42-52, 71-84.

179. **Strong L., Yarmush D. M., Yarmush M. L. (1994)**. Antibody-targeted photolysis photophysical, biochemical, and pharmacokinetic properties of antibacterial conjugates**,** *Annals New York Academy of Sciences* 745, 297-320.

180. **Szocs K., Gabor F., Csik G., Fidy J. (1999).** δ-Aminolaevulinic acid-induced porphyrin synthesis and photodynamic inactivation of *Escherichia coli B*, *J Photochem Photobiol B,* 50, 8-17.

181. **Tanford C. (1980).** The Hydrophobic Effect: formation of micelles and biological membranes, 2nd edition, John Wiley & Sons Inc; p 109.

182. **Tang H. M., Hamblin M. R., Yow C. M. (2007)**. A comparative in vitro photoinactivation study of clinical isolates of multidrug-resistant pathogens, *J Infect Chemother*, 13, 2, 87-91.

183. **Tatsumi R., Waschi M. (2008)**. TolC-dependent exclusion of porphyrins in *Escherichia coli*, *J Bacteriol*, 190, 18, 6228-6233.

184. **Taylor P. W., Stapleton P. D., Luzio J. P.(2002).** New ways to treat bacterial infections, *DDT*, 7, 21, 1086-1091.

185. **Tavares A., Carvalho C. M., Faustino M. A., Neves M. G., Tome J. P., Tome A. C., Cavaleiro J. A., Cunha A., Gomes N. C., Alves E., Almeida A. (2010)**. Antimicrobial photodynamic therapy: study of bacterial recovery viability and potential development of resistance after treatment, *Mar Drugs*, 8, 1, 91-105.

186. **Tegos G. P., Demidova T. N., Arcila-Lopez D., Lee H., Wharton T., Gali H., Hamblin M. R. (2005)** Cationic fullerenes are effective and selective antimicrobial photosensitizers, *Chem Biol*, 12, 1127-1135.

187. **Tegos G. P., Hamblin M. R. (2006a)**. Phenothiazinium antimicrobial photosensitizers are substrates of bacterial multidrug resistance pumps, *Antimicrob Agent Chemother*, 50, 1, 196-203.

188. **Tegos G. P., Anbe M., Yang C., Demidova T. N., Satti M., Mroz P., Janjua S., Gad F., Hamblin M. R. (2006b).** Protease-stable polycationic photosensitizer conjugates between polyethyleneimine and chlorine e6 for broad-spectrum antimicrobial photoinactivation, *Antimicrob Agents Chemother*, 50, 4, 1402-1410.

189. **Tegos G., Masago K., Aziz F., Higginbotham A., Stermitz F. R., Hamblin M. R. (2008)**. Inhibitors of bacterial multidrug efflux pumps potentiate antimicrobial photoinactivation, *Antimicrob Agents Chemother*, 52, 9, 3202-3209.

190. **Todar K.,** Todar's online textbook of bacteriology, ch. Bacterial resistance to antibiotics, 2011 05 06 address: http://www.textbookofbacteriology.net/resantimicrobial.html.

191. **Tuite E. M., Kelly J. M.(1993).** Photochemical interactions of methylene blue and analogues with DNA and other biological substrates, *Photochem Photobiol B*, 21, 103-124.

192. **Usatheva M. N., Teichert M. C., Biel M. A. (2001).** Comparison of the methylene blue and toluidine blue photobactericidal efficacy against Gram-positive and Gram-negative microorganisms, *Laser Surg Medicine*, 29, 165-173.

193. **Usatcheva M. N., Teichert M. C., Sievert C. E., Biel M. A, (2006)**. Effect of Ca+ on the photobacterial efficacy of methylen blue and toluidine blue against gram-negative bacteria and the dye affinity to lipopolysaccharides, *Lasers Surg Med* 38, 10, 946-954.

194. **Vaara M. (1992).** Agents that increase the permeability of the outer membrane, *Microbiological Reviews*, 56, 3, 395-411.

195. **Valduga G., Breda B., Giacometti G., Jori G., Reddi E. (1999).** Photosensitization of wild and mutant strains of *Escherichia coli* by meso-tetra(N-methyl-4-pyridyl)porphine, *Biochem Biophys Res Commun*, 256, 84-88.

196. **Wakayama Y., Takagi M., Yano K. (1980).** Photosensitized inactivation of *E coli*. cells in toluidine blue–light system, *Photochem Photobiol*, 32, 601–605.

197. **Wainwright M. (1998).** Photodynamic antimicrobial chemotherapy (PACT), *J Antimicrob Chemother*, 42, 13-28.

198. **Wainwright M. (2003).** The use of dyes in modern biomedicine, *Biotech Histochem*, 78, 147-155.

199. **Wainwright M. (2004)** Photoinactivation of viruses, *Photochem Photobiol Sci*, 3, 406-411.

200. **Wainwright M. (2009).** Photosensitizers in biomedicine, ch. 11 Antimicrobial application – photodynamic antimicrobial chemotherapy, ch. 7 Phthalocyanines, ch. 4 Azines, ch. 6 Porphyrins, John Wiley & Sons Ltd., 237-247; 147-165; 63-74, 113-141.

201. **Wang K., Zhang Z., Guo Q., Bao X., Li Z. (2008)** Interaction of water-soluble bridged porphyrin with DNA, *Front Chem China*, 3, 4, 406-412.

202. **Wardle B. (2009).** Principles and applications of photochemistry, , ch. 2 Light absorption and electronically-excited states, ch.3 **The Physical Deactivation of Excited States**, ch 7 Some Aspects of the Chemical Properties of Excited States, John Wiley & Sons Ltd., 29-43, 47-57, 119-133.

203. **Verkamp E., Backman V. G., Björnsson J. M., Söll D., Eggertsson G. (1993)**. The periplasmic dipeptide permease system transports 5-aminolevulinic acid into Escherichia coli, *J Bacteriol*, 175, 5, 1452-1456.

204. **Willing B. P., Russell S. L, Finlay B. B. (2011).** Shifting the balance: antibiotic effects on host-microbiota mutualism, *Nature Rewievs Microbiology*, doi:10.1038/nrmicro2536

205. **Wilson M. (1993).** Photolysis of oral bacteria and its potential use in the treatment of caries and periodontal disease, *J Appl Bacteriol,* 75, 299–306.

206. **Wilson M. & Mia N. (1994).** Effect of environmental factors on the lethal photosensitization of *Candida albicans in vitro, Lasers Med Sci,* 9, 105–109.

207. **Wilson M., Burns T., Pratten J., Pearson, G. J. (1995).** Bacteria in supragingival plaque samples can be killed by lowpower laser light in the presence of a photosensitizer, *J Appl Bacteriol,* 78, 569–574.

208. **Wilson M. (1996).** Susceptibility of oral microbial biofilms to antimicrobial agents, *J Med Microbiol*, 44, 79-87.

209. **Wilson M., Burns T., Pratten J. (1996).** Killing of *Streptococcus sanguis* in biofilm using a light-activated antimicrobial agent, *J Antimicrob Chemother*, 37, 377-381.

210. **Wilson M. (2004).** Lethal photosensitization of oral bacteria and its potential application in the photodynamic therapy of oral infections, *Photochem Photobiol Sci*, 3, 412-418.

211. **Wood S., Nattress B., Kirkham J., Shore R., Brookes S., Griffiths J., Robinson C. (1999).** An in vitro study of the use of photodynamic therapy for the treatment of natural oral plaque biofilms formed in vivo, *J Photochem Photobiol B*, 50, 1-7.

212. **Zolfaghari P. S., Packer S., Singer M., Nair S. P., Bennett J., Street C., Wilson M. (2009).** In vivo killing of *Staphylococcus aureus* using a light activated antimicrobial agent, *BMC Microbiol*, 9, 27, doi:10.1186/1471-2180-9-27

213. **Zupán K., Herényi L., Tóth K., Egyeki M., Czík G. (2005)**. Binding of cationic porphyrin to isolated DNA and nucleoprotein complex: quantitative analysis of binding forms under various experimental conditions, *Biochemistry*, 44, 45, 15000-15006.